UNIVERSITY OF AMSTERDAM

UvA-DARE (Digital Academic Repository)

Search for pair production of heavy vectorlike quarks decaying into hadronic final states in pp collisions at root √s=13 TeV with the ATLAS detector

Aaboud, M.; The ATLAS Collaboration

DOI
10.1103/PhysRevD.98.092005

Publication date
2018

Document Version
Final published version

Published in
Physical Review D. Particles and Fields

License
CC BY

Link to publication

Citation for published version (APA):
Aaboud, M., & The ATLAS Collaboration (2018). Search for pair production of heavy vectorlike quarks decaying into hadronic final states in pp collisions at root √s=13 TeV with the ATLAS detector. *Physical Review D. Particles and Fields*, *98*(9), Article 092005. https://doi.org/10.1103/PhysRevD.98.092005

General rights
It is not permitted to download or to forward/distribute the text or part of it without the consent of the author(s) and/or copyright holder(s), other than for strictly personal, individual use, unless the work is under an open content license (like Creative Commons).

Disclaimer/Complaints regulations
If you believe that digital publication of certain material infringes any of your rights or (privacy) interests, please let the Library know, stating your reasons. In case of a legitimate complaint, the Library will make the material inaccessible and/or remove it from the website. Please Ask the Library: https://uba.uva.nl/en/contact, or a letter to: Library of the University of Amsterdam, Secretariat, P.O. Box 19185, 1000 GD Amsterdam, The Netherlands. You will be contacted as soon as possible.

UvA-DARE is a service provided by the library of the University of Amsterdam (https://dare.uva.nl)

Download date:14 Sep 2026

Search for pair production of heavy vectorlike quarks decaying into hadronic final states in pp collisions at $\sqrt{s} = 13$ TeV with the ATLAS detector

M. Aaboud *et al.*[*]
(ATLAS Collaboration)

(Received 7 August 2018; published 9 November 2018)

A search is presented for the pair production of heavy vectorlike quarks, $T\bar{T}$ or $B\bar{B}$, that decay into final states with jets and no reconstructed leptons. Jets in the final state are classified using a deep neural network as arising from hadronically decaying W/Z bosons, Higgs bosons, top quarks, or background. The analysis uses data from the ATLAS experiment corresponding to 36.1 fb^{-1} of proton-proton collisions with a center-of-mass energy of $\sqrt{s} = 13$ TeV delivered by the Large Hadron Collider in 2015 and 2016. No significant deviation from the Standard Model expectation is observed. Results are interpreted assuming the vectorlike quarks decay into a Standard Model boson and a third-generation-quark, $T \to Wb, Ht, Zt$ or $B \to Wt, Hb, Zb$, for a variety of branching ratios. At 95% confidence level, the observed (expected) lower limit on the vectorlike B-quark mass for a weak-isospin doublet (B, Y) is 950 (890) GeV, and the lower limits on the masses for the pure decays $B \to Hb$ and $T \to Ht$, where these results are strongest, are 1010 (970) GeV and 1010 (1010) GeV, respectively.

DOI: 10.1103/PhysRevD.98.092005

I. INTRODUCTION

Many theories beyond the Standard Model (SM) are motivated by the naturalness problem [1], and are intended to resolve the quadratic divergences in the radiative corrections to the Higgs-boson mass. Several extensions to the SM, such as little Higgs [2,3] and composite Higgs [4,5] models, have been proposed to address this issue. A common feature of these models is the existence of TeV-scale vectorlike quarks (VLQs) that couple preferentially to third-generation SM quarks [6].

VLQs are spin-1/2 colored fermions with left-right symmetric transformation properties under the weak-isospin SU(2) gauge group. Unlike chiral quarks, which obtain mass through electroweak symmetry breaking [7–12], VLQs can have a gauge invariant mass term $m\bar{\psi}\psi$. Therefore, VLQs are not subject to the constraints from Higgs production which highly disfavor additional chiral quarks [13–16]. VLQs also couple to flavor-changing neutral currents, so a charge[1] $+2/3$ vectorlike partner of the top quark, T, could decay[2] into Wb, Zt or Ht, while a charge $-1/3$ bottom quark partner, B, could decay into Wt, Zb, or Hb [17–20]. The branching ratios depend on the VLQ mass and weak-isospin multiplet. Vectorlike T and B can occur alone in a singlet scenario. Doublet and triplet scenarios also allow for more exotic X and Y VLQs with charges $+5/3$ and $-4/3$, respectively. Charge conservation requires these to decay only via $X \to Wt$ and $Y \to Wb$. Because this search has not been optimized for X and Y vectorlike quarks, they will not be discussed in this paper.

Many previous searches for pair-produced VLQs by ATLAS and CMS at $\sqrt{s} = 8$ TeV [21–26] and $\sqrt{s} = 13$ TeV [27–34] have focused on final states with one or more leptons. Additionally, previous results from CMS at $\sqrt{s} = 8$ TeV and ATLAS at $\sqrt{s} = 13$ TeV have included fully hadronic as well as leptonic final states [35–37]. The previous fully hadronic search by ATLAS [37] only focuses on the high missing transverse momentum ($E_{\mathrm{T}}^{\mathrm{miss}}$) region ($E_{\mathrm{T}}^{\mathrm{miss}} > 200$ GeV). The analysis presented in this paper searches for heavy VLQs produced in pairs and decaying into fully hadronic final states in the low-$E_{\mathrm{T}}^{\mathrm{miss}}$ region ($E_{\mathrm{T}}^{\mathrm{miss}} < 200$ GeV). This channel is complementary to those used in previous ATLAS VLQ searches and is particularly powerful for the $B \to Hb$ decay mode, which is difficult to probe with leptonic final states.

[*] Full author list given at the end of the article.
[1] Electric charge is measured in units of e.

Published by the American Physical Society under the terms of the Creative Commons Attribution 4.0 International license. Further distribution of this work must maintain attribution to the author(s) and the published article's title, journal citation, and DOI. Funded by SCOAP[3].

[2] It is assumed that the VLQs decay only into SM particles, and couple to only third-generation quarks.

 © 2018 CERN, for the ATLAS Collaboration

II. ATLAS DETECTOR

The ATLAS detector [38] at the Large Hadron Collider (LHC) is centered on the collision point and covers nearly the entire solid angle.[3] It consists of an inner tracking detector surrounded by a 2 T superconducting solenoid, electromagnetic and hadronic calorimeters, and a muon spectrometer incorporating three large superconducting toroid magnets. The inner detector, including the insertable B-layer installed in 2014 [39,40], provides charged-particle tracking information from a pixel and silicon microstrip detector in the pseudorapidity range $|\eta| < 2.5$ and a transition radiation tracker covering $|\eta| < 2.0$.

The calorimeter system covers the pseudorapidity range $|\eta| < 4.9$ and measures the positions and energies of electrons, photons, and charged and neutral hadrons. Within the region $|\eta| < 3.2$, electromagnetic calorimetry is provided by barrel and end cap high-granularity lead and liquid-argon sampling calorimeters. The hadronic sampling calorimeter uses either scintillator tiles or liquid argon as active material and steel, copper or tungsten as absorber.

The muon spectrometer comprises separate trigger and high-precision tracking chambers measuring the tracks of muons in a magnetic field generated by superconducting air-core toroid magnets. The precision chamber system covers the region $|\eta| < 2.7$, while the muon trigger system covers the range $|\eta| < 2.4$.

A two-level trigger system is used to select which events to save for offline analysis [41]. The first level is implemented in hardware/firmware and uses a subset of the detector information to reduce the event rate from 40 MHz to less than 100 kHz. This is followed by the software-based high-level trigger that reduces the event rate to approximately 1 kHz.

III. DATA AND SIMULATED EVENTS

The data analyzed correspond to pp collisions with a center-of-mass energy of $\sqrt{s} = 13$ TeV recorded by the ATLAS detector in 2015 and 2016. Data quality requirements ensure that all components of the detector were functioning. The full data set corresponds to an integrated luminosity of 36.1 fb^{-1}.

The primary background for this search is multijet events, followed by $t\bar{t}$ events and minor contributions from single-top-quark and $t\bar{t} + \mathrm{X}$ ($\mathrm{X} = W$, Z, H) events. The multijet background is estimated using a data-driven method (Sec. V C), while signal events and other background contributions were simulated via Monte Carlo (MC) generation of LHC collisions that are then passed through a GEANT4 simulation [42] of the ATLAS detector [43]. All simulated events are reconstructed using the same analysis chain as the data. In all MC samples, the top-quark and Higgs-boson masses were set to 172.5 and 125.0 GeV, respectively, and the EVTGEN v1.2.0 program [44] was used to simulate the properties of bottom and charm hadron decays.

Simulated events of VLQ pair production, $Q\bar{Q}$, were produced with the leading-order (LO) generator PROTOS v2.2 [18,45] using the NNPDF2.3 LO parton distribution function (PDF) set [46] and passed to PYTHIA 8.186 [47] for parton showering and fragmentation. The A14 [48] set of tuned parameters is used. VLQs were produced for the isospin singlet scenario with a narrow width and for masses between 700 and 1200 GeV in steps of 50 GeV, with additional events produced at 500, 600, 1300, and 1400 GeV. Additional samples were produced assuming a doublet scenario for VLQ masses of 700, 950, and 1200 GeV, in order to study differences from the different chirality of VLQs arising in singlet and doublet models.

The pair production cross section varies from 3.38 ± 0.25 pb ($m_Q = 500$ GeV) to 3.50 ± 0.43 fb ($m_Q = 1400$ GeV), computed using TOP++v2.0 [49] at next-to-next-to-leading order (NNLO) in QCD, including resummation of next-to-next-to-leading logarithmic (NNLL) soft-gluon terms, and using the MSTW 2008 NNLO set of PDFs [50]. Theory uncertainties are estimated by variations of the factorization and renormalization scales and by taking uncertainties of the PDF and strong coupling constant, α_S, into account. The latter two represent the largest contribution to the overall theoretical uncertainty in the predicted cross section and are calculated using the PDF4LHC [51] prescription with the MSTW 2008 68% C.L. NNLO, CT10 NNLO [52,53], and NNPDF2.3 5f FFN PDF sets.

The $t\bar{t}$ events were generated using POWHEG-BOX v2 + PYTHIA 8.210 [54,55] with the CT10 NLO PDF set and the Perugia2012 set of tuned parameters [56] for parton showering. The NLO radiation factor, h_{damp}, was set to $1.5m_{\mathrm{top}}$. The $t\bar{t}$ background is split into $t\bar{t} +$ light-flavor jets ($t\bar{t} +$ light) and $t\bar{t} +$ heavy-flavor jets ($t\bar{t} +$ HF), where heavy flavor refers to c- and b-flavor. Single-top-quark production (Wt and t-channel) was generated using POWHEG-BOX v1+PYTHIA 6.428 [57–59] and the Perugia2012 set of tuned parameters for parton showering and the CT10 NLO PDF set. The $t\bar{t} + V$ ($V = W, Z$) and $t\bar{t} + H$ background was modeled using MADGRAPH5_aMC@NLO v2.3.2 [60] as the generator in LO precision with up to two additional partons and in NLO precision, respectively. The parton showering and fragmentation is performed using PYTHIA 8.210 [47] (PYTHIA 8.186) for $t\bar{t} + Z$ and $t\bar{t} + H$ ($t\bar{t} + W$). The contribution

[3] ATLAS uses a right-handed coordinate system with its origin at the nominal interaction point (IP) in the center of the detector and the z axis along the beam pipe. The x axis points from the IP to the center of the LHC ring, and the y axis points upwards. Cylindrical coordinates (r, ϕ) are used in the transverse plane, ϕ being the azimuthal angle around the z axis. The pseudorapidity is defined in terms of the polar angle θ as $\eta = -\ln\tan(\theta/2)$. Angular distance is measured in units of $\Delta R \equiv \sqrt{(\Delta\eta)^2 + (\Delta\phi)^2}$.

from single-top-quark and $t\bar{t}+\mathrm{X}$ events is less than 6% in all signal regions.

Finally, although a data-driven method is used to estimate the multijet background, a sample of simulated multijet events is used for the training of an algorithm employed to identify boosted objects (Sec. IV). The simulated multijet events were produced with PYTHIA 8.186 using the A14 set of tuned parameters for the underlying event and the NNPDF2.3 LO PDFs. The renormalization and factorization scales were set to the average transverse momentum (p_{T}) of the two leading jets.

IV. OBJECT DEFINITIONS

The main objects used in this search are small-radius (small-R) jets reconstructed from clusters of energy deposited in the calorimeter. A variable-radius reclustering algorithm [61,62] is then used to find groups of small-R jets that are consistent with the hadronic decays of high-momentum bosons and top quarks. To ensure orthogonality with ATLAS VLQ searches that include leptons [27–30,37], events containing electrons or muons with $p_{\mathrm{T}} > 20$ GeV are vetoed using the same tight object definitions as in those searches. For a given reconstructed event, the missing transverse momentum, with magnitude $E_{\mathrm{T}}^{\mathrm{miss}}$, is calculated from the negative vector sum of the p_{T} of all reconstructed jets, and any reconstructed electrons and muons. A soft energy term is included to account for nonreconstructed particles originating from the hard scatter. It is calculated using only charged tracks matched to the primary vertex to reduce contamination from particles originating from other pp interactions in the same or nearby bunch crossings (pileup) [63].

Small-R jets are reconstructed from calibrated topological energy clusters in the calorimeter using the anti-k_t algorithm [64,65] with a radius parameter of 0.4. They are required to have $p_{\mathrm{T}} > 25$ GeV and $|\eta| < 2.5$. Low-p_{T} jets produced in pileup interactions are suppressed using the jet vertex tagger (JVT) algorithm [66]. A jet is removed from the event if it has $p_{\mathrm{T}} < 60$ GeV, $|\eta| < 2.4$, and a JVT value lower than 0.59. This requirement on the JVT value has an efficiency of 92% for jets of $p_{\mathrm{T}} < 60$ GeV and $|\eta| < 2.4$ originating from the primary vertex. In order to avoid misidentification and overlap of objects, a jet is removed from the event if an electron or muon selected with loosened identification criteria is found within $\Delta R = 0.2$ or if a loosely selected muon is found in a jet that is not well matched to the primary vertex, as in Refs. [27,28].

A small-R jet is b-tagged if it satisfies the 77% working point criterion of the MV2c10 ATLAS b-tagging algorithm [67,68]. Working points are defined by a requirement on the output discriminant and are labeled by the b-jet efficiency they give on an inclusive $t\bar{t}$ sample. The 77% working point has rejection factors of 6.2 and 134 for jets containing charm hadrons (c-jets) and jets containing light-quark hadrons or gluons (light jets), respectively. Correction factors are applied to the simulated event samples to correct for differences in the b-tagging efficiencies for b-jets, c-jets, and light-jets between data and simulation. In addition to using b-tagging to select events with the 77% working point, three other working points (60%, 70%, 85%) are used in the context of the boosted-object tagging as described later in this section.

Small-R jets are reclustered [61] using the anti-k_t algorithm with a variable cone size [62] to create variable-radius reclustered jets (vRC jets). Constituent small-R jets are not allowed to be shared by multiple vRC jets. Because the small-R jets used in the reclustering are already calibrated, the vRC jets are also calibrated and their uncertainties are obtained directly from the small-R jet uncertainties [69]. A requirement on a p_{T}-dependent variable radius reduces the overlap of boosted objects in the high-multiplicity final state of this search and exploits the fact that the radius separation R between the decay products of a heavy, high-p_{T} particle of mass m can be approximated with $R \sim 2m/p_{\mathrm{T}}$. The radius parameter threshold is chosen to be $R_{\mathrm{eff}} = \rho/p_{\mathrm{T}}$, with $\rho = 315\,\mathrm{GeV}$, within the restriction of $0.4 \leq R_{\mathrm{eff}} \leq 1.2$. This results in a good compromise between the accuracy and efficiency of the reconstruction for the objects considered in the final state. To reduce contributions from low-energy pileup, a trimming procedure [70] removes small-R jets from a vRC jet if their p_{T} is less than 5% of the vRC jet p_{T}. The vRC jets are required to have mass greater than 40 GeV, $p_{\mathrm{T}} > 150$ GeV, and $|\eta| < 2.5$.

A multiclass deep neural network (DNN) is trained to identify the most likely parent particle of the vRC jets, distinguishing between four categories: V-boson (W- or Z-boson), Higgs-boson, top-quark, and *background* jets. In simulation the label for a reconstructed signal jet (V-boson, Higgs-boson, or top-quark jet) is obtained by matching the vRC jets to a hadronically decaying boson or top quark at generator level within a cone of $\Delta R = 0.75 \cdot \rho/p_{\mathrm{T}}$. For the Higgs boson, only direct decays into quark pairs are considered. All vRC jets matched to multiple generator-level V bosons, Higgs bosons, or top quarks are discarded. The *background* label is given to any vRC jets reconstructed from simulated multijet events. The DNN is trained using the mass, p_{T}, and number of constituent jets of the vRC jet, as well as the four-momentum vectors and b-tagging information of the three highest-p_{T} constituent small-R jets as input.

The KERAS software package [71] is used to build and train the DNN, using the THEANO backend [72]. The DNN has four fully connected hidden layers and a four-dimensional output layer, and is trained using the Adam [73] optimizer algorithm.[4] Hidden layers of the

[4]For an introduction to DNNs and related terminology, see Refs. [74,75].

DNN use batch normalization [76] and rectified-linear-unit activation functions, whereas the output layer uses a sigmoid function. As the performance of the DNN tagger is dependent on the architecture and training hyperparameters, DNNs with different number of layers, learning rate, L1 regularizer, and batch size are tested to define the architecture and training hyperparameters. The p_{T} distribution of the background is reweighted to match the signal distribution. In this way the DNN is prevented from learning the differences between the p_{T} distributions of signal and background jets, while allowing for learning relations between the p_{T} of the vRC jets and other input features. By using only properties of the calibrated small-R jets as input to the tagger, all jet-related systematic uncertainties can be propagated through the DNN by varying the corresponding properties of the small-R jets. To reduce the four-dimensional DNN output information (D_{DNN}), the outputs of the different classes are combined by building a discriminant function.

The discriminant function P for a V boson, Higgs boson, and top quark is given by

$$P(V)=\log_{10}\left(\frac{D^{V}_{\mathrm{DNN}}}{0.9\cdot D^{\mathrm{background}}_{\mathrm{DNN}}+0.05\cdot D^{t}_{\mathrm{DNN}}+0.05\cdot D^{H}_{\mathrm{DNN}}}\right),$$

$$P(H)=\log_{10}\left(\frac{D^{H}_{\mathrm{DNN}}}{0.9\cdot D^{\mathrm{background}}_{\mathrm{DNN}}+0.05\cdot D^{V}_{\mathrm{DNN}}+0.05\cdot D^{t}_{\mathrm{DNN}}}\right),$$

and

$$P(t)=\log_{10}\left(\frac{D^{t}_{\mathrm{DNN}}}{0.9\cdot D^{\mathrm{background}}_{\mathrm{DNN}}+0.05\cdot D^{H}_{\mathrm{DNN}}+0.05\cdot D^{V}_{\mathrm{DNN}}}\right),$$

respectively. The relative weighting factors of 0.9 for background jets and 0.05 for V-boson, Higgs-boson, or top-quark jets are chosen as a compromise between background rejection and the ability to discriminate amongst signal sources. For each signal discriminant P, an optimized working point is defined to obtain a boosted-object tagger with a specified signal efficiency. The discriminant functions and the corresponding thresholds for these working points are shown in Fig. 1, where $|\eta|$, p_{T}, and m refer to the pseudorapidity, transverse momentum, and mass of the vRC jet. The multipeak behavior in some of the discriminant functions is a result of differences in important vRC jet properties used as input to the DNN, such as the mass, number of constituent small-R jets, and whether the constituent small-R jets are b-tagged. These properties relate to, e.g., whether or not all of the decay products of the V boson, Higgs boson, or top quark are fully contained within the vRC jet. For example, the double-peak structure in the distribution of Higgs-boson jets in Fig. 1(c) arises predominantly from whether the vRC jet contains the two expected subjets from the Higgs-boson decay or if it contains additional hadronic energy.

The V- and Higgs-boson taggers use 70% working points, which correspond to the thresholds $P(V) > -0.2$ and $P(H) > 0.35$. The top-quark tagger operates at a 60% working point using a threshold of $P(t) > 0.1$. The resulting signal efficiency and background rejection (estimated from simulated multijet events) for each boosted-object tagger is shown as a function of p_{T} in Fig. 2.

To handle the ambiguities due to multiple-tagged vRC jets, additional discriminant functions, shown in Fig. 3, are defined. Optimized thresholds, shown in each subfigure, are chosen to resolve double-tagged vRC jets. Higgs bosons are more frequently triple-tagged than V bosons or top quarks, so triple-tagged vRC jets are tagged as a Higgs boson. The vRC jets that are tagged as a V boson, top quark, or Higgs boson are referred to as V-tagged, top-tagged, and Higgs-tagged, respectively.

The shape of the vRC jet mass distribution before and after the final boosted-object tagging is shown in Fig. 4 for each jet type. As expected, each tagger preferentially selects vRC jets with a mass near the mass of the desired particle. For the top quarks, vRC jets with a mass near the W-boson mass are generally V-tagged (dominant at low p_{T}) and Higgs-tagged.

V. ANALYSIS STRATEGY

The search presented in this paper focuses on all-hadronic final states with small $E_{\mathrm{T}}^{\mathrm{miss}}$, which allows it to be sensitive to all possible final states involving hadronic decays of W, Z, and Higgs bosons and top quarks. The key aspect of this search is to suppress multijet background and accurately model multijet events that satisfy the selection criteria. As a first step, the multijet background is reduced by requiring multiple high-p_{T} and b-tagged small-R jets. As a second step, events are rejected if they do not contain vRC jets that originate from either a V boson, Higgs boson, or top quark as identified using the DNN boosted-object tagger. Events are then categorized according to the numbers of V-tagged, Higgs-tagged, and top-tagged vRC jets and of b-tagged small-R jets and are divided into 12 nonoverlapping signal regions, in order to be sensitive to all possible VLQ decays. Finally, multijet events are distinguished from signal events by calculating, for each signal region, a signal probability using the matrix element method [77]. This signal probability is then used in a binned profile-likelihood fit in order to extract the signal strength and improve the background modeling. The multijet background is estimated in each signal region using a bin-by-bin "ABCD" method, which is described in Sec. V C. The analysis strategy is optimized while assuming pair production of VLQs and considering all possible fully hadronic decay modes.

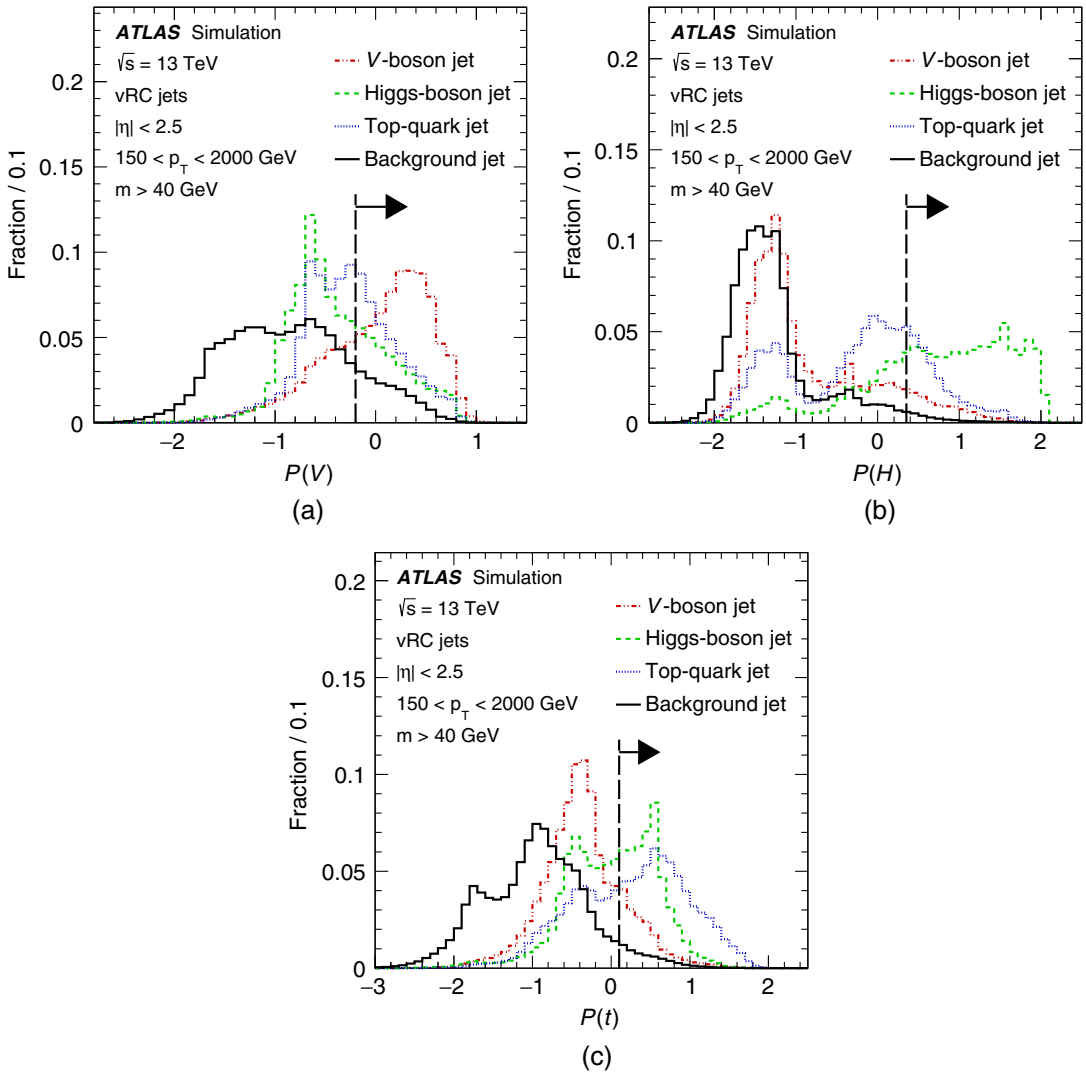

FIG. 1. The discriminant function P for the (a) V-tagger, (b) Higgs-tagger, and (c) top-tagger. Signal jets (V-boson, Higgs-boson, top-quark jets) are defined by matching the vRC jet to the corresponding object at generator level. The distributions are made by merging all simulated VLQ samples. Background jets are taken from simulated multijet events. The object selection applied to the vRC jets is shown on the left side of the figures. The dashed vertical line represents the applied tagging selection.

A. Event selection and classification

Data were collected using a combined trigger that requires a single jet with $p_{\mathrm{T}} > 100$ GeV at the first trigger level and a total scalar sum of the transverse momenta of all track particles and energy deposits $H_{\mathrm{T}} > 1000$ GeV at the high-level trigger. An offline threshold of $H_{\mathrm{T}} > 1250$ GeV ensures that this trigger is fully efficient. Events are required to have exactly zero leptons and $E_{\mathrm{T}}^{\mathrm{miss}} < 200$ GeV to remove background and maximize the significance of the signal. Events enter the signal regions if they contain at least four selected small-R jets with descending p_{T} thresholds of 300, 200, 125, and 75 GeV and at least two small-R jets that are b-tagged, where individual jets can satisfy one or both criteria. In addition, the events must have at least two vRC jets tagged as a V or Higgs boson and satisfy $E_{\mathrm{T}}^{\mathrm{miss}} > 40$ GeV. The $E_{\mathrm{T}}^{\mathrm{miss}}$ requirement rejects significantly more background than signal. For example, the $E_{\mathrm{T}}^{\mathrm{miss}}$ requirement is 71%–82% efficient for the various decay modes of a signal with a mass of $m_{VLQ} = 1$ TeV, but only 55% efficient for simulated multijet background events. Sources of $E_{\mathrm{T}}^{\mathrm{miss}}$ in VLQ pair production can include true sources, such as $Z \to \nu\nu$ decays or leptonic decays of W bosons and top quarks with a soft or misreconstructed lepton, as well as $E_{\mathrm{T}}^{\mathrm{miss}}$ from mismeasurement of high-energy jets.

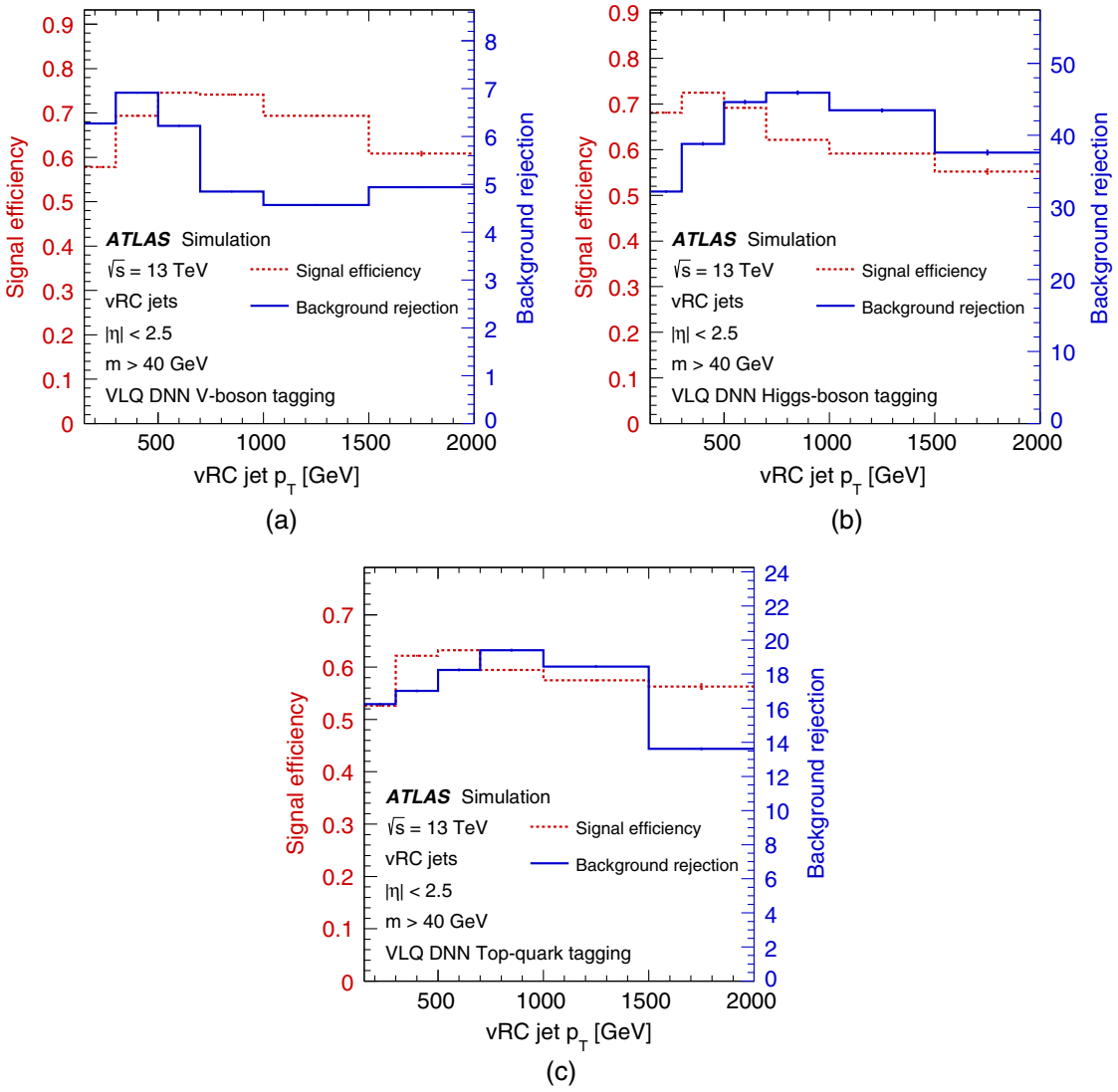

FIG. 2. The signal efficiency (dashed) and background rejection (solid) as a function of vRC jet p_T for the DNN VLQ (a) V-tagger, (b) Higgs-tagger, and (c) top-tagger. The dashed lines refer to the left y-axis scale, and the solid lines refer to the right. Signal jets (V-boson, Higgs-boson, top-quark jets) are defined by matching the vRC jet to the corresponding object at generator level. The distributions are made by merging all simulated VLQ samples. Background jets are taken from simulated multijet events. Statistical uncertainties are shown for signal and background.

The events are then classified into 12 different signal regions based on the number of V- and Higgs-tags (VV, VH, HH), top-tags (0, 1, ≥2), and b-tags (2, ≥3), as shown in Table I. The regions are designed to cover all of the possible VLQ decays and enhance the ratio of signal events to SM background events. Figure 5 shows the fraction of events from each background source that contributes to each signal region after the full event selection and the background-only fit to data described in Sec. VII. In addition to the signal regions, nine validation regions are also defined in order to validate the multijet background estimation and evaluate a closure uncertainty for the method. The two regions that are used to validate the multijet background estimation are defined to have exactly two b-tagged jets, two Higgs-tags, and no top-tags. The seven regions that are used to evaluate the closure uncertainty require exactly one b-tagged jet and the same number of V-, Higgs-, and top-tags as in each of the signal regions.

B. Matrix element method

The matrix element method [77] has been utilized for measurements [78–80] and searches for SM physics processes [81–87]. This analysis applies the method to a search for physics beyond the SM. This method requires the calculation of an event-based probability density function $P_i(\boldsymbol{x}|\boldsymbol{\alpha})$ for a given physics process i described

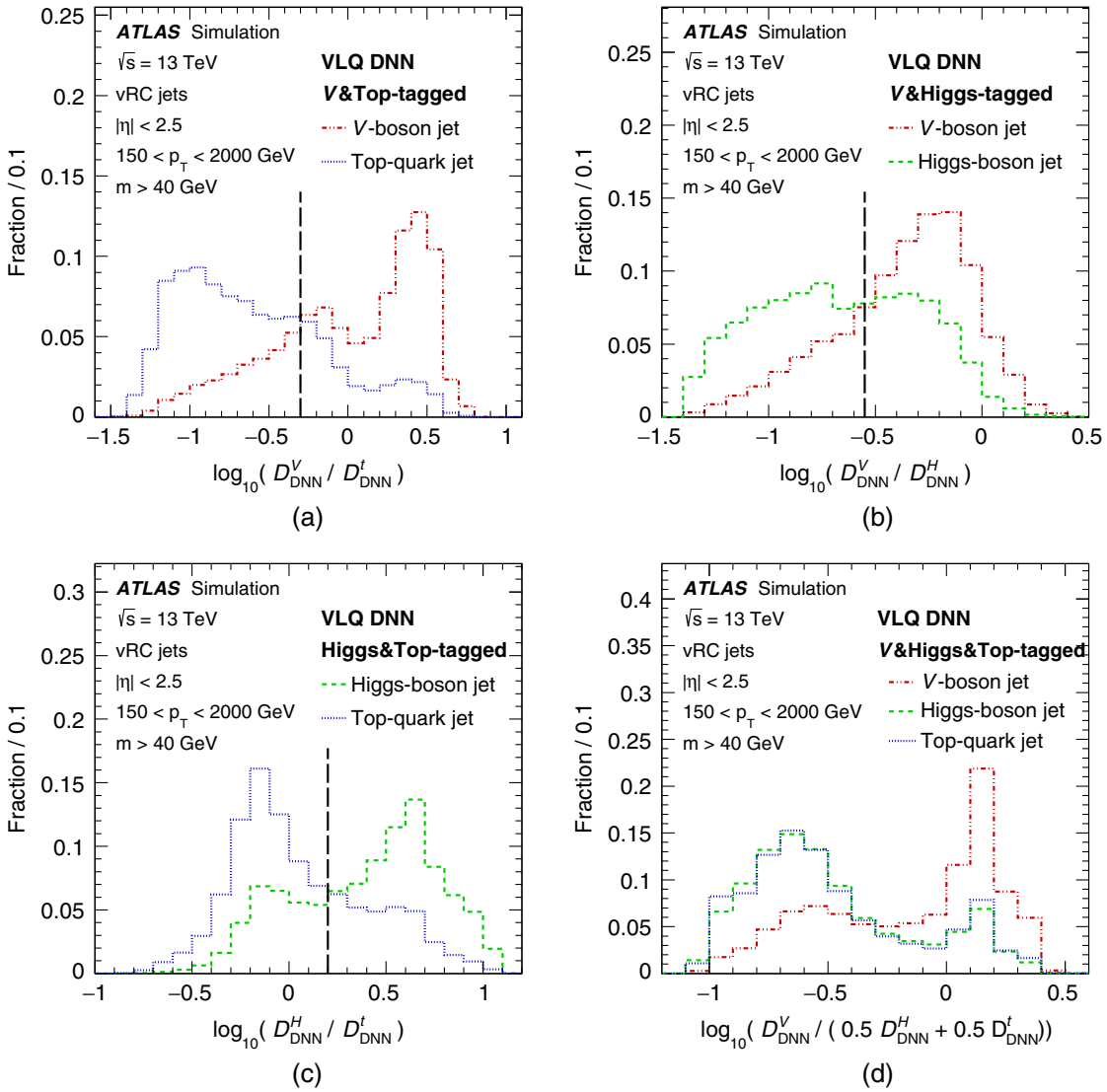

FIG. 3. The additional discriminant functions defined to resolve multiple-tagged vRC jets such as (a) DNN VLQ V- and top-tagged, (b) DNN VLQ V- and Higgs-tagged, (c) DNN VLQ Higgs- and top-tagged, and (d) DNN VLQ V-, Higgs-, and top-tagged. Signal (V-boson, Higgs-boson, top-quark) jets are defined by matching the vRC jet to the corresponding object at generator level. The distributions are made by merging all simulated VLQ samples. The dashed vertical line represents the applied selection.

by the matrix element of the process and a set of theoretical and experimental parameters α:

$$P_i(\boldsymbol{x}|\boldsymbol{\alpha}) = \frac{(2\pi)^4}{\sigma_i^{\text{eff}}(\boldsymbol{\alpha})} \int d\Phi_N(\boldsymbol{y}) \boldsymbol{f}(p_{\text{A}}) \boldsymbol{f}(p_{\text{B}}) \times \frac{|\mathcal{M}_i(\boldsymbol{y}|\boldsymbol{\alpha})|^2}{\mathcal{F}} W(\boldsymbol{y}|\boldsymbol{x}).$$

The numerical integration is performed over the phase space of the initial- and final-state particles and can be time consuming. In this equation, $\boldsymbol{x}$ and $\boldsymbol{y}$ represent the four-momentum vectors of all initial- and final-state particles at reconstruction and parton level, respectively. The Lorentz-invariant flux factor[5] $\mathcal{F}$ and phase-space element $d\Phi_N$ describe the kinematics of the process. The transition matrix element $\mathcal{M}_i$ is defined by the Feynman diagrams of the hard-scattering process. The functions $\boldsymbol{f}(p_{\text{A}})$ and $\boldsymbol{f}(p_{\text{B}})$ are the PDFs for the initial-state partons with momenta p_{A} and p_{B}. The transfer functions $W(\boldsymbol{y}|\boldsymbol{x})$ map the detector quantities $\boldsymbol{x}$ to the parton-level quantities $\boldsymbol{y}$. Finally, the effective cross section σ_i^{eff} normalizes P_i to unity taking acceptance and efficiency into account.

The reconstructed objects in an event can be combined to form multiple candidate VLQ final states. The process

[5] $\mathcal{F} = 4\sqrt{(p_{\text{A}}p_{\text{B}})^2 - m_{\text{A}}^2 m_{\text{B}}^2}$.

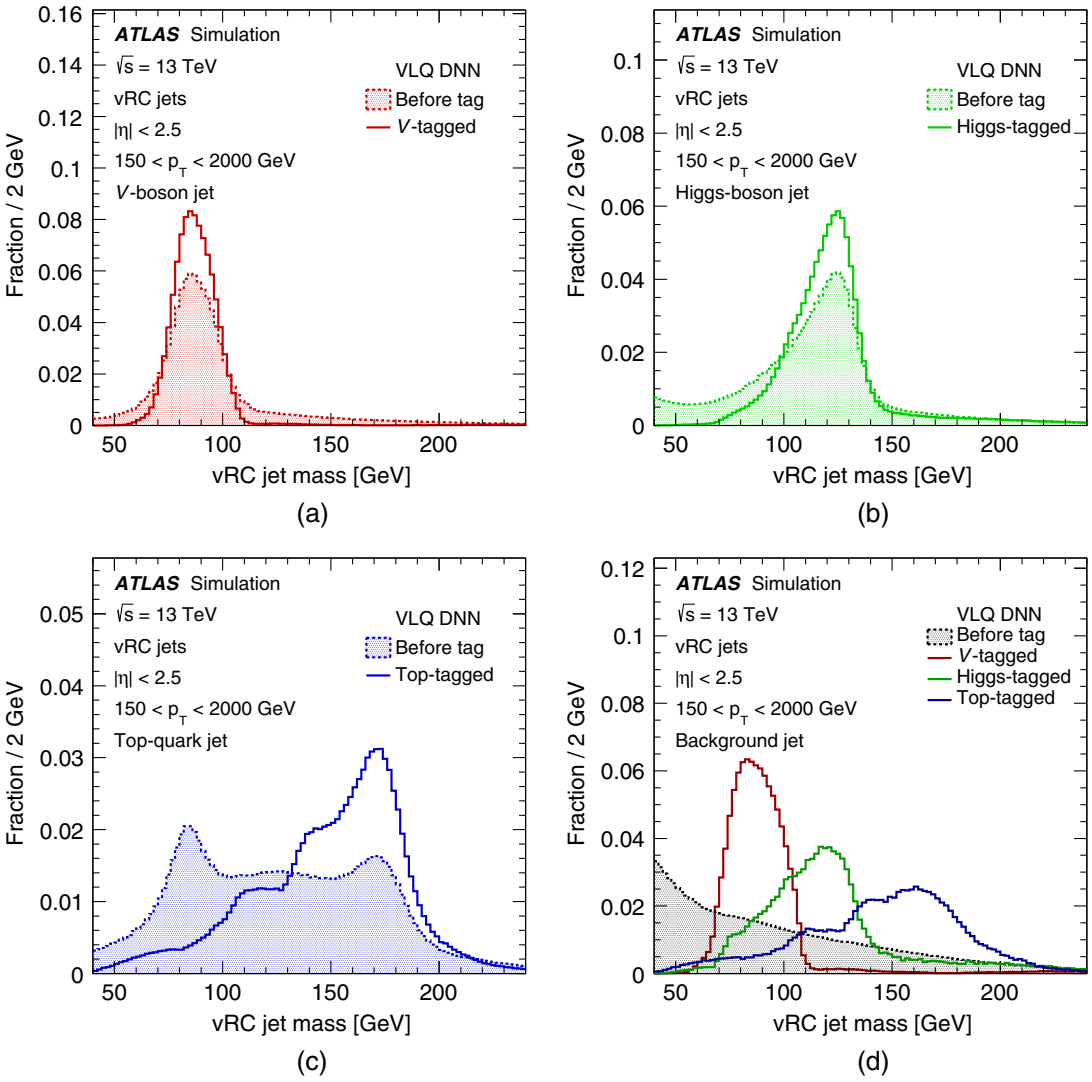

FIG. 4. The mass distribution of (a) V-boson jets, (b) Higgs-boson jets, (c) top-quark jets, and (d) background jets are shown before and after the final DNN VLQ boosted-object tagging. Signal (V-boson, Higgs-boson, top-quark) jets are defined by matching the vRC jet to the corresponding object at generator level. The distributions are made by merging all simulated VLQ samples. Background jets are taken from simulated multijet events. For signal jets, only the impact of the correct tag is shown, while for background jets the impact of each boosted-object tag is shown. All distributions are normalized to unit integral.

probability density is calculated for each allowed assignment permutation of the jets to the final-state quarks and bosons. A process likelihood function is then built by summing the process probabilities of each allowed assignment permutation. The vRC jets are assigned to final states according to their DNN VLQ boosted-object-tag label (V-tagged, Higgs-tagged, or top-tagged) and are permuted if they have the same label. If more than two vRC jets are tagged as a boson (V-tagged or Higgs-tagged), only the two with the highest transverse momenta are used. If b-quarks occur in the hypothesized final state, up to five different b-tagged small-R jets are assigned to the final state and freely permuted. These b-tagged jets are allowed to overlap with the vRC jets and could have been used already in the reconstruction of the vRC jet.

The transition matrix element defines the hypothesis being tested and is calculated using MadGraph5 in LO precision. The VLQ pair-production matrix element calculation is performed using the Feynrules [88] model as defined in Ref. [19]. In this analysis, only probabilities of signal hypotheses are calculated, since the dominant background is from multijet processes, for which it is difficult to define a model in the matrix element method. The second most important $t\bar{t}$ + jets background was studied as a background hypothesis, but its inclusion does not improve the sensitivity of the search. Top quarks, V bosons, and Higgs bosons are assumed to be reconstructed as vRC jets and are hence not decayed in the matrix element calculation.

In each signal region, the signal hypothesis is computed from all Feynman diagrams of vectorlike T or B pair

TABLE I. Summary of the definition of the 12 signal regions in the analysis. The number of b-tags is based on all small-R jets, including those used to construct vRC jets with V-, Higgs-, or top-tags. The last two signal regions require two bosons of any type X (V or Higgs boson). The rightmost column lists the matrix element method (MEM) final states used to define the signal hypothesis in Sec. V B.

Region name	V-tags	H-tags	Top-tags	b-tags	MEM final states
(VV, 0t, 2b)	2	0	0	2	WbWb, ZbZb
(VV, 0t, 3b)	2	0	0	≥3	WbWb, ZbZb
(VV, 1t, 2b)	2	0	1	2	ZtWb, WtZb
(VV, 1t, 3b)	2	0	1	≥3	ZtWb, WtZb
(VH, 0t, 2b)	1	1	0	2	WbWb, ZbZb
(VH, 0t, 3b)	1	1	0	≥3	WbWb, ZbZb
(VH, 1t, 2b)	1	1	1	2	HtWb, WtHb
(VH, 1t, 3b)	1	1	1	≥3	HtWb, WtHb
(HH, 0t, 3b)	0	2	0	≥3	HbHb
(HH, 1t, 3b)	0	2	1	≥3	HtWb, WtHb
(XX, 2t, 2b)	≥0	≥0	≥2	2	HtHt, ZtZt, WtWt, HtZt
(XX, 2t, 3b)	≥0	≥0	≥2	≥3	HtHt, ZtZt, WtWt, HtZt

production resulting in the same number of top quarks, V bosons, and Higgs bosons as defined in Table I. Following the definition of the signal regions (XX, 2t, 2b) and (XX, 2t, 3b), all Feynman diagrams resulting in final states with two top quarks are used and no distinction is made based on the number of V and Higgs bosons. Combining these diagrams into a single hypothesis increases the performance significantly and allows mistags of the V and Higgs bosons. Because there is no direct decay of VLQs into a final state with two Higgs bosons and one top quark, the same diagrams as used for the (VH, 1t, 2b) and (VH, 1t, 3b) signal regions are used in the (HH, 1t, 3b) region taking mistags into account. Preliminary studies indicated that this analysis would be sensitive to VLQ masses around 900 GeV; therefore, in the calculation of the matrix elements, the masses of the vectorlike B and T

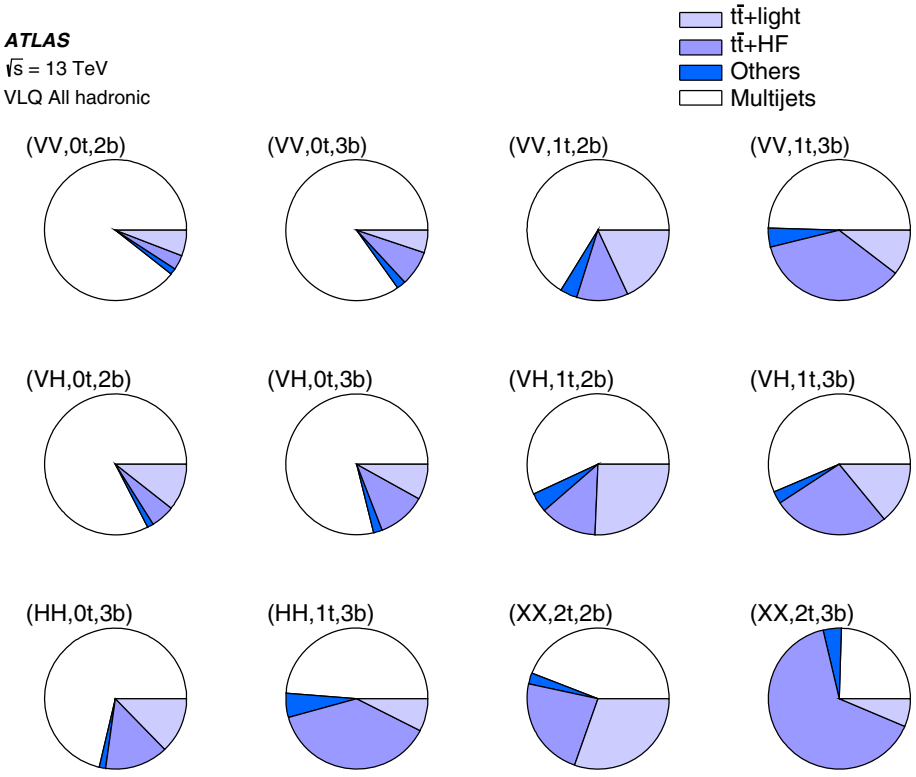

FIG. 5. Relative size of all background contributions in each signal region after the background-only fit to data described in Sec. VII. "Others" refers to backgrounds from single-top-quark and $t\bar{t}+\mathrm{X}$ production.

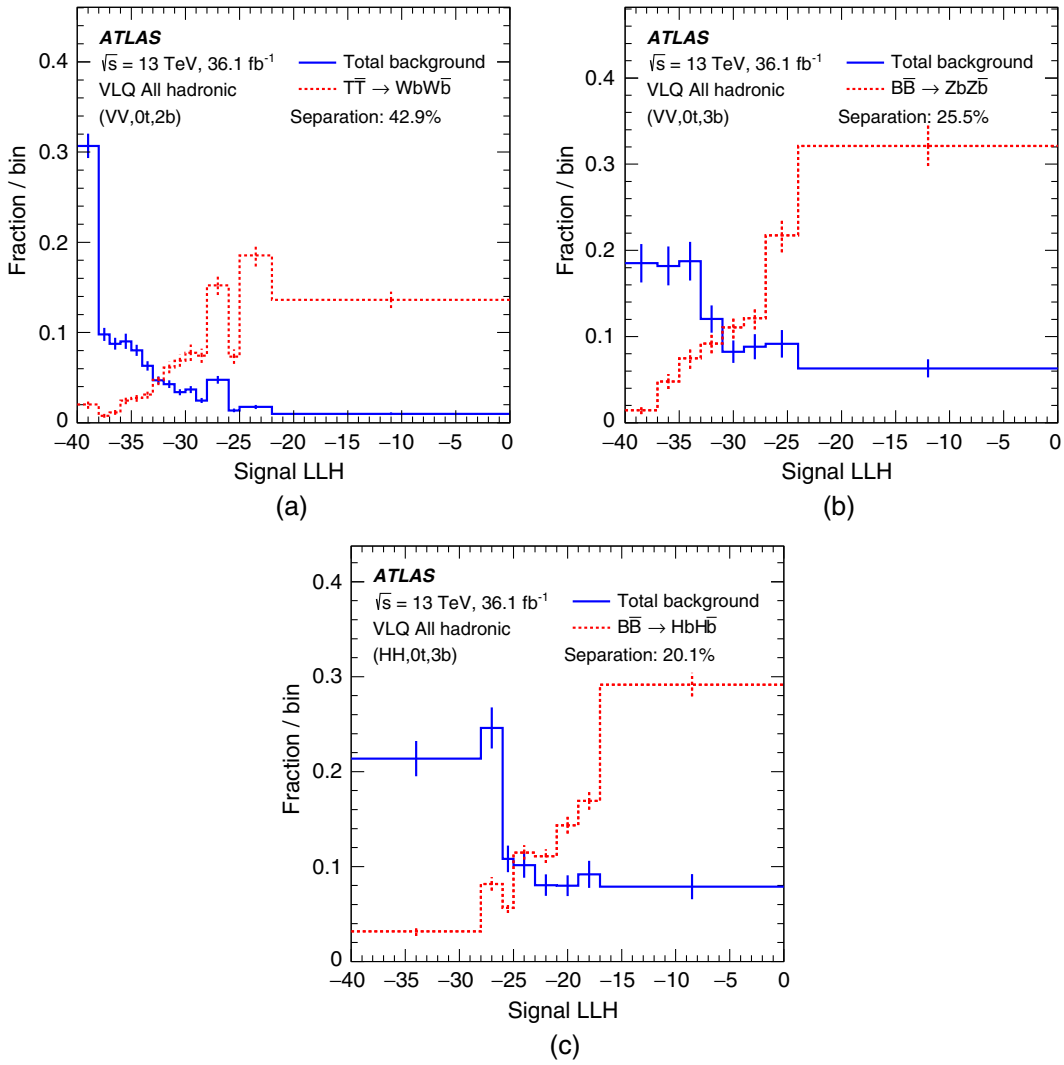

FIG. 6. The normalized signal LLH distributions of the total background and vectorlike $T\bar{T}$ and $B\bar{B}$ production ($m_{T/B} = 1$ TeV) assuming exclusive (a) $T \to Wb$, (b) $B \to Zb$, and (c) $B \to Hb$ decays are shown for the regions with the highest signal significance (VV, 0t, 2b), (VV, 0t, 3b), and (HH, 0t, 3b). The separation is defined by the formula in Eq. (1).

quarks are set to 900 GeV. The analysis sensitivity becomes slightly degraded when considering signal samples with a significantly higher VLQ mass.

The transfer functions are parametrized as single-Gaussian functions, which is a good compromise between separation power and reasonable integration time. For the modeling of the parton distribution functions, the CTEQ6L1 set from the LHAPDF package [89] is used. The integration is performed using VEGAS [90]. Due to the complexity and high dimensionality, adaptive MC techniques [91], simplifications, and approximations are needed in order to perform the integration in a reasonable time. The matrix element calculation is accelerated by evaluating only the most significant helicity states, which are identified at the beginning of each integration. The dimensionality of the integration is reduced by assuming that the final-state object directions in η and ϕ are measured with negligible uncertainty. The total momentum conservation and the negligible transverse momentum of the initial-state partons allow further reduction. No change of integration variables is performed in order to allow a general treatment of all signal regions. The integration variables are the energies of the top quarks, b-quarks, V, and Higgs bosons according to their numbers as defined for each region. The total integration volume is restricted by requiring the difference between the parton-level quantities and the observed values to be within five standard deviations of the width of the transfer functions. Finally, the likelihood contributions of all allowed assignment permutations are coarsely integrated and sorted by their contribution, then the full integration is performed with a decreasing precision. The logarithm of the resulting signal likelihoods (signal LLH) is used in each signal region as the final discriminating variable. Normalized distributions of the signal LLH for the total background and signal simulations in the most sensitive signal regions

assuming exclusive $T \to Wb$, $B \to Zb$, and $B \to Hb$ decays are shown as examples in Fig. 6. The binning in the signal LLH distribution is the same as that shown for the corresponding regions in Figs. 10–12. The separation given in Fig. 6 between signal and background is defined by the formula

$$\frac{1}{2}\int \frac{(S(x)-B(x))^2}{S(x)+B(x)}dx \tag{1}$$

where $S(x)$ and $B(x)$ are the signal and background yields per bin and S and B are normalized to unity.

C. Background estimation

The dominant multijet background is estimated using a data-driven double sideband method ('ABCD'). This method relies on three control regions (A, B, and C), defined by inverting two uncorrelated selection requirements, in order to predict the contribution of a background in a signal region (D). The two selection requirements of this method are applied on $E_{\mathrm{T}}^{\mathrm{miss}}$ and boson tagging. In order to invert the boson tagging, a 'loose-tagged' boson selection is defined. In contrast to the VLQ DNN tagger, this selection consists of a simple mass window for the vRC jet of 69–104 GeV for V bosons and 104–155 GeV for Higgs bosons. The regions used in the method are then defined as follows:

(1) Region A: ≥ 2 vRC jets that are V-tagged or Higgs-tagged or "loose-tagged') and < 2 vRC jets that are V-tagged or Higgs-tagged and $E_{\mathrm{T}}^{\mathrm{miss}} < 40$ GeV;
(2) Region B: ≥ 2 vRC jets that are V-tagged or Higgs-tagged and $E_{\mathrm{T}}^{\mathrm{miss}} < 40$ GeV;
(3) Region C: ≥ 2 vRC jets that are V-tagged or Higgs-tagged or loose-tagged and < 2 vRC jets that are V-tagged or Higgs-tagged and $E_{\mathrm{T}}^{\mathrm{miss}} \geq 40$ GeV; and
(4) Region D: "Signal region," ≥ 2 vRC jets that are V-tagged or Higgs-tagged and $E_{\mathrm{T}}^{\mathrm{miss}} \geq 40$ GeV.

The four regions are orthogonal and there is no significant correlation between boson tagging and $E_{\mathrm{T}}^{\mathrm{miss}}$. The level of correlation is evaluated by checking the correlation factor between the two variables in simulated multijet events, which is found to be consistent with zero.

In the control regions A, B, and C, the nonmultijet contributions are subtracted from the data using simulation. The relationship between the yields, N, in the signal region, D, and the control regions is given by $N_{\mathrm{D}} = N_{\mathrm{C}} \times (N_{\mathrm{B}}/N_{\mathrm{A}})$. This simple scaling is performed on a bin-by-bin basis in the signal LLH distribution to produce the expected multijet shape and normalization in the signal region. This procedure is followed separately for each of the 12 signal regions. Seven validation regions are also defined, with the same V-, Higgs-, and top-tagging requirements as the signal regions, but with exactly one b-tagged jet. These regions are used to evaluate a closure uncertainty, described in Sec. VI. Two examples of these validation regions can be seen in Fig. 7, where the only uncertainties taken into account are those from statistical sources and related to the detector simulation.

The binning that is used for each region is determined by the number of events in the A, B, and C control regions. It is

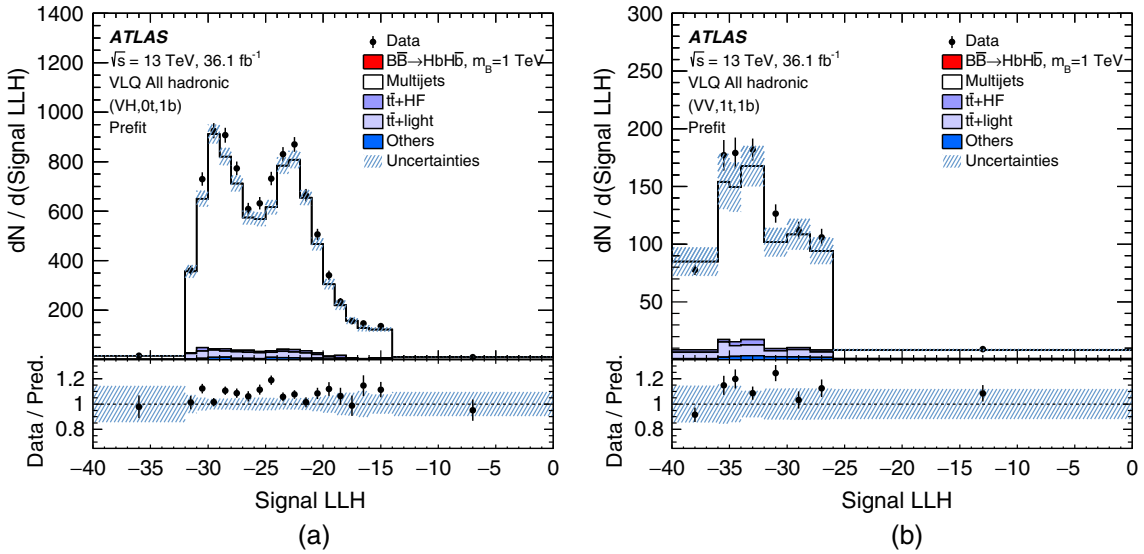

FIG. 7. Comparison between data and prediction for the signal LLH in the validation regions with two boson-tagged vRC jets, exactly one b-tagged small-R jet, and either (a) zero top-tagged vRC jets or (b) exactly one top-tagged vRC jet. The distributions show the number of events per width of 1.0 in the x axis. The hatched area represents the statistical and detector-related uncertainties of the background, added in quadrature. The deviation of the prediction from data is taken as the multijet closure uncertainty. The underflow and overflow are included in the first and last bins, respectively. These figures do not include any information from the fit described in Sec. VII, and are therefore described as "Prefit."

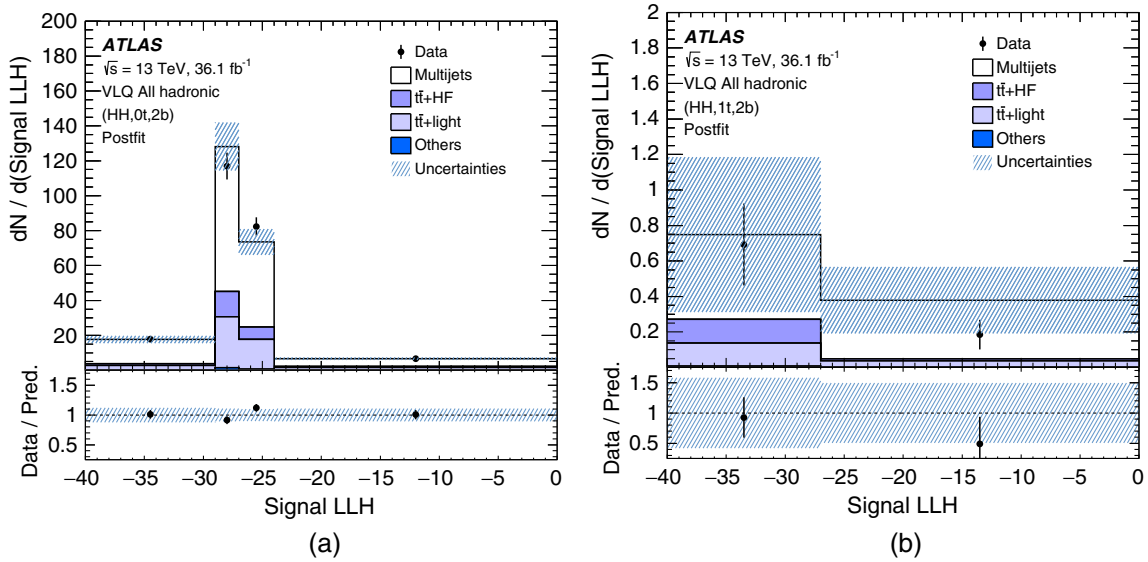

FIG. 8. Comparison between data and prediction for the signal LLH in the validation regions with two Higgs-tagged vRC jets, exactly two b-tagged small-R jets, and either (a) zero top-tagged vRC jets, or (b) exactly one top-tagged vRC jet. The distributions show the number of events per width of 1.0 in the x axis. The hatched area represents the uncertainty on the background from statistical uncertainty and all sources of systematic uncertainty described in Sec. VI. The background and uncertainty take into account the constraints, pulls and correlations of the background-only fit to data of the signal regions, described in Sec. VII, and are therefore described as "Postfit." The underflow and overflow are included in the first and last bins, respectively.

required that there are a sufficient number of events in each bin of the control regions (at least 50) to produce a sufficiently smooth distribution.

To evaluate the performance of the background estimation method with all uncertainties, two regions kinematically close to the signal regions, but with very low expected signal contribution, are also defined. These regions have two Higgs-tagged vRC jets, exactly two b-tagged small-R jets, and either zero or one top-tagged vRC jet. Good agreement is observed in these regions, as shown in Fig. 8.

Standard Model backgrounds from $t\bar{t}$, single-top-quark, and $t\bar{t}+\mathrm{X}$ processes are estimated with simulated events, described in Sec. III. The normalization and shape are taken directly from simulation for all of these processes.

VI. SYSTEMATIC UNCERTAINTIES

The systematic uncertainties considered in this analysis arise from uncertainties in the treatment of the luminosity, object reconstruction and background modeling. Each source of uncertainty is treated as a nuisance parameter in the final likelihood fit, as described in Sec. VII. Different sources of uncertainty are assumed to be uncorrelated; however, a given uncertainty is assumed to be 100% correlated across all regions and samples. For each source of systematic uncertainty, the effect on the analysis is evaluated by propagating a $\pm 1\sigma$ variation of the quantity in question.

A. Luminosity and pileup

The uncertainty in the integrated luminosity of the 2015 and 2016 data set is 2.1%. It is derived, following a methodology similar to that detailed in Ref. [92], from a calibration of the luminosity scale using x-y beam-separation scans performed in August 2015 and May 2016. Because MC events are simulated with different pileup conditions than observed in data, the events are corrected to have the same pileup distributions as the data and an uncertainty is assigned to account for the uncertainty in the ratio of the predicted and measured inelastic proton-proton cross section [93].

B. Reconstructed objects

Several systematic uncertainties in the simulated background and the signal predictions arise from the reconstruction and identification of the selected reconstructed objects, as described in Sec. IV, due to the determination of correction factors applied to compensate for differences between data and predictions. The most important sources in this category are the uncertainties associated with jets, missing transverse momentum, and flavor tagging. Other sources, such as lepton reconstruction (affecting the lepton veto), are also considered, but have a negligible impact on the results. The impact on both shape and normalization is taken into account for the following uncertainties.

1. Jets

In case of the small-R jet selection, uncertainties arise from the jet reconstruction, the jet energy and mass scale calibrations, the JVT requirement, and corrections to the jet energy and mass resolutions. The most significant uncertainties associated with small-R jets are from energy scale and energy resolution. The energy scale is determined using the transverse momentum balance between a jet and a reference object such as a photon, Z boson, or another jet [94]. The uncertainty in the energy scale ranges from less than 1% to around 5% for $|\eta| < 0.8$ and p_{T} up to 500 GeV. Jets with higher $|\eta|$ have an additional uncertainty of up to 2%. The jet energy resolution is measured by studying dijet events in data and simulation [95]. The jet energy resolution in data and simulation are found to agree within 10% and the differences are used to determine the relative systematic uncertainties, which range from 10% to 20%. Additional uncertainties are considered for the jet mass scale and mass resolution, but are found to have little impact on the search sensitivity. The uncertainties associated with vRC jets are inherited from the small-R jet uncertainties.

2. Missing transverse momentum

The $E_{\mathrm{T}}^{\mathrm{miss}}$ is sensitive to changes in the momenta of the reconstructed objects, namely the small-R jets, as well as the additional soft term that accounts for low-energy deposits not associated with a reconstructed object. Uncertainties from the reconstructed objects are already accounted for. A soft-term uncertainty is assigned to account for variations in the modeling of the underlying event that change the amount of unclustered energy. The uncertainties in the yields are in the range 0.0%–18.7% for simulated samples and 0.0%–8.2% for the multijet background.

3. Flavor tagging

Uncertainties in the correction factors for the b-tagging identification response are obtained by comparing the simulated event samples with dedicated flavor-enriched samples in data [67]. An additional term is included to extrapolate the measured uncertainties to the high-p_{T} region of interest. This term is calculated from simulated events by considering variations of the quantities affecting the b-tagging performance such as the impact parameter resolution, percentage of poorly measured tracks, description of the detector material, and track multiplicity per jet. The dominant effect on the uncertainty when extrapolating to high p_{T} is related to the different tagging efficiency when smearing the track impact parameters based on the resolution measured in data and simulation.

Most of the vRC jet-tagger flavor-tagging uncertainties can be derived by propagating the small-R jet uncertainties through the DNN. An additional uncertainty associated with b-tagging is evaluated to take into account the use of b-tagging information in the vRC jet-tagger. This is a p_{T}-dependent uncertainty in the vRC jet-tagging efficiency, considered separately for V-boson, Higgs-boson, and top-quark tagging. This uncertainty in the yields ranges from 4.0% to 11.9% for simulated samples and from 0.3% to 9.4% for the multijet background.

C. Background modeling

A theory cross-section uncertainty of 5.3% is taken for the combined small backgrounds, which are dominated by single-top-quark processes [96].

1. Multijet estimation

The dominant multijet background is estimated using a data-driven ABCD technique, as described in Sec. V C.

TABLE II. Event yields in all 12 signal regions after the fit to data under the background-only hypothesis, as well as the predicted signal event yields before the fit for a B VLQ with a mass of 1 TeV. The contribution labeled "Others" is the combination of single-top-quark and $t\bar{t}+\mathrm{X}$ backgrounds. The uncertainties include statistical and systematic uncertainties. The uncertainties of the individual background components can be larger than the uncertainty on the sum of the backgrounds due to correlations.

						$m_B = 1$ TeV	$m_T = 1$ TeV	
Region	Multijet	$t\bar{t}+$ light	$t\bar{t}+$ HF	Others	Total background	$\mathcal{B}(B \to Hb) = 1$	$\mathcal{B}(T \to Ht) = 1$	Data
(VV, 0t, 2b)	5890 ± 190	380 ± 170	230 ± 90	92 ± 12	6590 ± 110	8.0 ± 1.0	3.5 ± 0.5	6614
(VV, 0t, 3b)	1300 ± 60	80 ± 40	130 ± 60	31 ± 8	1540 ± 40	11.5 ± 1.0	3.8 ± 0.6	1534
(VV, 1t, 2b)	680 ± 80	190 ± 90	130 ± 60	41 ± 11	1040 ± 90	2.2 ± 0.4	11.6 ± 1.4	1044
(VV, 1t, 3b)	190 ± 40	40 ± 26	130 ± 70	16 ± 5	380 ± 60	3.1 ± 0.4	7.4 ± 1.1	409
(VH, 0t, 2b)	7500 ± 400	1000 ± 500	500 ± 210	129 ± 15	9150 ± 340	23.4 ± 3.1	1.33 ± 0.33	9202
(VH, 0t, 3b)	3010 ± 180	310 ± 140	430 ± 200	76 ± 17	3820 ± 170	70 ± 6	6.2 ± 0.7	3778
(VH, 1t, 2b)	360 ± 60	160 ± 70	80 ± 40	28 ± 6	640 ± 50	3.9 ± 0.7	6.1 ± 0.8	623
(VH, 1t, 3b)	370 ± 50	100 ± 60	180 ± 80	19 ± 5	660 ± 90	18.2 ± 2.2	37.3 ± 3.3	662
(HH, 0t, 3b)	990 ± 110	180 ± 90	200 ± 100	19 ± 5	1390 ± 110	77 ± 6	38 ± 4	1407
(HH, 1t, 3b)	56 ± 13	8 ± 5	44 ± 24	6.4 ± 1.6	115 ± 16	17.1 ± 2.0	39 ± 4	113
(XX, 2t, 2b)	13 ± 4	8 ± 5	7 ± 5	0.7 ± 0.4	29 ± 7	0.17 ± 0.10	35 ± 4	30
(XX, 2t, 3b)	11 ± 7	3 ± 4	30 ± 19	2.0 ± 0.8	47 ± 21	2.4 ± 0.5	16.1 ± 2.3	51

To quantify a closure uncertainty for this method, the difference between the prediction and data in the one-*b*-tag validation regions is propagated as an overall normalization uncertainty to the corresponding two- and three-*b*-tag signal regions. The impact of including shape information in this uncertainty is negligible. To allow potential differences in performance as a function of jet multiplicity, the uncertainties are taken to be uncorrelated

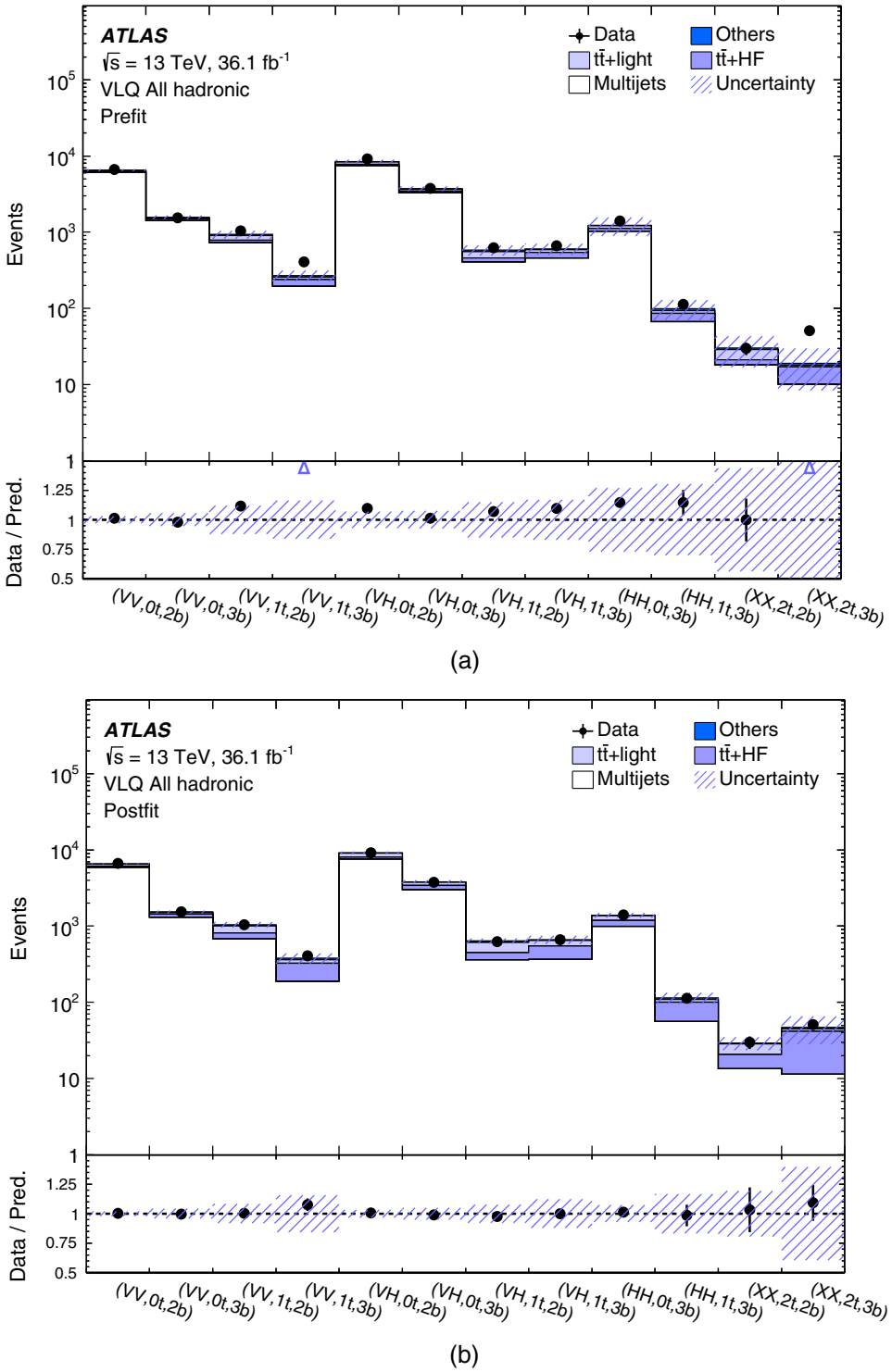

FIG. 9. Comparison between data and prediction for the event yields (a) before and (b) after the fit to the data under the background-only hypothesis. The figures show the total normalization across all signal regions. The contribution labeled "Others" is the combination of single-top-quark and $t\bar{t}+\mathrm{X}$ backgrounds. The hatched area represents the total uncertainty of the background.

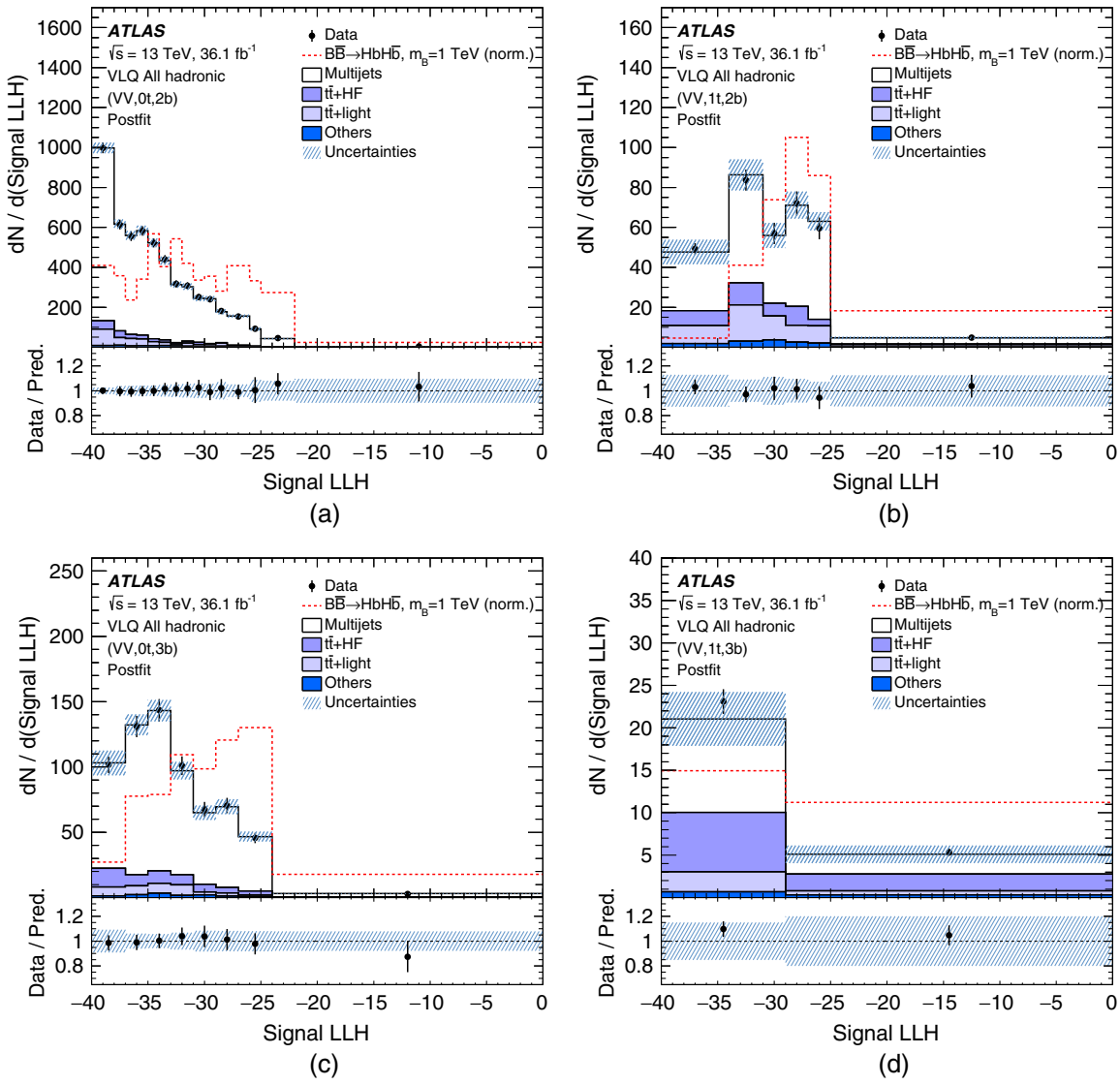

FIG. 10. Comparison between data and prediction for the signal LLH distribution after the fit to the data under the background-only hypothesis for the (a) (VV, 0t, 2b), (b) (VV, 1t, 2b), (c) (VV, 0t, 3b), and (d) (VV, 1t, 3b) signal regions. The contribution labeled "Others" is the combination of single-top-quark and $t\bar{t}+\mathrm{X}$ backgrounds. The distributions show the number of events per width of 1.0 in the x axis. The hatched area represents the total uncertainty of the background. The underflow and overflow are included in the first and last bins, respectively. A hypothetical signal for $\mathcal{B}(B \to Hb) = 100\%$ and $m_B = 1$ TeV is shown overlaid, normalized to the integral of the total background.

between the regions with exactly two b-tags and at least three b-tags.

Another uncertainty is taken from the impact on the multijet prediction of potential signal contamination in the validation regions. Detector-related uncertainties associated with all backgrounds estimated using simulation, as well as modeling uncertainties in $t\bar{t}$ processes, are also propagated through the multijet estimation via subtraction of nonmultijet events in the validation regions. These uncertainties take into account differences in both shape and normalization.

In addition to the systematic uncertainties, each bin of the multijet prediction is assigned an uncertainty to account for statistical uncertainties in the CRs propagated through the ABCD method. Along with the statistical uncertainty of the data in the SR, these tend to have the largest impact on the sensitivity of the analysis.

2. $t\bar{t}$ modeling

For the $t\bar{t}$ background, systematic uncertainties are considered for variations in initial- and final-state radiation, choice of parton shower, and choice of matrix-element generator. Each of these sources of uncertainty are considered as separate nuisance parameters in the likelihood fit. These are evaluated using alternative simulated $t\bar{t}$ samples.

The uncertainty in the treatment of radiative effects is estimated by varying the NLO radiation factor h_{damp} and the factorization and renormalization scales in a correlated way to produce more or less radiation. Alternative samples produced with MadGraph5_aMC@NLO v2.3.3+Pythia 8.212 and Powheg-Box v2+Herwig 7.0.1 [97] are used to evaluate generator and shower model uncertainties, respectively. Due to the limited number of events in the alternative $t\bar{t}$ samples, the uncertainties are taken into account after merging signal regions with two and at least three b-tagged jets. These uncertainties are in the range 1.4%–33% (13%–51%) for the normalization of $t\bar{t}+\mathrm{light}$ ($t\bar{t}+\mathrm{HF}$). Because the predicted cross sections of $t\bar{t}+\mathrm{light}$ and $t\bar{t}+\mathrm{HF}$ are not well known for the phase space of the signal regions, separate normalization factors are assigned to each of these two contributions and are allowed to float freely in the profile likelihood fit.

VII. STATISTICAL ANALYSIS

The statistical analysis quantifies the probability of compatibility between the measured data, expected SM background, and expected signal. The signal LLH distributions for the 12 signal regions are tested simultaneously

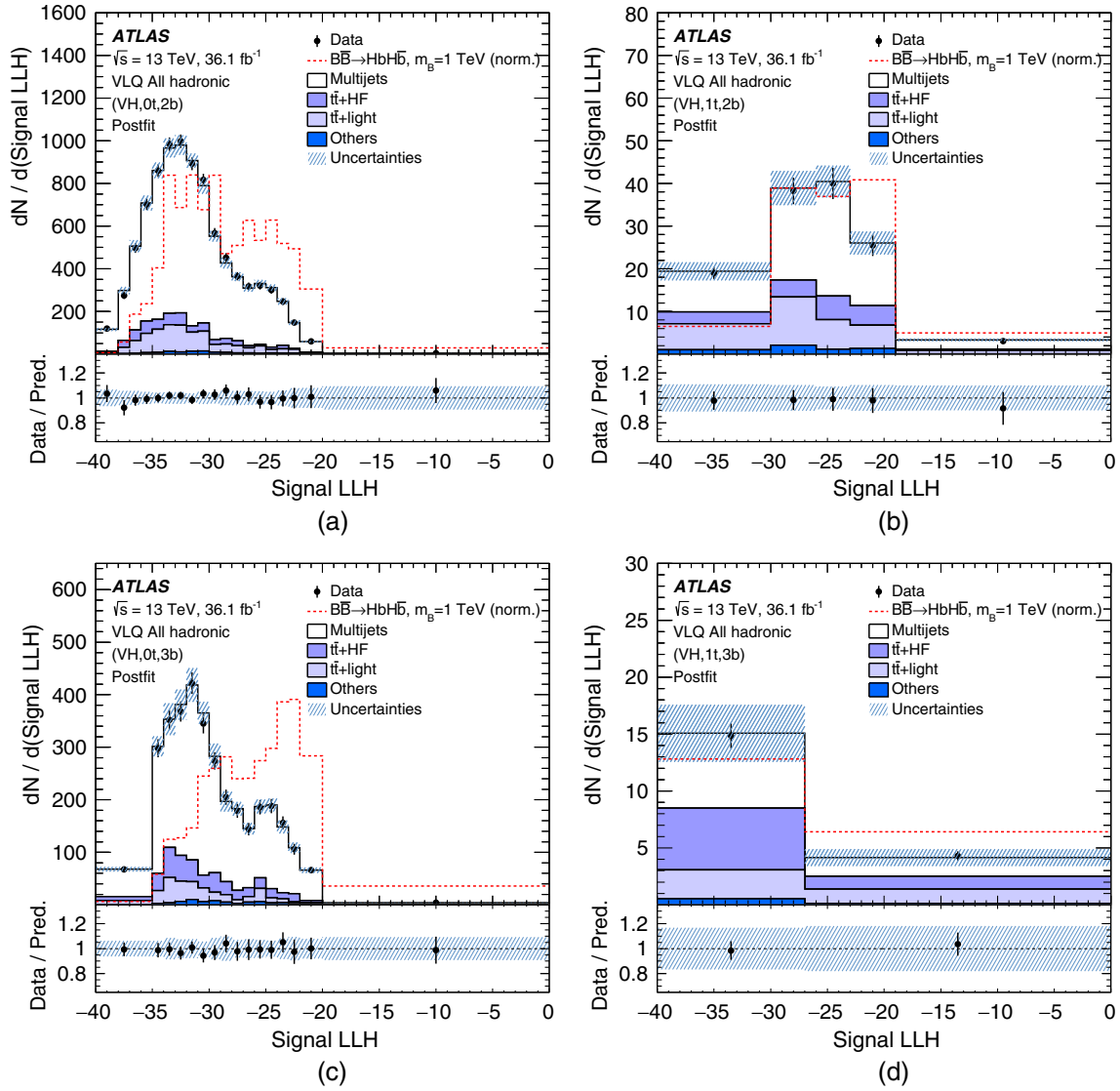

FIG. 11. Comparison between data and prediction for the signal LLH distribution after the fit to the data under the background-only hypothesis for the (a) (VH, 0t, 2b), (b) (VH, 1t, 2b), (c) (VH, 0t, 3b), and (d) (VH, 1t, 3b) signal regions. The contribution labeled "Others" is the combination of single-top-quark and $t\bar{t}+\mathrm{X}$ backgrounds. The distributions show the number of events per width of 1.0 in the x axis. The hatched area represents the total uncertainty of the background. The underflow and overflow are included in the first and last bins, respectively. A hypothetical signal for $\mathcal{B}(B\to Hb)=100\%$ and $m_B=1$ TeV is shown overlaid, normalized to the integral of the total background.

for the presence of a VLQ signal. Hypothesis testing is performed using a modified frequentist method based on a profile likelihood, taking into account systematic uncertainties as nuisance parameters. The statistical analysis is based on a binned likelihood function $\mathcal{L}(\mu,\theta)$ constructed as the product of Poisson probability terms over all bins. In this function, μ is a multiplicative factor applied to the predicted production cross section times branching ratio of the signal, and θ is the set of nuisance parameters, implemented in the likelihood function as Gaussian or log-normal priors. In addition, there are two unconstrained parameters in the fit, corresponding to the total normalization of $t\bar{t}+$ light and $t\bar{t}+$ HF.

The test statistic q_μ is defined as the profile likelihood ratio, $q_\mu = -2\ln(\mathcal{L}(\mu,\hat{\hat{\theta}}_\mu)/\mathcal{L}(\hat{\mu},\hat{\theta}))$,where $\hat{\mu}$ and $\hat{\theta}$ are the values of the parameters that maximize the likelihood function (with the constraint $0 \le \hat{\mu} \le \mu$), and $\hat{\hat{\theta}}_\mu$ are the values of the nuisance parameters that maximize the likelihood function for a given value of μ. Upper limits on the signal production cross section for each of the signal scenarios considered are derived by using q_μ in the CL_s method [98,99], where CL_s is computed using the asymptotic approximation [100]. For a given signal scenario, values of the production cross section that yield $CL_s < 0.05$ are excluded at ≥95% confidence level (C.L.).

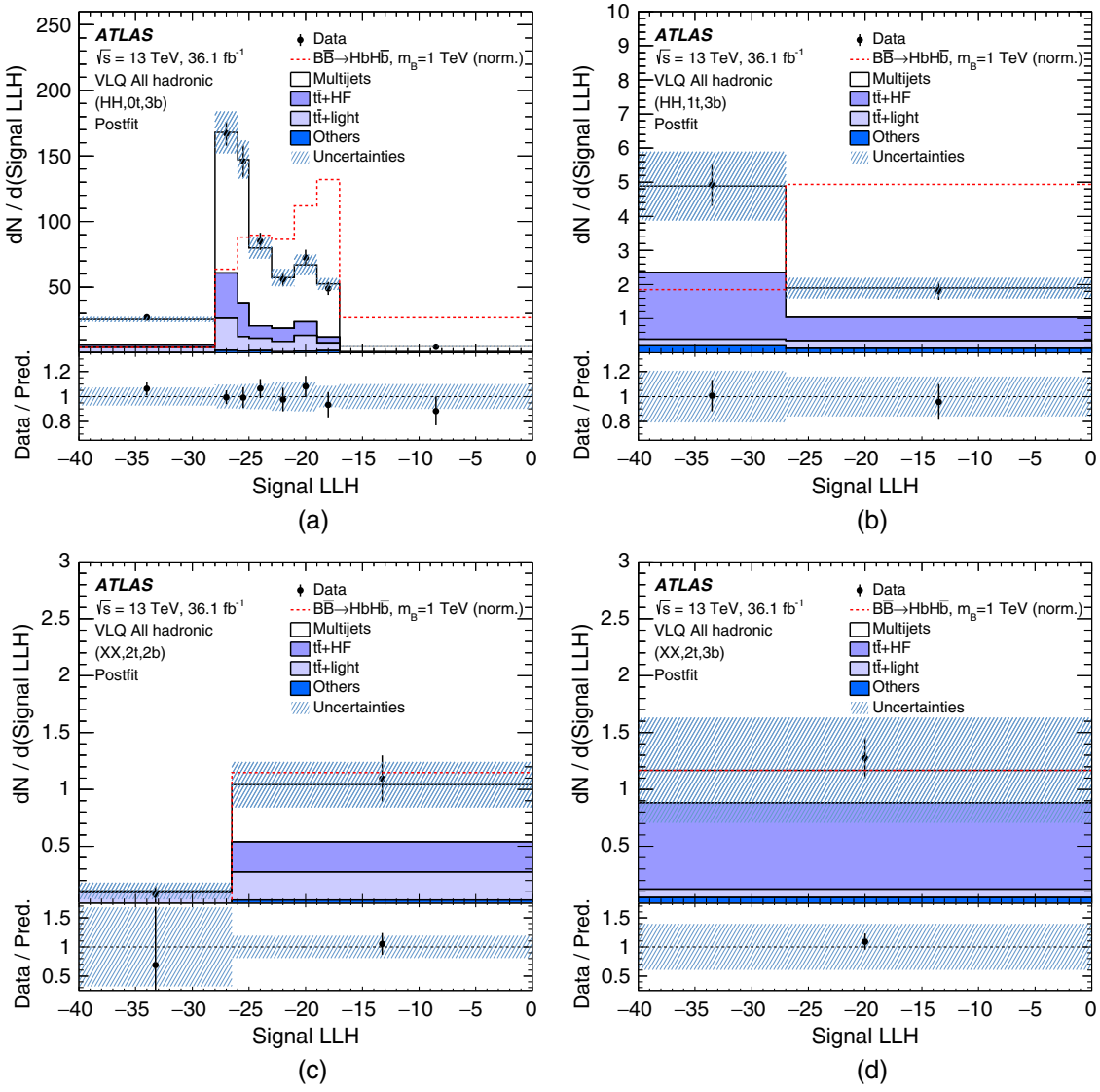

FIG. 12. Comparison between data and prediction for the signal LLH distribution after the fit to the data under the background-only hypothesis for the (a) (HH, 0t, 3b), (b) (HH, 1t, 3b), (c) (XX, 2t, 2b), and (d) (XX, 2t, 3b) signal regions. The contribution labeled "Others" is the combination of single-top-quark and $t\bar{t}+$ X backgrounds. The distributions show the number of events per width of 1.0 in the x axis. The hatched area represents the total uncertainty of the background. The underflow and overflow are included in the first and last bins, respectively. A hypothetical signal for $\mathcal{B}(B \to Hb) = 100\%$ and $m_B = 1$ TeV is shown overlaid, normalized to the integral of the total background.

VIII. RESULTS

Following the prescription described in Sec. VII, the profile likelihood fit for the background-only hypothesis is performed simultaneously in all signal regions. The postfit event yields are given in Table II and Fig. 9 shows a comparison between the predicted and observed numbers of events in all signal regions both before and after the fit.

The most notable shift in the postfit yields is that of the $t\bar{t}+\text{HF}$ normalization. The overall change in normalization is by a factor slightly greater than 2, which is achieved in the fit through a shift of the $t\bar{t}+\text{HF}$ normalization factor, as well as through pulls of systematic uncertainties, such as $t\bar{t}$ modeling and jet energy resolution uncertainties. The postfit distributions of the signal LLH from each signal region are shown in Figs. 10–12.

No significant excess of signal-like events is observed, and the analysis proceeds to set upper limits on the production cross section of $T\bar{T}$ and $B\bar{B}$ events in various scenarios. The sensitivity is mainly limited by the statistical uncertainty in the signal regions and in the control regions for the ABCD method. For example, if only statistical uncertainties and normalization factors are taken into account, the expected (observed) cross-section limit for $B\bar{B}\to HbH\bar{b}$ with $m_B=1$ TeV only changes by 5% (11%).

In a given scenario, a lower limit on the VLQ mass can be obtained by comparing the cross-section limits with the predicted cross section as a function of mass [49]. Figure 13 shows the expected and observed upper limits on the $T\bar{T}$ and $B\bar{B}$ cross section at 95% C.L. as a function of the VLQ mass in the scenario where the VLQ decays purely via the Higgs decay mode ($T\bar{T}\to HtH\bar{t}$ or $B\bar{B}\to HbH\bar{b}$), as well as in the benchmark scenario of the (B,Y) doublet. In this scenario, a B VLQ will decay almost equally into Zb and Hb, although the exact branching ratios depend on mass. For example, for $m_B=1$ TeV, $\mathcal{B}(B\to Zb)=0.51$ and $\mathcal{B}(B\to Hb)=0.49$ [45]. Only contributions from the B VLQ are considered, so the limit is conservative. In the case of a (B,Y) doublet, B masses below 950 GeV are excluded at 95% C.L.

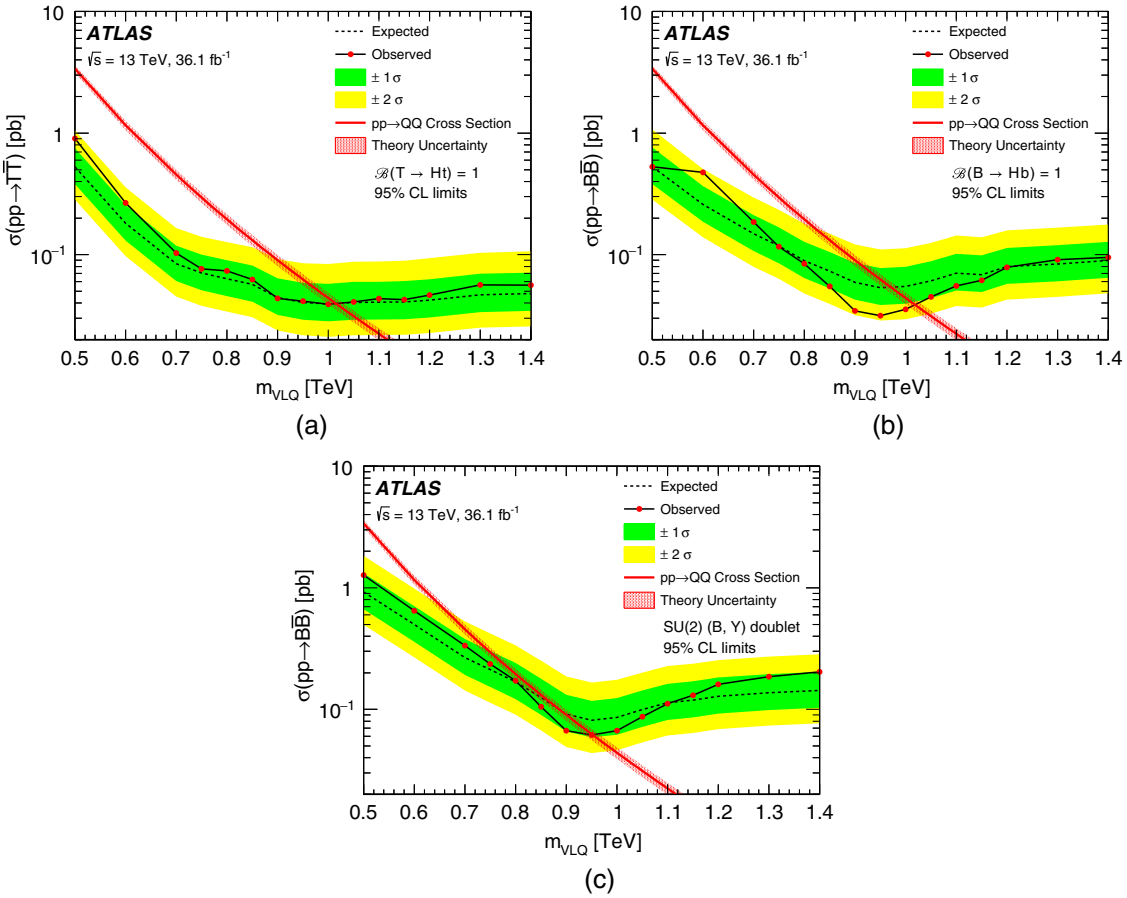

FIG. 13. Expected upper limits at the 95% C.L. on the (a) $T\bar{T}$ and (b) $B\bar{B}$ cross section as a function of the VLQ mass assuming $\mathcal{B}(T\to Ht)=1$ and $\mathcal{B}(B\to Hb)=1$, respectively, as well as on (c) the $B\bar{B}$ cross section with the assumption of branching ratios consistent with a weak-isospin doublet. In the doublet case, only contributions from the B VLQ are considered, making the result conservative. The green and yellow bands correspond to ±1 and ±2 standard deviations around the expected limit. The thin red line and band show the theoretical prediction and uncertainties, as described in Sec. III.

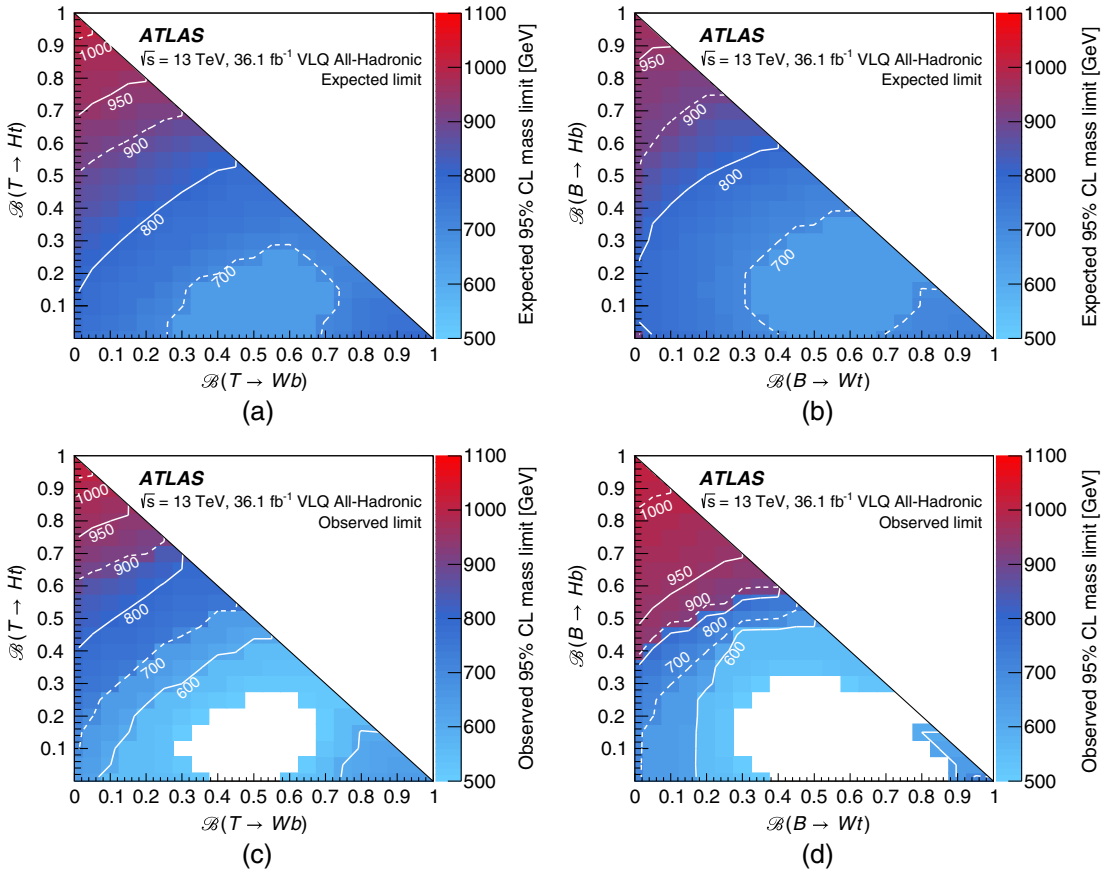

FIG. 14. Expected and observed 95% C.L. lower limits on (a),(c) m_T and (b),(d) m_B in the branching-ratio planes. Contour lines, alternating solid and dashed lines, are provided to show sensitivity to different VLQ masses across the planes. Signal hypotheses are considered in a mass range of 500–1400 GeV, so the white space on the observed limit figures corresponds to branching ratios where there is no observed exclusion above a mass of 500 GeV.

To evaluate the level of sensitivity of the results to the weak-isospin of the VLQ, samples of VLQ events with masses of 700, 950, and 1200 GeV were generated for an SU(2) doublet T and B quark and compared with the SU(2) singlet samples. Small differences between the limits are observed in decay modes with bottom quarks in the final state, where the SU(2) singlet produces a slightly weaker limit due to the slightly lower average momenta of decay products in the singlet final state. Thus, limits on the (B, Y) SU(2) doublet, which are taken from scaling the SU(2) singlet samples to doublet branching ratios, represent a slightly conservative limit. In final states with top quarks, the SU(2) singlet produces a slightly stronger limit, due to a slightly higher efficiency in VLQ DNN top tagging. Therefore, a limit on SU(2) doublets with T VLQs are not included here.

The largest difference between the observed and expected limits is for $\mathcal{B}(B \to Hb) = 1$ with a VLQ mass around 950 GeV. This results from a deficit in data in the final two bins of the (HH, 0t, 3b) signal region and the fact that the matrix element calculation for final states with two bottom quarks has its maximum sensitivity for masses near 900 GeV.

By reweighting the relative fractions of the three T (B) decay modes, it is possible to test all combinations of branching ratios. Figure 14 shows the lower limit on the T (B) mass as a function of $\mathcal{B}(T \to Ht)$ versus $\mathcal{B}(T \to Wb)$ $(\mathcal{B}(B \to Hb)$ versus $\mathcal{B}(B \to Wt))$. Each point on the figures have a total branching ratio of 1, so $\mathcal{B}(T \to Zt)$ $[\mathcal{B}(B \to Zb)]$ make up the remaining branching ratio for T (B). The expected and observed limits on the VLQ mass

TABLE III. Expected and observed 95% C.L. limits on the VLQ mass for $T\bar{T}$ and $B\bar{B}$ production. Different branching ratios are presented for T and B.

Branching ratio	Expected [GeV]	Observed [GeV]
$\mathcal{B}(B \to Wt) = 1$	730	710
$\mathcal{B}(B \to Zb) = 1$	910	710
$\mathcal{B}(B \to Hb) = 1$	970	1010
SU(2) (B, Y) doublet	890	950
$\mathcal{B}(T \to Wb) = 1$	790	650
$\mathcal{B}(T \to Zt) = 1$	780	650
$\mathcal{B}(T \to Ht) = 1$	1010	1010

for each corner of the branching-ratio plane are listed in Table III.

IX. CONCLUSION

A search for pair production of vectorlike quarks in the all-hadronic final state is presented using 36.1 fb^{-1} of collision data collected by the ATLAS detector at the LHC in 2015 and 2016. The analysis selects events with high-p_{T} small-R jets and multiple b-tags. Small-R jets are combined using a variable-R clustering algorithm and then classified with a neural network as a V-boson, Higgs-boson, top-quark, or background jet. A signal log likelihood calculated via the matrix element method is used as the final discriminant across multiple categories based on the number of V/H-tags, top-tags, and b-tags. The analysis targets all third-generation decays of VLQs, but it is particularly powerful for the $B \to Hb$ decay mode, which is difficult to probe with leptonic final states. The observed data are consistent with expected background and a 95% C.L. limit is placed on VLQ pair production as a function of the hypothetical VLQ mass. The observed (expected) mass exclusion limit for a weak-isospin (B, Y) doublet B is 950 (890) GeV, and the mass exclusion limits for the pure decays $B \to Hb$ and $T \to Ht$, where these results are strongest, are 1010 (970) GeV and 1010 (1010) GeV, respectively. Additionally, limits are placed across a two-dimensional plane of branching ratio values of Hb (Ht) vs Wt (Wb) for B (T) vectorlike quarks.

ACKNOWLEDGMENTS

We thank CERN for the very successful operation of the LHC, as well as the support staff from our institutions without whom ATLAS could not be operated efficiently. We acknowledge the support of ANPCyT, Argentina; YerPhI, Armenia; ARC, Australia; BMWFW and FWF, Austria; ANAS, Azerbaijan; SSTC, Belarus; CNPq and FAPESP, Brazil; NSERC, NRC and CFI, Canada; CERN; CONICYT, Chile; CAS, MOST and NSFC, China; COLCIENCIAS, Colombia; MSMT CR, MPO CR and VSC CR, Czech Republic; DNRF and DNSRC, Denmark; IN2P3-CNRS, CEA-DRF/IRFU, France; SRNSFG, Georgia; BMBF, HGF, and MPG, Germany; GSRT, Greece; RGC, Hong Kong SAR, China; ISF and Benoziyo Center, Israel; INFN, Italy; MEXT and JSPS, Japan; CNRST, Morocco; NWO, Netherlands; RCN, Norway; MNiSW and NCN, Poland; FCT, Portugal; MNE/IFA, Romania; MES of Russia and NRC KI, Russian Federation; JINR; MESTD, Serbia; MSSR, Slovakia; ARRS and MIZŠ, Slovenia; DST/NRF, South Africa; MINECO, Spain; SRC and Wallenberg Foundation, Sweden; SERI, SNSF and Cantons of Bern and Geneva, Switzerland; MOST, Taiwan; TAEK, Turkey; STFC, United Kingdom; DOE and NSF, United States of America. In addition, individual groups and members have received support from BCKDF, the Canada Council, CANARIE, CRC, Compute Canada, FQRNT, and the Ontario Innovation Trust, Canada; EPLANET, ERC, ERDF, FP7, Horizon 2020 and Marie Skłodowska-Curie Actions, European Union; Investissements d'Avenir Labex and Idex, ANR, Région Auvergne and Fondation Partager le Savoir, France; DFG and AvH Foundation, Germany; Herakleitos, Thales and Aristeia programmes co-financed by EU-ESF and the Greek NSRF; BSF, GIF and Minerva, Israel; BRF, Norway; CERCA Programme Generalitat de Catalunya, Generalitat Valenciana, Spain; the Royal Society and Leverhulme Trust, United Kingdom. The crucial computing support from all WLCG partners is acknowledged gratefully, in particular from CERN, the ATLAS Tier-1 facilities at TRIUMF (Canada), NDGF (Denmark, Norway, Sweden), CC-IN2P3 (France), KIT/GridKA (Germany), INFN-CNAF (Italy), NL-T1 (Netherlands), PIC (Spain), ASGC (Taiwan), RAL (UK) and BNL (USA), the Tier-2 facilities worldwide and large non-WLCG resource providers. Major contributors of computing resources are listed in Ref. [101].

[1] L. Susskind, Dynamics of spontaneous symmetry breaking in the Weinberg-Salam theory, Phys. Rev. D **20**, 2619 (1979).
[2] N. Arkani-Hamed, A. G. Cohen, E. Katz, and A. E. Nelson, The littlest Higgs, J. High Energy Phys. 07 (2002) 034.
[3] M. Schmaltz and D. Tucker-Smith, Little Higgs theories, Annu. Rev. Nucl. Part. Sci. **55**, 229 (2005).
[4] D. B. Kaplan, H. Georgi, and S. Dimopoulos, Composite Higgs scalars, Phys. Lett. B **136**, 187 (1984).
[5] K. Agashe, R. Contino, and A. Pomarol, The minimal composite Higgs model, Nucl. Phys. **B719**, 165 (2005).
[6] J. A. Aguilar-Saavedra, R. Benbrik, S. Heinemeyer, and M. Pérez-Victoria, Handbook of vectorlike quarks: Mixing and single production, Phys. Rev. D **88**, 094010 (2013).
[7] P. W. Higgs, Broken symmetries, massless particles and gauge fields, Phys. Lett. **12**, 132 (1964).
[8] F. Englert and R. Brout, Broken Symmetry and the Mass of Gauge Vector Mesons, Phys. Rev. Lett. **13**, 321 (1964).
[9] P. W. Higgs, Broken Symmetries and the Masses of Gauge Bosons, Phys. Rev. Lett. **13**, 508 (1964).
[10] G. S. Guralnik, C. R. Hagen, and T. W. B. Kibble, Global Conservation Laws and Massless Particles, Phys. Rev. Lett. **13**, 585 (1964).

[11] P. W. Higgs, Spontaneous symmetry breakdown without massless bosons, Phys. Rev. **145**, 1156 (1966).
[12] T. W. B. Kibble, Symmetry breaking in non-Abelian gauge theories, Phys. Rev. **155**, 1554 (1967).
[13] A. Djouadi and A. Lenz, Sealing the fate of a fourth generation of fermions, Phys. Lett. B **715**, 310 (2012).
[14] O. Eberhardt, G. Herbert, H. Lacker, A. Lenz, A. Menzel, U. Nierste, and M. Wiebusch, Impact of a Higgs Boson at a Mass of 126 GeV on the Standard Model with Three and Four Fermion Generations, Phys. Rev. Lett. **109**, 241802 (2012).
[15] ATLAS Collaboration, Observation of a new particle in the search for the Standard Model Higgs boson with the ATLAS detector at the LHC, Phys. Lett. B **716**, 1 (2012).
[16] CMS Collaboration, Observation of a new boson at a mass of 125 GeV with the CMS experiment at the LHC, Phys. Lett. B **716**, 30 (2012).
[17] F. del Aguila, L. Ametller, G. Kane, and J. Vidal, Vector-like fermion and standard Higgs production at hadron colliders, Nucl. Phys. **B334**, 1 (1990).
[18] J. A. Aguilar-Saavedra, Identifying top partners at LHC, J. High Energy Phys. 11 (2009) 030.
[19] M. Buchkremer, G. Cacciapaglia, A. Deandrea, and L. Panizzi, Model independent framework for searches of top partners, Nucl. Phys. **B876**, 376 (2013).
[20] K. Harigaya, S. Matsumoto, M. M. Nojiri, and K. Tobioka, Search for the top partner at the LHC using multi-b-jet channels, Phys. Rev. D **86**, 015005 (2012).
[21] ATLAS Collaboration, Analysis of events with b-jets and a pair of leptons of the same charge in pp collisions at $\sqrt{s} = 8$ TeV with the ATLAS detector, J. High Energy Phys. 10 (2015) 150.
[22] ATLAS Collaboration, Search for pair and single production of new heavy quarks that decay to a Z boson and a third-generation quark in pp collisions at $\sqrt{s} = 8$ TeV with the ATLAS detector, J. High Energy Phys. 11 (2014) 104.
[23] ATLAS Collaboration, Search for production of vector-like quark pairs and of four top quarks in the lepton-plus-jets final state in pp collisions at $\sqrt{s} = 8$ TeV with the ATLAS detector, J. High Energy Phys. 08 (2015) 105.
[24] ATLAS Collaboration, Search for pair production of a new heavy quark that decays into a W boson and a light quark in pp collisions at $\sqrt{s} = 8$ TeV with the ATLAS detector, Phys. Rev. D **92**, 112007 (2015).
[25] CMS Collaboration, Inclusive search for a vector-like T quark with charge $2/3$ in pp collisions at $\sqrt{s} = 8$ TeV, Phys. Lett. B **729**, 149 (2014).
[26] CMS Collaboration, Search for Top-Quark Partners with Charge $5/3$ in the Same-Sign Dilepton Final State, Phys. Rev. Lett. **112**, 171801 (2014).
[27] ATLAS Collaboration, Search for pair production of vector-like top quarks in events with one lepton, jets, and missing transverse momentum in $\sqrt{s} = 13$ TeV pp collisions with the ATLAS detector, J. High Energy Phys. 08 (2017) 052.
[28] ATLAS Collaboration, Search for pair production of heavy vector-like quarks decaying to high-p_T W bosons and b quarks in the lepton-plus-jets final state in pp collisions at $\sqrt{s} = 13$ TeV with the ATLAS detector, J. High Energy Phys. 10 (2017) 141.
[29] ATLAS Collaboration, Search for pair production of heavy vector-like quarks decaying into high-p_T W bosons and top quarks in the lepton-plus-jets final state in pp collisions at $\sqrt{s} = 13$ TeV with the ATLAS detector, J. High Energy Phys. 08 (2018) 048.
[30] ATLAS Collaboration, Search for pair- and single-production of vector-like quarks in final states with at least one Z boson decaying into a pair of electrons or muons in pp collision data collected with the ATLAS detector at $\sqrt{s} = 13$ TeV, arXiv:1806.10555.
[31] CMS Collaboration, Search for top quark partners with charge $5/3$ in proton-proton collisions at $\sqrt{s} = 13$ TeV, J. High Energy Phys. 08 (2017) 073.
[32] CMS Collaboration, Search for pair production of vector-like quarks in the $bW\bar{b}W$ channel from proton-proton collisions at $\sqrt{s} = 13$ TeV, Phys. Lett. B **779**, 82 (2018).
[33] CMS Collaboration, Search for pair production of vector-like T and B quarks in single-lepton final states using boosted jet substructure techniques at $\sqrt{s} = 13$ TeV, J. High Energy Phys. 11 (2017) 085.
[34] CMS Collaboration, Search for vector-like T and B quark pairs in final states with leptons at $\sqrt{s} = 13$ TeV, J. High Energy Phys. 08 (2018) 177.
[35] CMS Collaboration, Search for vectorlike charge $2/3$ T quarks in proton-proton collisions at $\sqrt{(s)} = 8$ TeV, Phys. Rev. D **93**, 012003 (2016).
[36] CMS Collaboration, Search for pair-produced vectorlike B quarks in proton-proton collisions at $\sqrt{s} = 8$ TeV, Phys. Rev. D **93**, 112009 (2016).
[37] ATLAS Collaboration, Search for pair production of up-type vector-like quarks and for four-top-quark events in final states with multiple b-jets with the ATLAS detector, J. High Energy Phys. 07 (2018) 089.
[38] ATLAS Collaboration, The ATLAS experiment at the CERN large hadron collider, J. Instrum. **3**, S08003 (2008).
[39] ATLAS Collaboration, ATLAS insertable B-layer technical design report addendum, Technical Reports No. CERN-LHCC-2012-009, No. ATLAS-TDR-19-ADD-1; Addendum to No. CERN-LHCC-2010-013, No. ATLAS-TDR-019, 2012, https://cds.cern.ch/record/1451888.
[40] B. Abbott *et al.*, Production and integration of the ATLAS insertable B-layer, J. Instrum. **13**, T05008 (2018).
[41] ATLAS Collaboration, Performance of the ATLAS trigger system in 2015, Eur. Phys. J. C **77**, 317 (2017).
[42] S. Agostinelli *et al.*, GEANT4: A simulation toolkit, Nucl. Instrum. Methods Phys. Res., Sect. A **506**, 250 (2003).
[43] ATLAS Collaboration, The ATLAS simulation infrastructure, Eur. Phys. J. C **70**, 823 (2010).
[44] D. J. Lange, The EVTGEN particle decay simulation package, Nucl. Instrum. Methods Phys. Res., Sect. A **462**, 152 (2001).
[45] J. Aguilar-Saavedra, PROTOS: Program for top simulations, Technical Report, http://jaguilar.web.cern.ch/jaguilar/protos/.
[46] R. D. Ball *et al.*, Parton distributions with LHC data, Nucl. Phys. **B867**, 244 (2013).

[47] T. Sjöstrand, S. Mrenna, and P. Z. Skands, A brief introduction to PYTHIA 8.1, Comput. Phys. Commun. **178**, 852 (2008).

[48] ATLAS Collaboration, ATLAS PYTHIA 8 tunes to 7 TeV data, Report No. ATL-PHYS-PUB-2014-021, 2014, https://cds.cern.ch/record/1966419.

[49] M. Czakon and A. Mitov, TOP++: A program for the calculation of the top-pair cross-section at hadron colliders, Comput. Phys. Commun. **185**, 2930 (2014).

[50] A. D. Martin, W. J. Stirling, R. S. Thorne, and G. Watt, Parton distributions for the LHC, Eur. Phys. J. C **63**, 189 (2009).

[51] J. Butterworth *et al.*, PDF4LHC recommendations for LHC Run II, J. Phys. G **43**, 023001 (2016).

[52] H.-L. Lai, M. Guzzi, J. Huston, Z. Li, P. M. Nadolsky, J. Pumplin, and C.-P. Yuan, New parton distributions for collider physics, Phys. Rev. D **82**, 074024 (2010).

[53] J. Gao, M. Guzzi, J. Huston, H.-L. Lai, Z. Li, P. Nadolsky, J. Pumplin, D. Stump, and C.-P. Yuan, CT10 next-to-next-to-leading order global analysis of QCD, Phys. Rev. D **89**, 033009 (2014).

[54] S. Alioli, P. Nason, C. Oleari, and E. Re, A general framework for implementing NLO calculations in shower Monte Carlo programs: The POWHEG BOX, J. High Energy Phys. 06 (2010) 043.

[55] J. M. Campbell, R. K. Ellis, P. Nason, and E. Re, Top-pair production and decay at NLO matched with parton showers, J. High Energy Phys. 04 (2015) 114.

[56] P. Z. Skands, Tuning Monte Carlo generators: The Perugia tunes, Phys. Rev. D **82**, 074018 (2010).

[57] E. Re, Single-top *Wt*-channel production matched with parton showers using the POWHEG method, Eur. Phys. J. C **71**, 1547 (2011).

[58] S. Alioli, P. Nason, C. Oleari, and E. Re, NLO single-top production matched with shower in POWHEG: *s*- and *t*-channel contributions, J. High Energy Phys. 09 (2009) 111; Erratum 02 (2010) 11.

[59] T. Sjöstrand, S. Mrenna, and P. Z. Skands, PYTHIA 6.4 physics and manual, J. High Energy Phys. 05 (2006) 026.

[60] J. Alwall, R. Frederix, S. Frixione, V. Hirschi, F. Maltoni, O. Mattelaer, H.-S. Shao, T. Stelzer, P. Torrielli, and M. Zaro, The automated computation of tree-level and next-to-leading order differential cross sections, and their matching to parton shower simulations, J. High Energy Phys. 07 (2014) 079.

[61] B. Nachman, P. Nef, A. Schwartzman, M. Swiatlowski, and C. Wanotayaroj, Jets from jets: Reclustering as a tool for large radius jet reconstruction and grooming at the LHC, J. High Energy Phys. 02 (2015) 075.

[62] D. Krohn, J. Thaler, and L.-T.Wang, Jets with variable *R*, J. High Energy Phys. 06 (2009) 059.

[63] ATLAS Collaboration, Performance of missing transverse momentum reconstruction with the ATLAS detector using proton-proton collisions at $\sqrt{s} = 13$ TeV, arXiv:1802.08168.

[64] M. Cacciari, G. P. Salam, and G. Soyez, The anti-k_t jet clustering algorithm, J. High Energy Phys. 04 (2008) 063.

[65] M. Cacciari and G. P. Salam, Dispelling the N^3 myth for the k_t jet-finder, Phys. Lett. B **641**, 57 (2006).

[66] ATLAS Collaboration, Tagging and suppression of pileup jets with the ATLAS detector, Report No. ATLASCONF-2014-018, 2014, https://cds.cern.ch/record/1700870.

[67] ATLAS Collaboration, Optimisation of the ATLAS *b*-tagging performance for the 2016 LHC Run, Report No. ATL-PHYS-PUB-2016-012, 2016, https://cds.cern.ch/record/2160731.

[68] ATLAS Collaboration, Measurements of *b*-jet tagging efficiency with the ATLAS detector using $t\bar{t}$ events at $\sqrt{s} = 13$ TeV, J. High Energy Phys. 08 (2018) 89.

[69] ATLAS Collaboration, Jet reclustering and close-by effects in ATLAS Run II, Report No. ATLAS-CONF-2017-062, 2017, https://cds.cern.ch/record/2275649.

[70] ATLAS Collaboration, Performance of jet substructure techniques for large-*R* jets in proton-proton collisions at $\sqrt{s} = 7$ TeV using the ATLAS detector, J. High Energy Phys. 09 (2013) 076.

[71] F. Chollet, KERAS, https://github.com/fchollet/keras, 2017.

[72] R. Al-Rfou *et al.* (THEANO Development Team), THEANO: A PYTHON framework for fast computation of mathematical expressions, arXiv:1605.02688.

[73] D. P. Kingma and J. Ba, Adam: A method for stochastic optimization, arXiv:1412.6980.

[74] J. Schmidhuber, Deep learning in neural networks: An overview, Neural Netw. **61**, 85 (2015).

[75] I. Goodfellow, Y. Bengio, and A. Courville, *Deep Learning* (MIT Press, Cambridge, MA, 2016), http://www.deeplearningbook.org.

[76] S. Ioffe and C. Szegedy, Batch normalization: Accelerating deep network training by reducing internal covariate shift, arXiv:1502.03167.

[77] K. Kondo, Dynamical likelihood method for reconstruction of events with missing momentum. 1: Method and toy models, J. Phys. Soc. Jpn. **57**, 4126 (1988).

[78] V. M. Abazov *et al.* (D0 Collaboration), A precision measurement of the mass of the top quark, Nature (London) **429**, 638 (2004).

[79] A. Abulencia *et al.* (CDF Collaboration), Precision measurement of the top-quark mass from dilepton events at CDF II, Phys. Rev. D **75**, 031105 (2007).

[80] V. M. Abazov *et al.* (D0 Collaboration), Measurement of Spin Correlation in $t\bar{t}$ Production Using a Matrix Element Approach, Phys. Rev. Lett. **107**, 032001 (2011).

[81] V. M. Abazov *et al.* (D0 Collaboration), Observation of Single Top-Quark Production, Phys. Rev. Lett. **103**, 092001 (2009).

[82] T. Aaltonen *et al.* (CDF Collaboration), Observation of Electroweak Single Top-Quark Production, Phys. Rev. Lett. **103**, 092002 (2009).

[83] ATLAS Collaboration, Evidence for single top-quark production in the *s*-channel in proton-proton collisions at $\sqrt{s} = 8$ TeV with the ATLAS detector using the matrix element method, Phys. Lett. B **756**, 228 (2016).

[84] T. Aaltonen *et al.* (CDF Collaboration), Search for a Standard Model Higgs Boson in $WH \to \ell\nu b\bar{b}$ in $p\bar{p}$ Collisions at $\sqrt{s} = 1.96$ TeV, Phys. Rev. Lett. **103**, 101802 (2009).

[85] T. Aaltonen *et al.* (CDF Collaboration), Search for standard model Higgs boson production in association with a *W* boson using a matrix element technique at CDF in $p\bar{p}$ collisions at $\sqrt{s} = 1.96$ TeV, Phys. Rev. D **85**, 072001 (2012).

[86] ATLAS Collaboration, Search for the standard model Higgs boson produced in association with top quarks and decaying into $b\bar{b}$ in pp collisions at $\sqrt{s} = 8$ TeV with the ATLAS detector, Eur. Phys. J. C **75**, 349 (2015).
[87] CMS Collaboration, Search for a standard model Higgs boson produced in association with a top-quark pair and decaying to bottom quarks using a matrix element method, Eur. Phys. J. C **75**, 251 (2015).
[88] N. D. Christensen and C. Duhr, FeynRules: Feynman rules made easy, Comput. Phys. Commun. **180**, 1614 (2009).
[89] M. R. Whalley, D. Bourilkov, and R. C. Group, The Les Houches accord PDFs (LHAPDF) and LHAGLUE, arXiv: hep-ph/0508110.
[90] G. P. Lepage, A new algorithm for adaptive multidimensional integration, J. Comput. Phys. **27**, 192 (1978).
[91] M. Galassi, J. Davies, J. Theiler, B. Gough, G. Jungman, P. Alken, M. Booth, and F. Rossi, *GNU Scientific Library Reference Manual*, 3rd ed. (Network Theory Limited, United Kingdom, 2009).
[92] ATLAS Collaboration, Luminosity determination in pp collisions at $\sqrt{s} = 8$ TeV using the ATLAS detector at the LHC, Eur. Phys. J. C **76**, 653 (2016).
[93] ATLAS Collaboration, Measurement of the Inelastic Proton-Proton Cross Section at $\sqrt{s} = 13$ TeV with the ATLAS Detector at the LHC, Phys. Rev. Lett. **117**, 182002 (2016).
[94] ATLAS Collaboration, Jet energy scale measurements and their systematic uncertainties in proton-proton collisions at $\sqrt{s} = 13$ TeV with the ATLAS detector, Phys. Rev. D **96**, 072002 (2017).
[95] ATLAS Collaboration, Jet energy resolution in proton-proton collisions at $\sqrt{s} = 7$ TeV recorded in 2010 with the ATLAS detector, Eur. Phys. J. C **73**, 2306 (2013).
[96] N. Kidonakis, Two-loop soft anomalous dimensions for single top quark associated production with a W- or H-, Phys. Rev. D **82**, 054018 (2010).
[97] G. Corcella, I. G. Knowles, G. Marchesini, S. Moretti, K. Odagiri, P. Richardson, M. H. Seymour, and B. R. Webber, HERWIG 6: An event generator for hadron emission reactions with interfering gluons (including supersymmetric processes), J. High Energy Phys. 01 (2001) 010.
[98] A. L. Read, Presentation of search results: The CLs technique, J. Phys. G **28**, 2693 (2002).
[99] T. Junk, Confidence level computation for combining searches with small statistics, Nucl. Instrum. Methods Phys. Res., Sect. A **434**, 435 (1999).
[100] G. Cowan, K. Cranmer, E. Gross, and O. Vitells, Asymptotic formulae for likelihood-based tests of new physics, Eur. Phys. J. C **71**, 1554 (2011).
[101] ATLAS Collaboration, ATLAS computing acknowledgements, Report No. ATL-GEN-PUB-2016-002, https://cds.cern.ch/record/2202407.

M. Aaboud,[34d] G. Aad,[99] B. Abbott,[124] O. Abdinov,[13,a] B. Abeloos,[128] D. K. Abhayasinghe,[91] S. H. Abidi,[164] O. S. AbouZeid,[143] N. L. Abraham,[153] H. Abramowicz,[158] H. Abreu,[157] Y. Abulaiti,[6] B. S. Acharya,[64a,64b,b] S. Adachi,[160] L. Adamczyk,[81a] J. Adelman,[119] M. Adersberger,[112] A. Adiguzel,[12c,c] T. Adye,[141] A. A. Affolder,[143] Y. Afik,[157] C. Agheorghiesei,[27c] J. A. Aguilar-Saavedra,[136f,136a] F. Ahmadov,[77,d] G. Aielli,[71a,71b] S. Akatsuka,[83] T. P. A. Åkesson,[94] E. Akilli,[52] A. V. Akimov,[108] G. L. Alberghi,[23b,23a] J. Albert,[173] P. Albicocco,[49] M. J. Alconada Verzini,[86] S. Alderweireldt,[117] M. Aleksa,[35] I. N. Aleksandrov,[77] C. Alexa,[27b] T. Alexopoulos,[10] M. Alhroob,[124] B. Ali,[138] G. Alimonti,[66a] J. Alison,[36] S. P. Alkire,[145] C. Allaire,[128] B. M. M. Allbrooke,[153] B. W. Allen,[127] P. P. Allport,[21] A. Aloisio,[67a,67b] A. Alonso,[39] F. Alonso,[86] C. Alpigiani,[145] A. A. Alshehri,[55] M. I. Alstaty,[99] B. Alvarez Gonzalez,[35] D. Álvarez Piqueras,[171] M. G. Alviggi,[67a,67b] B. T. Amadio,[18] Y. Amaral Coutinho,[78b] L. Ambroz,[131] C. Amelung,[26] D. Amidei,[103] S. P. Amor Dos Santos,[136a,136c] S. Amoroso,[35] C. S. Amrouche,[52] C. Anastopoulos,[146] L. S. Ancu,[52] N. Andari,[21] T. Andeen,[11] C. F. Anders,[59b] J. K. Anders,[20] K. J. Anderson,[36] A. Andreazza,[66a,66b] V. Andrei,[59a] C. R. Anelli,[173] S. Angelidakis,[37] I. Angelozzi,[118] A. Angerami,[38] A. V. Anisenkov,[120b,120a] A. Annovi,[69a] C. Antel,[59a] M. T. Anthony,[146] M. Antonelli,[49] D. J. A. Antrim,[168] F. Anulli,[70a] M. Aoki,[79] L. Aperio Bella,[35] G. Arabidze,[104] Y. Arai,[79] J. P. Araque,[136a] V. Araujo Ferraz,[78b] R. Araujo Pereira,[78b] A. T. H. Arce,[47] R. E. Ardell,[91] F. A. Arduh,[86] J-F. Arguin,[107] S. Argyropoulos,[75] A. J. Armbruster,[35] L. J. Armitage,[90] A Armstrong,[168] O. Arnaez,[164] H. Arnold,[118] M. Arratia,[31] O. Arslan,[24] A. Artamonov,[109,a] G. Artoni,[131] S. Artz,[97] S. Asai,[160] N. Asbah,[44] A. Ashkenazi,[158] E. M. Asimakopoulou,[169] L. Asquith,[153] K. Assamagan,[29] R. Astalos,[28a] R. J. Atkin,[32a] M. Atkinson,[170] N. B. Atlay,[148] K. Augsten,[138] G. Avolio,[35] R. Avramidou,[58a] B. Axen,[18] M. K. Ayoub,[15a] G. Azuelos,[107,e] A. E. Baas,[59a] M. J. Baca,[21] H. Bachacou,[142] K. Bachas,[65a,65b] M. Backes,[131] P. Bagnaia,[70a,70b] M. Bahmani,[82] H. Bahrasemani,[149] A. J. Bailey,[171] J. T. Baines,[141] M. Bajic,[39] C. Bakalis,[10] O. K. Baker,[180] P. J. Bakker,[118] D. Bakshi Gupta,[93] E. M. Baldin,[120b,120a] P. Balek,[177] F. Balli,[142] W. K. Balunas,[133] J. Balz,[97] E. Banas,[82] A. Bandyopadhyay,[24] S. Banerjee,[178,f] A. A. E. Bannoura,[179] L. Barak,[158] W. M. Barbe,[37] E. L. Barberio,[102] D. Barberis,[53b,53a] M. Barbero,[99] T. Barillari,[113] M-S. Barisits,[35] J. Barkeloo,[127] T. Barklow,[150] N. Barlow,[31] R. Barnea,[157] S. L. Barnes,[58c] B. M. Barnett,[141] R. M. Barnett,[18] Z. Barnovska-Blenessy,[58a] A. Baroncelli,[72a] G. Barone,[26] A. J. Barr,[131] L. Barranco Navarro,[171] F. Barreiro,[96] J. Barreiro Guimarães da Costa,[15a] R. Bartoldus,[150] A. E. Barton,[87] P. Bartos,[28a]

A. Basalaev,[134] A. Bassalat,[128] R. L. Bates,[55] S. J. Batista,[164] S. Batlamous,[34e] J. R. Batley,[31] M. Battaglia,[143] M. Bauce,[70a,70b] F. Bauer,[142] K. T. Bauer,[168] H. S. Bawa,[150,g] J. B. Beacham,[122] M. D. Beattie,[87] T. Beau,[132] P. H. Beauchemin,[167] P. Bechtle,[24] H. C. Beck,[51] H. P. Beck,[20,h] K. Becker,[50] M. Becker,[97] C. Becot,[44] A. Beddall,[12d] A. J. Beddall,[12a] V. A. Bednyakov,[77] M. Bedognetti,[118] C. P. Bee,[152] T. A. Beermann,[35] M. Begalli,[78b] M. Begel,[29] A. Behera,[152] J. K. Behr,[44] A. S. Bell,[92] G. Bella,[158] L. Bellagamba,[23b] A. Bellerive,[33] M. Bellomo,[157] P. Bellos,[9] K. Belotskiy,[110] N. L. Belyaev,[110] O. Benary,[158,a] D. Benchekroun,[34a] M. Bender,[112] N. Benekos,[10] Y. Benhammou,[158] E. Benhar Noccioli,[180] J. Benitez,[75] D. P. Benjamin,[47] M. Benoit,[52] J. R. Bensinger,[26] S. Bentvelsen,[118] L. Beresford,[131] M. Beretta,[49] D. Berge,[44] E. Bergeaas Kuutmann,[169] N. Berger,[5] L. J. Bergsten,[26] J. Beringer,[18] S. Berlendis,[7] N. R. Bernard,[100] G. Bernardi,[132] C. Bernius,[150] F. U. Bernlochner,[24] T. Berry,[91] P. Berta,[97] C. Bertella,[15a] G. Bertoli,[43a,43b] I. A. Bertram,[87] G. J. Besjes,[39] O. Bessidskaia Bylund,[43a,43b] M. Bessner,[44] N. Besson,[142] A. Bethani,[98] S. Bethke,[113] A. Betti,[24] A. J. Bevan,[90] J. Beyer,[113] R. M. Bianchi,[135] O. Biebel,[112] D. Biedermann,[19] R. Bielski,[98] K. Bierwagen,[97] N. V. Biesuz,[69a,69b] M. Biglietti,[72a] T. R. V. Billoud,[107] M. Bindi,[51] A. Bingul,[12d] C. Bini,[70a,70b] S. Biondi,[23b,23a] T. Bisanz,[51] J. P. Biswal,[158] C. Bittrich,[46] D. M. Bjergaard,[47] J. E. Black,[150] K. M. Black,[25] R. E. Blair,[6] T. Blazek,[28a] I. Bloch,[44] C. Blocker,[26] A. Blue,[55] U. Blumenschein,[90] Dr. Blunier,[144a] G. J. Bobbink,[118] V. S. Bobrovnikov,[120b,120a] S. S. Bocchetta,[94] A. Bocci,[47] D. Boerner,[179] D. Bogavac,[112] A. G. Bogdanchikov,[120b,120a] C. Bohm,[43a] V. Boisvert,[91] P. Bokan,[169,i] T. Bold,[81a] A. S. Boldyrev,[111] A. E. Bolz,[59b] M. Bomben,[132] M. Bona,[90] J. S. Bonilla,[127] M. Boonekamp,[142] A. Borisov,[140] G. Borissov,[87] J. Bortfeldt,[35] D. Bortoletto,[131] V. Bortolotto,[71a,61b,61c,71b] D. Boscherini,[23b] M. Bosman,[14] J. D. Bossio Sola,[30] K. Bouaouda,[34a] J. Boudreau,[135] E. V. Bouhova-Thacker,[87] D. Boumediene,[37] C. Bourdarios,[128] S. K. Boutle,[55] A. Boveia,[122] J. Boyd,[35] I. R. Boyko,[77] A. J. Bozson,[91] J. Bracinik,[21] N. Brahimi,[99] A. Brandt,[8] G. Brandt,[179] O. Brandt,[59a] F. Braren,[44] U. Bratzler,[161] B. Brau,[100] J. E. Brau,[127] W. D. Breaden Madden,[55] K. Brendlinger,[44] A. J. Brennan,[102] L. Brenner,[44] R. Brenner,[169] S. Bressler,[177] B. Brickwedde,[97] D. L. Briglin,[21] D. Britton,[55] D. Britzger,[59b] I. Brock,[24] R. Brock,[104] G. Brooijmans,[38] T. Brooks,[91] W. K. Brooks,[144b] E. Brost,[119] J. H Broughton,[21] P. A. Bruckman de Renstrom,[82] D. Bruncko,[28b] A. Bruni,[23b] G. Bruni,[23b] L. S. Bruni,[118] S. Bruno,[71a,71b] B. H. Brunt,[31] M. Bruschi,[23b] N. Bruscino,[135] P. Bryant,[36] L. Bryngemark,[44] T. Buanes,[17] Q. Buat,[35] P. Buchholz,[148] A. G. Buckley,[55] I. A. Budagov,[77] F. Buehrer,[50] M. K. Bugge,[130] O. Bulekov,[110] D. Bullock,[8] T. J. Burch,[119] S. Burdin,[88] C. D. Burgard,[118] A. M. Burger,[5] B. Burghgrave,[119] K. Burka,[82] S. Burke,[141] I. Burmeister,[45] J. T. P. Burr,[131] D. Büscher,[50] V. Büscher,[97] E. Buschmann,[51] P. Bussey,[55] J. M. Butler,[25] C. M. Buttar,[55] J. M. Butterworth,[92] P. Butti,[35] W. Buttinger,[35] A. Buzatu,[155] A. R. Buzykaev,[120b,120a] G. Cabras,[23b,23a] S. Cabrera Urbán,[171] D. Caforio,[138] H. Cai,[170] V. M. M. Cairo,[2] O. Cakir,[4a] N. Calace,[52] P. Calafiura,[18] A. Calandri,[99] G. Calderini,[132] P. Calfayan,[63] G. Callea,[40b,40a] L. P. Caloba,[78b] S. Calvente Lopez,[96] D. Calvet,[37] S. Calvet,[37] T. P. Calvet,[152] M. Calvetti,[69a,69b] R. Camacho Toro,[132] S. Camarda,[35] P. Camarri,[71a,71b] D. Cameron,[130] R. Caminal Armadans,[100] C. Camincher,[35] S. Campana,[35] M. Campanelli,[92] A. Camplani,[39] A. Campoverde,[148] V. Canale,[67a,67b] M. Cano Bret,[58c] J. Cantero,[125] T. Cao,[158] Y. Cao,[170] M. D. M. Capeans Garrido,[35] I. Caprini,[27b] M. Caprini,[27b] M. Capua,[40b,40a] R. M. Carbone,[38] R. Cardarelli,[71a] F. C. Cardillo,[50] I. Carli,[139] T. Carli,[35] G. Carlino,[67a] B. T. Carlson,[135] L. Carminati,[66a,66b] R. M. D. Carney,[43a,43b] S. Caron,[117] E. Carquin,[144b] S. Carrá,[66a,66b] G. D. Carrillo-Montoya,[35] D. Casadei,[32b] M. P. Casado,[14,j] A. F. Casha,[164] M. Casolino,[14] D. W. Casper,[168] R. Castelijn,[118] F. L. Castillo,[171] V. Castillo Gimenez,[171] N. F. Castro,[136a,136e] A. Catinaccio,[35] J. R. Catmore,[130] A. Cattai,[35] J. Caudron,[24] V. Cavaliere,[29] E. Cavallaro,[14] D. Cavalli,[66a] M. Cavalli-Sforza,[14] V. Cavasinni,[69a,69b] E. Celebi,[12b] F. Ceradini,[72a,72b] L. Cerda Alberich,[171] A. S. Cerqueira,[78a] A. Cerri,[153] L. Cerrito,[71a,71b] F. Cerutti,[18] A. Cervelli,[23b,23a] S. A. Cetin,[12b] A. Chafaq,[34a] D Chakraborty,[119] S. K. Chan,[57] W. S. Chan,[118] Y. L. Chan,[61a] J. D. Chapman,[31] D. G. Charlton,[21] C. C. Chau,[33] C. A. Chavez Barajas,[153] S. Che,[122] A. Chegwidden,[104] S. Chekanov,[6] S. V. Chekulaev,[165a] G. A. Chelkov,[77,k] M. A. Chelstowska,[35] C. Chen,[58a] C. H. Chen,[76] H. Chen,[29] J. Chen,[58a] J. Chen,[38] S. Chen,[133] S. J. Chen,[15c] X. Chen,[15b,l] Y. Chen,[80] Y-H. Chen,[44] H. C. Cheng,[103] H. J. Cheng,[15d] A. Cheplakov,[77] E. Cheremushkina,[140] R. Cherkaoui El Moursli,[34e] E. Cheu,[7] K. Cheung,[62] L. Chevalier,[142] V. Chiarella,[49] G. Chiarelli,[69a] G. Chiodini,[65a] A. S. Chisholm,[35] A. Chitan,[27b] I. Chiu,[160] Y. H. Chiu,[173] M. V. Chizhov,[77] K. Choi,[63] A. R. Chomont,[128] S. Chouridou,[159] Y. S. Chow,[118] V. Christodoulou,[92] M. C. Chu,[61a] J. Chudoba,[137] A. J. Chuinard,[101] J. J. Chwastowski,[82] L. Chytka,[126] D. Cinca,[45] V. Cindro,[89] I. A. Cioară,[24] A. Ciocio,[18] F. Cirotto,[67a,67b] Z. H. Citron,[177] M. Citterio,[66a] A. Clark,[52] M. R. Clark,[38] P. J. Clark,[48] C. Clement,[43a,43b] Y. Coadou,[99] M. Cobal,[64a,64c] A. Coccaro,[53b,53a] J. Cochran,[76] A. E. C. Coimbra,[177] L. Colasurdo,[117] B. Cole,[38] A. P. Colijn,[118] J. Collot,[56] P. Conde Muiño,[136a,136b] E. Coniavitis,[50] S. H. Connell,[32b] I. A. Connelly,[98] S. Constantinescu,[27b] F. Conventi,[67a,m] A. M. Cooper-Sarkar,[131] F. Cormier,[172] K. J. R. Cormier,[164]

M. Corradi,[70a,70b] E. E. Corrigan,[94] F. Corriveau,[101,n] A. Cortes-Gonzalez,[35] M. J. Costa,[171] D. Costanzo,[146] G. Cottin,[31] G. Cowan,[91] B. E. Cox,[98] J. Crane,[98] K. Cranmer,[121] S. J. Crawley,[55] R. A. Creager,[133] G. Cree,[33] S. Crépé-Renaudin,[56] F. Crescioli,[132] M. Cristinziani,[24] V. Croft,[121] G. Crosetti,[40b,40a] A. Cueto,[96] T. Cuhadar Donszelmann,[146] A. R. Cukierman,[150] M. Curatolo,[49] J. Cúth,[97] S. Czekierda,[82] P. Czodrowski,[35] M. J. Da Cunha Sargedas De Sousa,[58b,136b] C. Da Via,[98] W. Dabrowski,[81a] T. Dado,[28a,i] S. Dahbi,[34e] T. Dai,[103] F. Dallaire,[107] C. Dallapiccola,[100] M. Dam,[39] G. D'amen,[23b,23a] J. Damp,[97] J. R. Dandoy,[133] M. F. Daneri,[30] N. P. Dang,[178,f] N. D Dann,[98] M. Danninger,[172] V. Dao,[35] G. Darbo,[53b] S. Darmora,[8] O. Dartsi,[5] A. Dattagupta,[127] T. Daubney,[44] S. D'Auria,[55] W. Davey,[24] C. David,[44] T. Davidek,[139] D. R. Davis,[47] E. Dawe,[102] I. Dawson,[146] K. De,[8] R. De Asmundis,[67a] A. De Benedetti,[124] S. De Castro,[23b,23a] S. De Cecco,[70a,70b] N. De Groot,[117] P. de Jong,[118] H. De la Torre,[104] F. De Lorenzi,[76] A. De Maria,[51,o] D. De Pedis,[70a] A. De Salvo,[70a] U. De Sanctis,[71a,71b] A. De Santo,[153] K. De Vasconcelos Corga,[99] J. B. De Vivie De Regie,[128] C. Debenedetti,[143] D. V. Dedovich,[77] N. Dehghanian,[3] M. Del Gaudio,[40b,40a] J. Del Peso,[96] D. Delgove,[128] F. Deliot,[142] C. M. Delitzsch,[7] M. Della Pietra,[67a,67b] D. Della Volpe,[52] A. Dell'Acqua,[35] L. Dell'Asta,[25] M. Delmastro,[5] C. Delporte,[128] P. A. Delsart,[56] D. A. DeMarco,[164] S. Demers,[180] M. Demichev,[77] S. P. Denisov,[140] D. Denysiuk,[118] L. D'Eramo,[132] D. Derendarz,[82] J. E. Derkaoui,[34d] F. Derue,[132] P. Dervan,[88] K. Desch,[24] C. Deterre,[44] K. Dette,[164] M. R. Devesa,[30] P. O. Deviveiros,[35] A. Dewhurst,[141] S. Dhaliwal,[26] F. A. Di Bello,[52] A. Di Ciaccio,[71a,71b] L. Di Ciaccio,[5] W. K. Di Clemente,[133] C. Di Donato,[67a,67b] A. Di Girolamo,[35] B. Di Micco,[72a,72b] R. Di Nardo,[35] K. F. Di Petrillo,[57] A. Di Simone,[50] R. Di Sipio,[164] D. Di Valentino,[33] C. Diaconu,[99] M. Diamond,[164] F. A. Dias,[39] T. Dias Do Vale,[136a] M. A. Diaz,[144a] J. Dickinson,[18] E. B. Diehl,[103] J. Dietrich,[19] S. Díez Cornell,[44] A. Dimitrievska,[18] J. Dingfelder,[24] F. Dittus,[35] F. Djama,[99] T. Djobava,[156b] J. I. Djuvsland,[59a] M. A. B. Do Vale,[78c] M. Dobre,[27b] D. Dodsworth,[26] C. Doglioni,[94] J. Dolejsi,[139] Z. Dolezal,[139] M. Donadelli,[78d] J. Donini,[37] A. D'onofrio,[90] M. D'Onofrio,[88] J. Dopke,[141] A. Doria,[67a] M. T. Dova,[86] A. T. Doyle,[55] E. Drechsler,[51] E. Dreyer,[149] T. Dreyer,[51] M. Dris,[10] Y. Du,[58b] J. Duarte-Campderros,[158] F. Dubinin,[108] M. Dubovsky,[28a] A. Dubreuil,[52] E. Duchovni,[177] G. Duckeck,[112] A. Ducourthial,[132] O. A. Ducu,[107,p] D. Duda,[113] A. Dudarev,[35] A. C. Dudder,[97] E. M. Duffield,[18] L. Duflot,[128] M. Dührssen,[35] C. Dülsen,[179] M. Dumancic,[177] A. E. Dumitriu,[27b,q] A. K. Duncan,[55] M. Dunford,[59a] A. Duperrin,[99] H. Duran Yildiz,[4a] M. Düren,[54] A. Durglishvili,[156b] D. Duschinger,[46] B. Dutta,[44] D. Duvnjak,[1] M. Dyndal,[44] S. Dysch,[98] B. S. Dziedzic,[82] C. Eckardt,[44] K. M. Ecker,[113] R. C. Edgar,[103] T. Eifert,[35] G. Eigen,[17] K. Einsweiler,[18] T. Ekelof,[169] M. El Kacimi,[34c] R. El Kosseifi,[99] V. Ellajosyula,[99] M. Ellert,[169] F. Ellinghaus,[179] A. A. Elliot,[90] N. Ellis,[35] J. Elmsheuser,[29] M. Elsing,[35] D. Emeliyanov,[141] Y. Enari,[160] J. S. Ennis,[175] M. B. Epland,[47] J. Erdmann,[45] A. Ereditato,[20] S. Errede,[170] M. Escalier,[128] C. Escobar,[171] B. Esposito,[49] O. Estrada Pastor,[171] A. I. Etienvre,[142] E. Etzion,[158] H. Evans,[63] A. Ezhilov,[134] M. Ezzi,[34e] F. Fabbri,[55] L. Fabbri,[23b,23a] V. Fabiani,[117] G. Facini,[92] R. M. Faisca Rodrigues Pereira,[136a] R. M. Fakhrutdinov,[140] S. Falciano,[70a] P. J. Falke,[5] S. Falke,[5] J. Faltova,[139] Y. Fang,[15a] M. Fanti,[66a,66b] A. Farbin,[8] A. Farilla,[72a] E. M. Farina,[68a,68b] T. Farooque,[104] S. Farrell,[18] S. M. Farrington,[175] P. Farthouat,[35] F. Fassi,[34e] P. Fassnacht,[35] D. Fassouliotis,[9] M. Faucci Giannelli,[48] A. Favareto,[53b,53a] W. J. Fawcett,[52] L. Fayard,[128] O. L. Fedin,[134,r] W. Fedorko,[172] M. Feickert,[41] S. Feigl,[130] L. Feligioni,[99] C. Feng,[58b] E. J. Feng,[35] M. Feng,[47] M. J. Fenton,[55] A. B. Fenyuk,[140] L. Feremenga,[8] J. Ferrando,[44] A. Ferrari,[169] P. Ferrari,[118] R. Ferrari,[68a] D. E. Ferreira de Lima,[59b] A. Ferrer,[171] D. Ferrere,[52] C. Ferretti,[103] F. Fiedler,[97] A. Filipčič,[89] F. Filthaut,[117] K. D. Finelli,[25] M. C. N. Fiolhais,[136a,136c,s] L. Fiorini,[171] C. Fischer,[14] W. C. Fisher,[104] N. Flaschel,[44] I. Fleck,[148] P. Fleischmann,[103] R. R. M. Fletcher,[133] T. Flick,[179] B. M. Flierl,[112] L. M. Flores,[133] L. R. Flores Castillo,[61a] N. Fomin,[17] G. T. Forcolin,[98] A. Formica,[142] F. A. Förster,[14] A. C. Forti,[98] A. G. Foster,[21] D. Fournier,[128] H. Fox,[87] S. Fracchia,[146] P. Francavilla,[69a,69b] M. Franchini,[23b,23a] S. Franchino,[59a] D. Francis,[35] L. Franconi,[130] M. Franklin,[57] M. Frate,[168] M. Fraternali,[68a,68b] D. Freeborn,[92] S. M. Fressard-Batraneanu,[35] B. Freund,[107] W. S. Freund,[78b] D. Froidevaux,[35] J. A. Frost,[131] C. Fukunaga,[161] T. Fusayasu,[114] J. Fuster,[171] O. Gabizon,[157] A. Gabrielli,[23b,23a] A. Gabrielli,[18] G. P. Gach,[81a] S. Gadatsch,[52] P. Gadow,[113] G. Gagliardi,[53b,53a] L. G. Gagnon,[107] C. Galea,[27b] B. Galhardo,[136a,136c] E. J. Gallas,[131] B. J. Gallop,[141] P. Gallus,[138] G. Galster,[39] R. Gamboa Goni,[90] K. K. Gan,[122] S. Ganguly,[177] Y. Gao,[88] Y. S. Gao,[150,g] C. García,[171] J. E. García Navarro,[171] J. A. García Pascual,[15a] M. Garcia-Sciveres,[18] R. W. Gardner,[36] N. Garelli,[150] V. Garonne,[130] K. Gasnikova,[44] A. Gaudiello,[53b,53a] G. Gaudio,[68a] I. L. Gavrilenko,[108] A. Gavrilyuk,[109] C. Gay,[172] G. Gaycken,[24] E. N. Gazis,[10] C. N. P. Gee,[141] J. Geisen,[51] M. Geisen,[97] M. P. Geisler,[59a] K. Gellerstedt,[43a,43b] C. Gemme,[53b] M. H. Genest,[56] C. Geng,[103] S. Gentile,[70a,70b] C. Gentsos,[159] S. George,[91] D. Gerbaudo,[14] G. Gessner,[45] S. Ghasemi,[148] M. Ghasemi Bostanabad,[173] M. Ghneimat,[24] B. Giacobbe,[23b] S. Giagu,[70a,70b] N. Giangiacomi,[23b,23a] P. Giannetti,[69a] S. M. Gibson,[91] M. Gignac,[143] D. Gillberg,[33] G. Gilles,[179] D. M. Gingrich,[3,e] M. P. Giordani,[64a,64c] F. M. Giorgi,[23b]

P. F. Giraud,[142] P. Giromini,[57] G. Giugliarelli,[64a,64c] D. Giugni,[66a] F. Giuli,[131] M. Giulini,[59b] S. Gkaitatzis,[159] I. Gkialas,[9,t] E. L. Gkougkousis,[14] P. Gkountoumis,[10] L. K. Gladilin,[111] C. Glasman,[96] J. Glatzer,[14] P. C. F. Glaysher,[44] A. Glazov,[44] M. Goblirsch-Kolb,[26] J. Godlewski,[82] S. Goldfarb,[102] T. Golling,[52] D. Golubkov,[140] A. Gomes,[136a,136b,136d] R. Goncalves Gama,[78a] R. Gonçalo,[136a] G. Gonella,[50] L. Gonella,[21] A. Gongadze,[77] F. Gonnella,[21] J. L. Gonski,[57] S. González de la Hoz,[171] S. Gonzalez-Sevilla,[52] L. Goossens,[35] P. A. Gorbounov,[109] H. A. Gordon,[29] B. Gorini,[35] E. Gorini,[65a,65b] A. Gorišek,[89] A. T. Goshaw,[47] C. Gössling,[45] M. I. Gostkin,[77] C. A. Gottardo,[24] C. R. Goudet,[128] D. Goujdami,[34c] A. G. Goussiou,[145] N. Govender,[32b,u] C. Goy,[5] E. Gozani,[157] I. Grabowska-Bold,[81a] P. O. J. Gradin,[169] E. C. Graham,[88] J. Gramling,[168] E. Gramstad,[130] S. Grancagnolo,[19] V. Gratchev,[134] P. M. Gravila,[27f] C. Gray,[55] H. M. Gray,[18] Z. D. Greenwood,[93,v] C. Grefe,[24] K. Gregersen,[92] I. M. Gregor,[44] P. Grenier,[150] K. Grevtsov,[44] J. Griffiths,[8] A. A. Grillo,[143] K. Grimm,[150] S. Grinstein,[14,w] Ph. Gris,[37] J.-F. Grivaz,[128] S. Groh,[97] E. Gross,[177] J. Grosse-Knetter,[51] G. C. Grossi,[93] Z. J. Grout,[92] C. Grud,[103] A. Grummer,[116] L. Guan,[103] W. Guan,[178] J. Guenther,[35] A. Guerguichon,[128] F. Guescini,[165a] D. Guest,[168] R. Gugel,[50] B. Gui,[122] T. Guillemin,[5] S. Guindon,[35] U. Gul,[55] C. Gumpert,[35] J. Guo,[58c] W. Guo,[103] Y. Guo,[58a,x] Z. Guo,[99] R. Gupta,[41] S. Gurbuz,[12c] G. Gustavino,[124] B. J. Gutelman,[157] P. Gutierrez,[124] C. Gutschow,[92] C. Guyot,[142] M. P. Guzik,[81a] C. Gwenlan,[131] C. B. Gwilliam,[88] A. Haas,[121] C. Haber,[18] H. K. Hadavand,[8] N. Haddad,[34e] A. Hadef,[58a] S. Hageböck,[24] M. Hagihara,[166] H. Hakobyan,[181,a] M. Haleem,[174] J. Haley,[125] G. Halladjian,[104] G. D. Hallewell,[99] K. Hamacher,[179] P. Hamal,[126] K. Hamano,[173] A. Hamilton,[32a] G. N. Hamity,[146] K. Han,[58a,y] L. Han,[58a] S. Han,[15d] K. Hanagaki,[79,z] M. Hance,[143] D. M. Handl,[112] B. Haney,[133] R. Hankache,[132] P. Hanke,[59a] E. Hansen,[94] J. B. Hansen,[39] J. D. Hansen,[39] M. C. Hansen,[24] P. H. Hansen,[39] K. Hara,[166] A. S. Hard,[178] T. Harenberg,[179] S. Harkusha,[105] P. F. Harrison,[175] N. M. Hartmann,[112] Y. Hasegawa,[147] A. Hasib,[48] S. Hassani,[142] S. Haug,[20] R. Hauser,[104] L. Hauswald,[46] L. B. Havener,[38] M. Havranek,[138] C. M. Hawkes,[21] R. J. Hawkings,[35] D. Hayden,[104] C. Hayes,[152] C. P. Hays,[131] J. M. Hays,[90] H. S. Hayward,[88] S. J. Haywood,[141] M. P. Heath,[48] V. Hedberg,[94] L. Heelan,[8] S. Heer,[24] K. K. Heidegger,[50] J. Heilman,[33] S. Heim,[44] T. Heim,[18] B. Heinemann,[44,aa] J. J. Heinrich,[112] L. Heinrich,[121] C. Heinz,[54] J. Hejbal,[137] L. Helary,[35] A. Held,[172] S. Hellesund,[130] S. Hellman,[43a,43b] C. Helsens,[35] R. C. W. Henderson,[87] Y. Heng,[178] S. Henkelmann,[172] A. M. Henriques Correia,[35] G. H. Herbert,[19] H. Herde,[26] V. Herget,[174] Y. Hernández Jiménez,[32c] H. Herr,[97] G. Herten,[50] R. Hertenberger,[112] L. Hervas,[35] T. C. Herwig,[133] G. G. Hesketh,[92] N. P. Hessey,[165a] J. W. Hetherly,[41] S. Higashino,[79] E. Higón-Rodriguez,[171] K. Hildebrand,[36] E. Hill,[173] J. C. Hill,[31] K. K. Hill,[29] K. H. Hiller,[44] S. J. Hillier,[21] M. Hils,[46] I. Hinchliffe,[18] M. Hirose,[129] D. Hirschbuehl,[179] B. Hiti,[89] O. Hladik,[137] D. R. Hlaluku,[32c] X. Hoad,[48] J. Hobbs,[152] N. Hod,[165a] M. C. Hodgkinson,[146] A. Hoecker,[35] M. R. Hoeferkamp,[116] F. Hoenig,[112] D. Hohn,[24] D. Hohov,[128] T. R. Holmes,[36] M. Holzbock,[112] M. Homann,[45] S. Honda,[166] T. Honda,[79] T. M. Hong,[135] A. Hönle,[113] B. H. Hooberman,[170] W. H. Hopkins,[127] Y. Horii,[115] P. Horn,[46] A. J. Horton,[149] L. A. Horyn,[36] J-Y. Hostachy,[56] A. Hostiuc,[145] S. Hou,[155] A. Hoummada,[34a] J. Howarth,[98] J. Hoya,[86] M. Hrabovsky,[126] J. Hrdinka,[35] I. Hristova,[19] J. Hrivnac,[128] A. Hrynevich,[106] T. Hryn'ova,[5] P. J. Hsu,[62] S.-C. Hsu,[145] Q. Hu,[29] S. Hu,[58c] Y. Huang,[15a] Z. Hubacek,[138] F. Hubaut,[99] M. Huebner,[24] F. Huegging,[24] T. B. Huffman,[131] E. W. Hughes,[38] M. Huhtinen,[35] R. F. H. Hunter,[33] P. Huo,[152] A. M. Hupe,[33] N. Huseynov,[77,d] J. Huston,[104] J. Huth,[57] R. Hyneman,[103] G. Iacobucci,[52] G. Iakovidis,[29] I. Ibragimov,[148] L. Iconomidou-Fayard,[128] Z. Idrissi,[34e] P. Iengo,[35] R. Ignazzi,[39] O. Igonkina,[118,bb] R. Iguchi,[160] T. Iizawa,[52] Y. Ikegami,[79] M. Ikeno,[79] D. Iliadis,[159] N. Ilic,[150] F. Iltzsche,[46] G. Introzzi,[68a,68b] M. Iodice,[72a] K. Iordanidou,[38] V. Ippolito,[70a,70b] M. F. Isacson,[169] N. Ishijima,[129] M. Ishino,[160] M. Ishitsuka,[162] W. Islam,[125] C. Issever,[131] S. Istin,[12c,cc] F. Ito,[166] J. M. Iturbe Ponce,[61a] R. Iuppa,[73a,73b] A. Ivina,[177] H. Iwasaki,[79] J. M. Izen,[42] V. Izzo,[67a] S. Jabbar,[3] P. Jacka,[137] P. Jackson,[1] R. M. Jacobs,[24] V. Jain,[2] G. Jäkel,[179] K. B. Jakobi,[97] K. Jakobs,[50] S. Jakobsen,[74] T. Jakoubek,[137] D. O. Jamin,[125] D. K. Jana,[93] R. Jansky,[52] J. Janssen,[24] M. Janus,[51] P. A. Janus,[81a] G. Jarlskog,[94] N. Javadov,[77,d] T. Javůrek,[50] M. Javurkova,[50] F. Jeanneau,[142] L. Jeanty,[18] J. Jejelava,[156a,dd] A. Jelinskas,[175] P. Jenni,[50,ee] J. Jeong,[44] C. Jeske,[175] S. Jézéquel,[5] H. Ji,[178] J. Jia,[152] H. Jiang,[76] Y. Jiang,[58a] Z. Jiang,[150,ff] S. Jiggins,[50] F. A. Jimenez Morales,[37] J. Jimenez Pena,[171] S. Jin,[15c] A. Jinaru,[27b] O. Jinnouchi,[162] H. Jivan,[32c] P. Johansson,[146] K. A. Johns,[7] C. A. Johnson,[63] W. J. Johnson,[145] K. Jon-And,[43a,43b] R. W. L. Jones,[87] S. D. Jones,[153] S. Jones,[7] T. J. Jones,[88] J. Jongmanns,[59a] P. M. Jorge,[136a,136b] J. Jovicevic,[165a] X. Ju,[178] J. J. Junggeburth,[113] A. Juste Rozas,[14,w] A. Kaczmarska,[82] M. Kado,[128] H. Kagan,[122] M. Kagan,[150] T. Kaji,[176] E. Kajomovitz,[157] C. W. Kalderon,[94] A. Kaluza,[97] S. Kama,[41] A. Kamenshchikov,[140] L. Kanjir,[89] Y. Kano,[160] V. A. Kantserov,[110] J. Kanzaki,[79] B. Kaplan,[121] L. S. Kaplan,[178] D. Kar,[32c] M. J. Kareem,[165b] E. Karentzos,[10] S. N. Karpov,[77] Z. M. Karpova,[77] V. Kartvelishvili,[87] A. N. Karyukhin,[140] K. Kasahara,[166] L. Kashif,[178] R. D. Kass,[122] A. Kastanas,[151] Y. Kataoka,[160] C. Kato,[160] J. Katzy,[44] K. Kawade,[80] K. Kawagoe,[85] T. Kawamoto,[160] G. Kawamura,[51] E. F. Kay,[88]

V. F. Kazanin,[120b,120a] R. Keeler,[173] R. Kehoe,[41] J. S. Keller,[33] E. Kellermann,[94] J. J. Kempster,[21] J. Kendrick,[21] O. Kepka,[137] S. Kersten,[179] B. P. Kerševan,[89] R. A. Keyes,[101] M. Khader,[170] F. Khalil-Zada,[13] A. Khanov,[125] A. G. Kharlamov,[120b,120a] T. Kharlamova,[120b,120a] A. Khodinov,[163] T. J. Khoo,[52] E. Khramov,[77] J. Khubua,[156b] S. Kido,[80] M. Kiehn,[52] C. R. Kilby,[91] S. H. Kim,[166] Y. K. Kim,[36] N. Kimura,[64a,64c] O. M. Kind,[19] B. T. King,[88] D. Kirchmeier,[46] J. Kirk,[141] A. E. Kiryunin,[113] T. Kishimoto,[160] D. Kisielewska,[81a] V. Kitali,[44] O. Kivernyk,[5] E. Kladiva,[28b] T. Klapdor-Kleingrothaus,[50] M. H. Klein,[103] M. Klein,[88] U. Klein,[88] K. Kleinknecht,[97] P. Klimek,[119] A. Klimentov,[29] R. Klingenberg,[45,a] T. Klingl,[24] T. Klioutchnikova,[35] F. F. Klitzner,[112] P. Kluit,[118] S. Kluth,[113] E. Kneringer,[74] E. B. F. G. Knoops,[99] A. Knue,[50] A. Kobayashi,[160] D. Kobayashi,[85] T. Kobayashi,[160] M. Kobel,[46] M. Kocian,[150] P. Kodys,[139] T. Koffas,[33] E. Koffeman,[118] N. M. Köhler,[113] T. Koi,[150] M. Kolb,[59b] I. Koletsou,[5] T. Kondo,[79] N. Kondrashova,[58c] K. Köneke,[50] A. C. König,[117] T. Kono,[79] R. Konoplich,[121,gg] V. Konstantinides,[92] N. Konstantinidis,[92] B. Konya,[94] R. Kopeliansky,[63] S. Koperny,[81a] K. Korcyl,[82] K. Kordas,[159] A. Korn,[92] I. Korolkov,[14] E. V. Korolkova,[146] O. Kortner,[113] S. Kortner,[113] T. Kosek,[139] V. V. Kostyukhin,[24] A. Kotwal,[47] A. Koulouris,[10] A. Kourkoumeli-Charalampidi,[68a,68b] C. Kourkoumelis,[9] E. Kourlitis,[146] V. Kouskoura,[29] A. B. Kowalewska,[82] R. Kowalewski,[173] T. Z. Kowalski,[81a] C. Kozakai,[160] W. Kozanecki,[142] A. S. Kozhin,[140] V. A. Kramarenko,[111] G. Kramberger,[89] D. Krasnopevtsev,[110] M. W. Krasny,[132] A. Krasznahorkay,[35] D. Krauss,[113] J. A. Kremer,[81a] J. Kretzschmar,[88] P. Krieger,[164] K. Krizka,[18] K. Kroeninger,[45] H. Kroha,[113] J. Kroll,[137] J. Kroll,[133] J. Krstic,[16] U. Kruchonak,[77] H. Krüger,[24] N. Krumnack,[76] M. C. Kruse,[47] T. Kubota,[102] S. Kuday,[4b] J. T. Kuechler,[179] S. Kuehn,[35] A. Kugel,[59a] F. Kuger,[174] T. Kuhl,[44] V. Kukhtin,[77] R. Kukla,[99] Y. Kulchitsky,[105] S. Kuleshov,[144b] Y. P. Kulinich,[170] M. Kuna,[56] T. Kunigo,[83] A. Kupco,[137] T. Kupfer,[45] O. Kuprash,[158] H. Kurashige,[80] L. L. Kurchaninov,[165a] Y. A. Kurochkin,[105] M. G. Kurth,[15d] E. S. Kuwertz,[173] M. Kuze,[162] J. Kvita,[126] T. Kwan,[101] A. La Rosa,[113] J. L. La Rosa Navarro,[78d] L. La Rotonda,[40b,40a] F. La Ruffa,[40b,40a] C. Lacasta,[171] F. Lacava,[70a,70b] J. Lacey,[44] D. P. J. Lack,[98] H. Lacker,[19] D. Lacour,[132] E. Ladygin,[77] R. Lafaye,[5] B. Laforge,[132] T. Lagouri,[32c] S. Lai,[51] S. Lammers,[63] W. Lampl,[7] E. Lançon,[29] U. Landgraf,[50] M. P. J. Landon,[90] M. C. Lanfermann,[52] V. S. Lang,[44] J. C. Lange,[14] R. J. Langenberg,[35] A. J. Lankford,[168] F. Lanni,[29] K. Lantzsch,[24] A. Lanza,[68a] A. Lapertosa,[53b,53a] S. Laplace,[132] J. F. Laporte,[142] T. Lari,[66a] F. Lasagni Manghi,[23b,23a] M. Lassnig,[35] T. S. Lau,[61a] A. Laudrain,[128] A. T. Law,[143] P. Laycock,[88] M. Lazzaroni,[66a,66b] B. Le,[102] O. Le Dortz,[132] E. Le Guirriec,[99] E. P. Le Quilleuc,[142] M. LeBlanc,[7] T. LeCompte,[6] F. Ledroit-Guillon,[56] C. A. Lee,[29] G. R. Lee,[144a] L. Lee,[57] S. C. Lee,[155] B. Lefebvre,[101] M. Lefebvre,[173] F. Legger,[112] C. Leggett,[18] N. Lehmann,[179] G. Lehmann Miotto,[35] W. A. Leight,[44] A. Leisos,[159,hh] M. A. L. Leite,[78d] R. Leitner,[139] D. Lellouch,[177] B. Lemmer,[51] K. J. C. Leney,[92] T. Lenz,[24] B. Lenzi,[35] R. Leone,[7] S. Leone,[69a] C. Leonidopoulos,[48] G. Lerner,[153] C. Leroy,[107] R. Les,[164] A. A. J. Lesage,[142] C. G. Lester,[31] M. Levchenko,[134] J. Levêque,[5] D. Levin,[103] L. J. Levinson,[177] D. Lewis,[90] B. Li,[103] C-Q. Li,[58a] H. Li,[58b] L. Li,[58c] Q. Li,[15d] Q. Y. Li,[58a] S. Li,[58d,58c] X. Li,[58c] Y. Li,[148] Z. Liang,[15a] B. Liberti,[71a] A. Liblong,[164] K. Lie,[61c] S. Liem,[118] A. Limosani,[154] C. Y. Lin,[31] K. Lin,[104] T. H. Lin,[97] R. A. Linck,[63] B. E. Lindquist,[152] A. L. Lionti,[52] E. Lipeles,[133] A. Lipniacka,[17] M. Lisovyi,[59b] T. M. Liss,[170,ii] A. Lister,[172] A. M. Litke,[143] J. D. Little,[8] B. Liu,[76] B. L Liu,[6] H. B. Liu,[29] H. Liu,[103] J. B. Liu,[58a] J. K. K. Liu,[131] K. Liu,[132] M. Liu,[58a] P. Liu,[18] Y. Liu,[15a] Y. L. Liu,[58a] Y. W. Liu,[58a] M. Livan,[68a,68b] A. Lleres,[56] J. Llorente Merino,[15a] S. L. Lloyd,[90] C. Y. Lo,[61b] F. Lo Sterzo,[41] E. M. Lobodzinska,[44] P. Loch,[7] F. K. Loebinger,[98] A. Loesle,[50] K. M. Loew,[26] T. Lohse,[19] K. Lohwasser,[146] M. Lokajicek,[137] B. A. Long,[25] J. D. Long,[170] R. E. Long,[87] L. Longo,[65a,65b] K. A. Looper,[122] J. A. Lopez,[144b] I. Lopez Paz,[14] A. Lopez Solis,[146] J. Lorenz,[112] N. Lorenzo Martinez,[5] M. Losada,[22] P. J. Lösel,[112] X. Lou,[44] X. Lou,[15a] A. Lounis,[128] J. Love,[6] P. A. Love,[87] J. J. Lozano Bahilo,[171] H. Lu,[61a] M. Lu,[58a] N. Lu,[103] Y. J. Lu,[62] H. J. Lubatti,[145] C. Luci,[70a,70b] A. Lucotte,[56] C. Luedtke,[50] F. Luehring,[63] I. Luise,[132] W. Lukas,[74] L. Luminari,[70a] B. Lund-Jensen,[151] M. S. Lutz,[100] P. M. Luzi,[132] D. Lynn,[29] R. Lysak,[137] E. Lytken,[94] F. Lyu,[15a] V. Lyubushkin,[77] H. Ma,[29] L. L. Ma,[58b] Y. Ma,[58b] G. Maccarrone,[49] A. Macchiolo,[113] C. M. Macdonald,[146] J. Machado Miguens,[133,136b] D. Madaffari,[171] R. Madar,[37] W. F. Mader,[46] A. Madsen,[44] N. Madysa,[46] J. Maeda,[80] K. Maekawa,[160] S. Maeland,[17] T. Maeno,[29] A. S. Maevskiy,[111] V. Magerl,[50] C. Maidantchik,[78b] T. Maier,[112] A. Maio,[136a,136b,136d] O. Majersky,[28a] S. Majewski,[127] Y. Makida,[79] N. Makovec,[128] B. Malaescu,[132] Pa. Malecki,[82] V. P. Maleev,[134] F. Malek,[56] U. Mallik,[75] D. Malon,[6] C. Malone,[31] S. Maltezos,[10] S. Malyukov,[35] J. Mamuzic,[171] G. Mancini,[49] I. Mandić,[89] J. Maneira,[136a] L. Manhaes de Andrade Filho,[78a] J. Manjarres Ramos,[46] K. H. Mankinen,[94] A. Mann,[112] A. Manousos,[74] B. Mansoulie,[142] J. D. Mansour,[15a] M. Mantoani,[51] S. Manzoni,[66a,66b] G. Marceca,[30] L. March,[52] L. Marchese,[131] G. Marchiori,[132] M. Marcisovsky,[137] C. A. Marin Tobon,[35] M. Marjanovic,[37] D. E. Marley,[103] F. Marroquim,[78b] Z. Marshall,[18] M. U. F Martensson,[169] S. Marti-Garcia,[171] C. B. Martin,[122] T. A. Martin,[175] V. J. Martin,[48] B. Martin dit Latour,[17] M. Martinez,[14,w] V. I. Martinez Outschoorn,[100]

S. Martin-Haugh,[141] V. S. Martoiu,[27b] A. C. Martyniuk,[92] A. Marzin,[35] L. Masetti,[97] T. Mashimo,[160] R. Mashinistov,[108] J. Masik,[98] A. L. Maslennikov,[120b,120a] L. H. Mason,[102] L. Massa,[71a,71b] P. Mastrandrea,[5] A. Mastroberardino,[40b,40a] T. Masubuchi,[160] P. Mättig,[179] J. Maurer,[27b] B. Maček,[89] S. J. Maxfield,[88] D. A. Maximov,[120b,120a] R. Mazini,[155] I. Maznas,[159] S. M. Mazza,[143] N. C. Mc Fadden,[116] G. Mc Goldrick,[164] S. P. Mc Kee,[103] A. McCarn,[103] T. G. McCarthy,[113] L. I. McClymont,[92] E. F. McDonald,[102] J. A. Mcfayden,[35] G. Mchedlidze,[51] M. A. McKay,[41] K. D. McLean,[173] S. J. McMahon,[141] P. C. McNamara,[102] C. J. McNicol,[175] R. A. McPherson,[173,n] J. E. Mdhluli,[32c] Z. A. Meadows,[100] S. Meehan,[145] T. M. Megy,[50] S. Mehlhase,[112] A. Mehta,[88] T. Meideck,[56] B. Meirose,[42] D. Melini,[171,jj] B. R. Mellado Garcia,[32c] J. D. Mellenthin,[51] M. Melo,[28a] F. Meloni,[20] A. Melzer,[24] S. B. Menary,[98] E. D. Mendes Gouveia,[136a] L. Meng,[88] X. T. Meng,[103] A. Mengarelli,[23b,23a] S. Menke,[113] E. Meoni,[40b,40a] S. Mergelmeyer,[19] C. Merlassino,[20] P. Mermod,[52] L. Merola,[67a,67b] C. Meroni,[66a] F. S. Merritt,[36] A. Messina,[70a,70b] J. Metcalfe,[6] A. S. Mete,[168] C. Meyer,[133] J. Meyer,[157] J-P. Meyer,[142] H. Meyer Zu Theenhausen,[59a] F. Miano,[153] R. P. Middleton,[141] L. Mijović,[48] G. Mikenberg,[177] M. Mikestikova,[137] M. Mikuž,[89] M. Milesi,[102] A. Milic,[164] D. A. Millar,[90] D. W. Miller,[36] A. Milov,[177] D. A. Milstead,[43a,43b] A. A. Minaenko,[140] M. Miñano Moya,[171] I. A. Minashvili,[156b] A. I. Mincer,[121] B. Mindur,[81a] M. Mineev,[77] Y. Minegishi,[160] Y. Ming,[178] L. M. Mir,[14] A. Mirto,[65a,65b] K. P. Mistry,[133] T. Mitani,[176] J. Mitrevski,[112] V. A. Mitsou,[171] A. Miucci,[20] P. S. Miyagawa,[146] A. Mizukami,[79] J. U. Mjörnmark,[94] T. Mkrtchyan,[181] M. Mlynarikova,[139] T. Moa,[43a,43b] K. Mochizuki,[107] P. Mogg,[50] S. Mohapatra,[38] S. Molander,[43a,43b] R. Moles-Valls,[24] M. C. Mondragon,[104] K. Mönig,[44] J. Monk,[39] E. Monnier,[99] A. Montalbano,[149] J. Montejo Berlingen,[35] F. Monticelli,[86] S. Monzani,[66a] R. W. Moore,[3] N. Morange,[128] D. Moreno,[22] M. Moreno Llácer,[35] P. Morettini,[53b] M. Morgenstern,[118] S. Morgenstern,[35] D. Mori,[149] T. Mori,[160] M. Morii,[57] M. Morinaga,[176] V. Morisbak,[130] A. K. Morley,[35] G. Mornacchi,[35] A. P. Morris,[92] J. D. Morris,[90] L. Morvaj,[152] P. Moschovakos,[10] M. Mosidze,[156b] H. J. Moss,[146] J. Moss,[150,kk] K. Motohashi,[162] R. Mount,[150] E. Mountricha,[35] E. J. W. Moyse,[100] S. Muanza,[99] F. Mueller,[113] J. Mueller,[135] R. S. P. Mueller,[112] D. Muenstermann,[87] P. Mullen,[55] G. A. Mullier,[20] F. J. Munoz Sanchez,[98] P. Murin,[28b] W. J. Murray,[175,141] A. Murrone,[66a,66b] M. Muškinja,[89] C. Mwewa,[32a] A. G. Myagkov,[140,ll] J. Myers,[127] M. Myska,[138] B. P. Nachman,[18] O. Nackenhorst,[45] K. Nagai,[131] K. Nagano,[79] Y. Nagasaka,[60] K. Nagata,[166] M. Nagel,[50] E. Nagy,[99] A. M. Nairz,[35] Y. Nakahama,[115] K. Nakamura,[79] T. Nakamura,[160] I. Nakano,[123] H. Nanjo,[129] F. Napolitano,[59a] R. F. Naranjo Garcia,[44] R. Narayan,[11] D. I. Narrias Villar,[59a] I. Naryshkin,[134] T. Naumann,[44] G. Navarro,[22] R. Nayyar,[7] H. A. Neal,[103] P. Y. Nechaeva,[108] T. J. Neep,[142] A. Negri,[68a,68b] M. Negrini,[23b] S. Nektarijevic,[117] C. Nellist,[51] M. E. Nelson,[131] S. Nemecek,[137] P. Nemethy,[121] M. Nessi,[35,mm] M. S. Neubauer,[170] M. Neumann,[179] P. R. Newman,[21] T. Y. Ng,[61c] Y. S. Ng,[19] H. D. N. Nguyen,[99] T. Nguyen Manh,[107] E. Nibigira,[37] R. B. Nickerson,[131] R. Nicolaidou,[142] J. Nielsen,[143] N. Nikiforou,[11] V. Nikolaenko,[140,ll] I. Nikolic-Audit,[132] K. Nikolopoulos,[21] P. Nilsson,[29] Y. Ninomiya,[79] A. Nisati,[70a] N. Nishu,[58c] R. Nisius,[113] I. Nitsche,[45] T. Nitta,[176] T. Nobe,[160] Y. Noguchi,[83] M. Nomachi,[129] I. Nomidis,[132] M. A. Nomura,[29] T. Nooney,[90] M. Nordberg,[35] N. Norjoharuddeen,[131] T. Novak,[89] O. Novgorodova,[46] R. Novotny,[138] M. Nozaki,[79] L. Nozka,[126] K. Ntekas,[168] E. Nurse,[92] F. Nuti,[102] F. G. Oakham,[33,e] H. Oberlack,[113] T. Obermann,[24] J. Ocariz,[132] A. Ochi,[80] I. Ochoa,[38] J. P. Ochoa-Ricoux,[144a] K. O'Connor,[26] S. Oda,[85] S. Odaka,[79] A. Oh,[98] S. H. Oh,[47] C. C. Ohm,[151] H. Oide,[53b,53a] H. Okawa,[166] Y. Okazaki,[83] Y. Okumura,[160] T. Okuyama,[79] A. Olariu,[27b] L. F. Oleiro Seabra,[136a] S. A. Olivares Pino,[144a] D. Oliveira Damazio,[29] J. L. Oliver,[1] M. J. R. Olsson,[36] A. Olszewski,[82] J. Olszowska,[82] D. C. O'Neil,[149] A. Onofre,[136a,136e] K. Onogi,[115] P. U. E. Onyisi,[11] H. Oppen,[130] M. J. Oreglia,[36] Y. Oren,[158] D. Orestano,[72a,72b] E. C. Orgill,[98] N. Orlando,[61b] A. A. O'Rourke,[44] R. S. Orr,[164] B. Osculati,[53b,53a,a] V. O'Shea,[55] R. Ospanov,[58a] G. Otero y Garzon,[30] H. Otono,[85] M. Ouchrif,[34d] F. Ould-Saada,[130] A. Ouraou,[142] Q. Ouyang,[15a] M. Owen,[55] R. E. Owen,[21] V. E. Ozcan,[12c] N. Ozturk,[8] J. Pacalt,[126] H. A. Pacey,[31] K. Pachal,[149] A. Pacheco Pages,[14] L. Pacheco Rodriguez,[142] C. Padilla Aranda,[14] S. Pagan Griso,[18] M. Paganini,[180] G. Palacino,[63] S. Palazzo,[40b,40a] S. Palestini,[35] M. Palka,[81b] D. Pallin,[37] I. Panagoulias,[10] C. E. Pandini,[35] J. G. Panduro Vazquez,[91] P. Pani,[35] G. Panizzo,[64a,64c] L. Paolozzi,[52] T. D. Papadopoulou,[10] K. Papageorgiou,[9,t] A. Paramonov,[6] D. Paredes Hernandez,[61b] S. R. Paredes Saenz,[131] B. Parida,[58c] A. J. Parker,[87] K. A. Parker,[44] M. A. Parker,[31] F. Parodi,[53b,53a] J. A. Parsons,[38] U. Parzefall,[50] V. R. Pascuzzi,[164] J. M. P. Pasner,[143] E. Pasqualucci,[70a] S. Passaggio,[53b] F. Pastore,[91] P. Pasuwan,[43a,43b] S. Pataraia,[97] J. R. Pater,[98] A. Pathak,[178,f] T. Pauly,[35] B. Pearson,[113] M. Pedersen,[130] L. Pedraza Diaz,[117] S. Pedraza Lopez,[171] R. Pedro,[136a,136b] S. V. Peleganchuk,[120b,120a] O. Penc,[137] C. Peng,[15d] H. Peng,[58a] B. S. Peralva,[78a] M. M. Perego,[142] A. P. Pereira Peixoto,[136a] D. V. Perepelitsa,[29] F. Peri,[19] L. Perini,[66a,66b] H. Pernegger,[35] S. Perrella,[67a,67b] V. D. Peshekhonov,[77,a] K. Peters,[44] R. F. Y. Peters,[98] B. A. Petersen,[35] T. C. Petersen,[39] E. Petit,[56] A. Petridis,[1] C. Petridou,[159] P. Petroff,[128] E. Petrolo,[70a] M. Petrov,[131] F. Petrucci,[72a,72b]

M. Pettee,[180] N. E. Pettersson,[100] A. Peyaud,[142] R. Pezoa,[144b] T. Pham,[102] F. H. Phillips,[104] P. W. Phillips,[141] G. Piacquadio,[152] E. Pianori,[18] A. Picazio,[100] M. A. Pickering,[131] R. Piegaia,[30] J. E. Pilcher,[36] A. D. Pilkington,[98] M. Pinamonti,[71a,71b] J. L. Pinfold,[3] M. Pitt,[177] M-A. Pleier,[29] V. Pleskot,[139] E. Plotnikova,[77] D. Pluth,[76] P. Podberezko,[120b,120a] R. Poettgen,[94] R. Poggi,[52] L. Poggioli,[128] I. Pogrebnyak,[104] D. Pohl,[24] I. Pokharel,[51] G. Polesello,[68a] A. Poley,[44] A. Policicchio,[40b,40a] R. Polifka,[35] A. Polini,[23b] C. S. Pollard,[44] V. Polychronakos,[29] D. Ponomarenko,[110] L. Pontecorvo,[70a] G. A. Popeneciu,[27d] D. M. Portillo Quintero,[132] S. Pospisil,[138] K. Potamianos,[44] I. N. Potrap,[77] C. J. Potter,[31] H. Potti,[11] T. Poulsen,[94] J. Poveda,[35] T. D. Powell,[146] M. E. Pozo Astigarraga,[35] P. Pralavorio,[99] S. Prell,[76] D. Price,[98] M. Primavera,[65a] S. Prince,[101] N. Proklova,[110] K. Prokofiev,[61c] F. Prokoshin,[144b] S. Protopopescu,[29] J. Proudfoot,[6] M. Przybycien,[81a] A. Puri,[170] P. Puzo,[128] J. Qian,[103] Y. Qin,[98] A. Quadt,[51] M. Queitsch-Maitland,[44] A. Qureshi,[1] P. Rados,[102] F. Ragusa,[66a,66b] G. Rahal,[95] J. A. Raine,[98] S. Rajagopalan,[29] A. Ramirez Morales,[90] T. Rashid,[128] S. Raspopov,[5] M. G. Ratti,[66a,66b] D. M. Rauch,[44] F. Rauscher,[112] S. Rave,[97] B. Ravina,[146] I. Ravinovich,[177] J. H. Rawling,[98] M. Raymond,[35] A. L. Read,[130] N. P. Readioff,[56] M. Reale,[65a,65b] D. M. Rebuzzi,[68a,68b] A. Redelbach,[174] G. Redlinger,[29] R. Reece,[143] R. G. Reed,[32c] K. Reeves,[42] L. Rehnisch,[19] J. Reichert,[133] A. Reiss,[97] C. Rembser,[35] H. Ren,[15d] M. Rescigno,[70a] S. Resconi,[66a] E. D. Resseguie,[133] S. Rettie,[172] E. Reynolds,[21] O. L. Rezanova,[120b,120a] P. Reznicek,[139] R. Richter,[113] S. Richter,[92] E. Richter-Was,[81b] O. Ricken,[24] M. Ridel,[132] P. Rieck,[113] C. J. Riegel,[179] O. Rifki,[44] M. Rijssenbeek,[152] A. Rimoldi,[68a,68b] M. Rimoldi,[20] L. Rinaldi,[23b] G. Ripellino,[151] B. Ristić,[87] E. Ritsch,[35] I. Riu,[14] J. C. Rivera Vergara,[144a] F. Rizatdinova,[125] E. Rizvi,[90] C. Rizzi,[14] R. T. Roberts,[98] S. H. Robertson,[101,n] A. Robichaud-Veronneau,[101] D. Robinson,[31] J. E. M. Robinson,[44] A. Robson,[55] E. Rocco,[97] C. Roda,[69a,69b] Y. Rodina,[99] S. Rodriguez Bosca,[171] A. Rodriguez Perez,[14] D. Rodriguez Rodriguez,[171] A. M. Rodríguez Vera,[165b] S. Roe,[35] C. S. Rogan,[57] O. Røhne,[130] R. Röhrig,[113] C. P. A. Roland,[63] J. Roloff,[57] A. Romaniouk,[110] M. Romano,[23b,23a] N. Rompotis,[88] M. Ronzani,[121] L. Roos,[132] S. Rosati,[70a] K. Rosbach,[50] P. Rose,[143] N-A. Rosien,[51] E. Rossi,[67a,67b] L. P. Rossi,[53b] L. Rossini,[66a,66b] J. H. N. Rosten,[31] R. Rosten,[14] M. Rotaru,[27b] J. Rothberg,[145] D. Rousseau,[128] D. Roy,[32c] A. Rozanov,[99] Y. Rozen,[157] X. Ruan,[32c] F. Rubbo,[150] F. Rühr,[50] A. Ruiz-Martinez,[33] Z. Rurikova,[50] N. A. Rusakovich,[77] H. L. Russell,[101] J. P. Rutherfoord,[7] N. Ruthmann,[35] E. M. Rüttinger,[44,nn] Y. F. Ryabov,[134] M. Rybar,[170] G. Rybkin,[128] S. Ryu,[6] A. Ryzhov,[140] G. F. Rzehorz,[51] P. Sabatini,[51] G. Sabato,[118] S. Sacerdoti,[128] H. F-W. Sadrozinski,[143] R. Sadykov,[77] F. Safai Tehrani,[70a] P. Saha,[119] M. Sahinsoy,[59a] A. Sahu,[179] M. Saimpert,[44] M. Saito,[160] T. Saito,[160] H. Sakamoto,[160] A. Sakharov,[121,gg] D. Salamani,[52] G. Salamanna,[72a,72b] J. E. Salazar Loyola,[144b] D. Salek,[118] P. H. Sales De Bruin,[169] D. Salihagic,[113] A. Salnikov,[150] J. Salt,[171] D. Salvatore,[40b,40a] F. Salvatore,[153] A. Salvucci,[61a,61b,61c] A. Salzburger,[35] D. Sammel,[50] D. Sampsonidis,[159] D. Sampsonidou,[159] J. Sánchez,[171] A. Sanchez Pineda,[64a,64c] H. Sandaker,[130] C. O. Sander,[44] M. Sandhoff,[179] C. Sandoval,[22] D. P. C. Sankey,[141] M. Sannino,[53b,53a] Y. Sano,[115] A. Sansoni,[49] C. Santoni,[37] H. Santos,[136a] I. Santoyo Castillo,[153] A. Sapronov,[77] J. G. Saraiva,[136a,136d] O. Sasaki,[79] K. Sato,[166] E. Sauvan,[5] P. Savard,[164,e] N. Savic,[113] R. Sawada,[160] C. Sawyer,[141] L. Sawyer,[93,v] C. Sbarra,[23b] A. Sbrizzi,[23b,23a] T. Scanlon,[92] J. Schaarschmidt,[145] P. Schacht,[113] B. M. Schachtner,[112] D. Schaefer,[36] L. Schaefer,[133] J. Schaeffer,[97] S. Schaepe,[35] U. Schäfer,[97] A. C. Schaffer,[128] D. Schaile,[112] R. D. Schamberger,[152] N. Scharmberg,[98] V. A. Schegelsky,[134] D. Scheirich,[139] F. Schenck,[19] M. Schernau,[168] C. Schiavi,[53b,53a] S. Schier,[143] L. K. Schildgen,[24] Z. M. Schillaci,[26] E. J. Schioppa,[35] M. Schioppa,[40b,40a] K. E. Schleicher,[50] S. Schlenker,[35] K. R. Schmidt-Sommerfeld,[113] K. Schmieden,[35] C. Schmitt,[97] S. Schmitt,[44] S. Schmitz,[97] U. Schnoor,[50] L. Schoeffel,[142] A. Schoening,[59b] E. Schopf,[24] M. Schott,[97] J. F. P. Schouwenberg,[117] J. Schovancova,[35] S. Schramm,[52] A. Schulte,[97] H-C. Schultz-Coulon,[59a] M. Schumacher,[50] B. A. Schumm,[143] Ph. Schune,[142] A. Schwartzman,[150] T. A. Schwarz,[103] H. Schweiger,[98] Ph. Schwemling,[142] R. Schwienhorst,[104] A. Sciandra,[24] G. Sciolla,[26] M. Scornajenghi,[40b,40a] F. Scuri,[69a] F. Scutti,[102] L. M. Scyboz,[113] J. Searcy,[103] C. D. Sebastiani,[70a,70b] P. Seema,[24] S. C. Seidel,[116] A. Seiden,[143] T. Seiss,[36] J. M. Seixas,[78b] G. Sekhniaidze,[67a] K. Sekhon,[103] S. J. Sekula,[41] N. Semprini-Cesari,[23b,23a] S. Sen,[47] S. Senkin,[37] C. Serfon,[130] L. Serin,[128] L. Serkin,[64a,64b] M. Sessa,[72a,72b] H. Severini,[124] F. Sforza,[167] A. Sfyrla,[52] E. Shabalina,[51] J. D. Shahinian,[143] N. W. Shaikh,[43a,43b] L. Y. Shan,[15a] R. Shang,[170] J. T. Shank,[25] M. Shapiro,[18] A. S. Sharma,[1] A. Sharma,[131] P. B. Shatalov,[109] K. Shaw,[153] S. M. Shaw,[98] A. Shcherbakova,[134] Y. Shen,[124] N. Sherafati,[33] A. D. Sherman,[25] P. Sherwood,[92] L. Shi,[155,oo] S. Shimizu,[80] C. O. Shimmin,[180] M. Shimojima,[114] I. P. J. Shipsey,[131] S. Shirabe,[85] M. Shiyakova,[77] J. Shlomi,[177] A. Shmeleva,[108] D. Shoaleh Saadi,[107] M. J. Shochet,[36] S. Shojaii,[102] D. R. Shope,[124] S. Shrestha,[122] E. Shulga,[110] P. Sicho,[137] A. M. Sickles,[170] P. E. Sidebo,[151] E. Sideras Haddad,[32c] O. Sidiropoulou,[174] A. Sidoti,[23b,23a] F. Siegert,[46] Dj. Sijacki,[16] J. Silva,[136a] M. Silva Jr.,[178] M. V. Silva Oliveira,[78a] S. B. Silverstein,[43a] L. Simic,[77] S. Simion,[128] E. Simioni,[97] M. Simon,[97] P. Sinervo,[164] N. B. Sinev,[127]

M. Sioli,[23b,23a] G. Siragusa,[174] I. Siral,[103] S. Yu. Sivoklokov,[111] J. Sjölin,[43a,43b] M. B. Skinner,[87] P. Skubic,[124] M. Slater,[21] T. Slavicek,[138] M. Slawinska,[82] K. Sliwa,[167] R. Slovak,[139] V. Smakhtin,[177] B. H. Smart,[5] J. Smiesko,[28a] N. Smirnov,[110] S. Yu. Smirnov,[110] Y. Smirnov,[110] L. N. Smirnova,[111] O. Smirnova,[94] J. W. Smith,[51] M. N. K. Smith,[38] R. W. Smith,[38] M. Smizanska,[87] K. Smolek,[138] A. A. Snesarev,[108] I. M. Snyder,[127] S. Snyder,[29] R. Sobie,[173,n] A. M. Soffa,[168] A. Soffer,[158] A. Søgaard,[48] D. A. Soh,[155] G. Sokhrannyi,[89] C. A. Solans Sanchez,[35] M. Solar,[138] E. Yu. Soldatov,[110] U. Soldevila,[171] A. A. Solodkov,[140] A. Soloshenko,[77] O. V. Solovyanov,[140] V. Solovyev,[134] P. Sommer,[146] H. Son,[167] W. Song,[141] A. Sopczak,[138] F. Sopkova,[28b] D. Sosa,[59b] C. L. Sotiropoulou,[69a,69b] S. Sottocornola,[68a,68b] R. Soualah,[64a,64c,pp] A. M. Soukharev,[120b,120a] D. South,[44] B. C. Sowden,[91] S. Spagnolo,[65a,65b] M. Spalla,[113] M. Spangenberg,[175] F. Spanò,[91] D. Sperlich,[19] F. Spettel,[113] T. M. Spieker,[59a] R. Spighi,[23b] G. Spigo,[35] L. A. Spiller,[102] D. P. Spiteri,[55] M. Spousta,[139] A. Stabile,[66a,66b] R. Stamen,[59a] S. Stamm,[19] E. Stanecka,[82] R. W. Stanek,[6] C. Stanescu,[72a] B. Stanislaus,[131] M. M. Stanitzki,[44] B. Stapf,[118] S. Stapnes,[130] E. A. Starchenko,[140] G. H. Stark,[36] J. Stark,[56] S. H Stark,[39] P. Staroba,[137] P. Starovoitov,[59a] S. Stärz,[35] R. Staszewski,[82] M. Stegler,[44] P. Steinberg,[29] B. Stelzer,[149] H. J. Stelzer,[35] O. Stelzer-Chilton,[165a] H. Stenzel,[54] T. J. Stevenson,[90] G. A. Stewart,[55] M. C. Stockton,[127] G. Stoicea,[27b] P. Stolte,[51] S. Stonjek,[113] A. Straessner,[46] J. Strandberg,[151] S. Strandberg,[43a,43b] M. Strauss,[124] P. Strizenec,[28b] R. Ströhmer,[174] D. M. Strom,[127] R. Stroynowski,[41] A. Strubig,[48] S. A. Stucci,[29] B. Stugu,[17] J. Stupak,[124] N. A. Styles,[44] D. Su,[150] J. Su,[135] S. Suchek,[59a] Y. Sugaya,[129] M. Suk,[138] V. V. Sulin,[108] D. M. S. Sultan,[52] S. Sultansoy,[4c] T. Sumida,[83] S. Sun,[103] X. Sun,[3] K. Suruliz,[153] C. J. E. Suster,[154] M. R. Sutton,[153] S. Suzuki,[79] M. Svatos,[137] M. Swiatlowski,[36] S. P. Swift,[2] A. Sydorenko,[97] I. Sykora,[28a] T. Sykora,[139] D. Ta,[97] K. Tackmann,[44,qq] J. Taenzer,[158] A. Taffard,[168] R. Tafirout,[165a] E. Tahirovic,[90] N. Taiblum,[158] H. Takai,[29] R. Takashima,[84] E. H. Takasugi,[113] K. Takeda,[80] T. Takeshita,[147] Y. Takubo,[79] M. Talby,[99] A. A. Talyshev,[120b,120a] J. Tanaka,[160] M. Tanaka,[162] R. Tanaka,[128] R. Tanioka,[80] B. B. Tannenwald,[122] S. Tapia Araya,[144b] S. Tapprogge,[97] A. Tarek Abouelfadl Mohamed,[132] S. Tarem,[157] G. Tarna,[27b,q] G. F. Tartarelli,[66a] P. Tas,[139] M. Tasevsky,[137] T. Tashiro,[83] E. Tassi,[40b,40a] A. Tavares Delgado,[136a,136b] Y. Tayalati,[34e] A. C. Taylor,[116] A. J. Taylor,[48] G. N. Taylor,[102] P. T. E. Taylor,[102] W. Taylor,[165b] A. S. Tee,[87] P. Teixeira-Dias,[91] H. Ten Kate,[35] P. K. Teng,[155] J. J. Teoh,[129] F. Tepel,[179] S. Terada,[79] K. Terashi,[160] J. Terron,[96] S. Terzo,[14] M. Testa,[49] R. J. Teuscher,[164,n] S. J. Thais,[180] T. Theveneaux-Pelzer,[44] F. Thiele,[39] J. P. Thomas,[21] A. S. Thompson,[55] P. D. Thompson,[21] L. A. Thomsen,[180] E. Thomson,[133] Y. Tian,[38] R. E. Ticse Torres,[51] V. O. Tikhomirov,[108,rr] Yu. A. Tikhonov,[120b,120a] S. Timoshenko,[110] P. Tipton,[180] S. Tisserant,[99] K. Todome,[162] S. Todorova-Nova,[5] S. Todt,[46] J. Tojo,[85] S. Tokár,[28a] K. Tokushuku,[79] E. Tolley,[122] K. G. Tomiwa,[32c] M. Tomoto,[115] L. Tompkins,[150,ff] K. Toms,[116] B. Tong,[57] P. Tornambe,[50] E. Torrence,[127] H. Torres,[46] E. Torró Pastor,[145] C. Tosciri,[131] J. Toth,[99,ss] F. Touchard,[99] D. R. Tovey,[146] C. J. Treado,[121] T. Trefzger,[174] F. Tresoldi,[153] A. Tricoli,[29] I. M. Trigger,[165a] S. Trincaz-Duvoid,[132] M. F. Tripiana,[14] W. Trischuk,[164] B. Trocmé,[56] A. Trofymov,[128] C. Troncon,[66a] M. Trovatelli,[173] F. Trovato,[153] L. Truong,[32b] M. Trzebinski,[82] A. Trzupek,[82] F. Tsai,[44] J. C-L. Tseng,[131] P. V. Tsiareshka,[105] N. Tsirintanis,[9] V. Tsiskaridze,[152] E. G. Tskhadadze,[156a] I. I. Tsukerman,[109] V. Tsulaia,[18] S. Tsuno,[79] D. Tsybychev,[152] Y. Tu,[61b] A. Tudorache,[27b] V. Tudorache,[27b] T. T. Tulbure,[27a] A. N. Tuna,[57] S. Turchikhin,[77] D. Turgeman,[177] I. Turk Cakir,[4b,tt] R. Turra,[66a] P. M. Tuts,[38] E. Tzovara,[97] G. Ucchielli,[23b,23a] I. Ueda,[79] M. Ughetto,[43a,43b] F. Ukegawa,[166] G. Unal,[35] A. Undrus,[29] G. Unel,[168] F. C. Ungaro,[102] Y. Unno,[79] K. Uno,[160] J. Urban,[28b] P. Urquijo,[102] P. Urrejola,[97] G. Usai,[8] J. Usui,[79] L. Vacavant,[99] V. Vacek,[138] B. Vachon,[101] K. O. H. Vadla,[130] A. Vaidya,[92] C. Valderanis,[112] E. Valdes Santurio,[43a,43b] M. Valente,[52] S. Valentinetti,[23b,23a] A. Valero,[171] L. Valéry,[44] R. A. Vallance,[21] A. Vallier,[5] J. A. Valls Ferrer,[171] T. R. Van Daalen,[14] W. Van Den Wollenberg,[118] H. Van der Graaf,[118] P. Van Gemmeren,[6] J. Van Nieuwkoop,[149] I. Van Vulpen,[118] M. C. van Woerden,[118] M. Vanadia,[71a,71b] W. Vandelli,[35] A. Vaniachine,[163] P. Vankov,[118] R. Vari,[70a] E. W. Varnes,[7] C. Varni,[53b,53a] T. Varol,[41] D. Varouchas,[128] K. E. Varvell,[154] G. A. Vasquez,[144b] J. G. Vasquez,[180] F. Vazeille,[37] D. Vazquez Furelos,[14] T. Vazquez Schroeder,[101] J. Veatch,[51] V. Vecchio,[72a,72b] L. M. Veloce,[164] F. Veloso,[136a,136c] S. Veneziano,[70a] A. Ventura,[65a,65b] M. Venturi,[173] N. Venturi,[35] V. Vercesi,[68a] M. Verducci,[72a,72b] C. M. Vergel Infante,[76] W. Verkerke,[118] A. T. Vermeulen,[118] J. C. Vermeulen,[118] M. C. Vetterli,[149,e] N. Viaux Maira,[144b] O. Viazlo,[94] I. Vichou,[170,a] T. Vickey,[146] O. E. Vickey Boeriu,[146] G. H. A. Viehhauser,[131] S. Viel,[18] L. Vigani,[131] M. Villa,[23b,23a] M. Villaplana Perez,[66a,66b] E. Vilucchi,[49] M. G. Vincter,[33] V. B. Vinogradov,[77] A. Vishwakarma,[44] C. Vittori,[23b,23a] I. Vivarelli,[153] S. Vlachos,[10] M. Vogel,[179] P. Vokac,[138] G. Volpi,[14] S. E. von Buddenbrock,[32c] E. Von Toerne,[24] V. Vorobel,[139] K. Vorobev,[110] M. Vos,[171] J. H. Vossebeld,[88] N. Vranjes,[16] M. Vranjes Milosavljevic,[16] V. Vrba,[138] M. Vreeswijk,[118] T. Šfiligoj,[89] R. Vuillermet,[35] I. Vukotic,[36] T. Ženiš,[28a] L. Živković,[16] P. Wagner,[24] W. Wagner,[179] J. Wagner-Kuhr,[112] H. Wahlberg,[86] S. Wahrmund,[46] K. Wakamiya,[80] V. M. Walbrecht,[113] J. Walder,[87]

R. Walker,[112] W. Walkowiak,[148] V. Wallangen,[43a,43b] A. M. Wang,[57] C. Wang,[58b,q] F. Wang,[178] H. Wang,[18] H. Wang,[3] J. Wang,[154] J. Wang,[59b] P. Wang,[41] Q. Wang,[124] R.-J. Wang,[132] R. Wang,[58a] R. Wang,[6] S. M. Wang,[155] W. T. Wang,[58a] W. Wang,[155,uu] W. X. Wang,[58a,vv] Y. Wang,[58a] Z. Wang,[58c] C. Wanotayaroj,[44] A. Warburton,[101] C. P. Ward,[31] D. R. Wardrope,[92] A. Washbrook,[48] P. M. Watkins,[21] A. T. Watson,[21] M. F. Watson,[21] G. Watts,[145] S. Watts,[98] B. M. Waugh,[92] A. F. Webb,[11] S. Webb,[97] C. Weber,[180] M. S. Weber,[20] S. A. Weber,[33] S. M. Weber,[59a] J. S. Webster,[6] A. R. Weidberg,[131] B. Weinert,[63] J. Weingarten,[51] M. Weirich,[97] C. Weiser,[50] P. S. Wells,[35] T. Wenaus,[29] T. Wengler,[35] S. Wenig,[35] N. Wermes,[24] M. D. Werner,[76] P. Werner,[35] M. Wessels,[59a] T. D. Weston,[20] K. Whalen,[127] N. L. Whallon,[145] A. M. Wharton,[87] A. S. White,[103] A. White,[8] M. J. White,[1] R. White,[144b] D. Whiteson,[168] B. W. Whitmore,[87] F. J. Wickens,[141] W. Wiedenmann,[178] M. Wielers,[141] C. Wiglesworth,[39] L. A. M. Wiik-Fuchs,[50] A. Wildauer,[113] F. Wilk,[98] H. G. Wilkens,[35] L. J. Wilkins,[91] H. H. Williams,[133] S. Williams,[31] C. Willis,[104] S. Willocq,[100] J. A. Wilson,[21] I. Wingerter-Seez,[5] E. Winkels,[153] F. Winklmeier,[127] O. J. Winston,[153] B. T. Winter,[24] M. Wittgen,[150] M. Wobisch,[93] A. Wolf,[97] T. M. H. Wolf,[118] R. Wolff,[99] M. W. Wolter,[82] H. Wolters,[136a,136c] V. W. S. Wong,[172] N. L. Woods,[143] S. D. Worm,[21] B. K. Wosiek,[82] K. W. Woźniak,[82] K. Wraight,[55] M. Wu,[36] S. L. Wu,[178] X. Wu,[52] Y. Wu,[58a] T. R. Wyatt,[98] B. M. Wynne,[48] S. Xella,[39] Z. Xi,[103] L. Xia,[175] D. Xu,[15a] H. Xu,[58a] L. Xu,[29] T. Xu,[142] W. Xu,[103] B. Yabsley,[154] S. Yacoob,[32a] K. Yajima,[129] D. P. Yallup,[92] D. Yamaguchi,[162] Y. Yamaguchi,[162] A. Yamamoto,[79] T. Yamanaka,[160] F. Yamane,[80] M. Yamatani,[160] T. Yamazaki,[160] Y. Yamazaki,[80] Z. Yan,[25] H. J. Yang,[58c,58d] H. T. Yang,[18] S. Yang,[75] Y. Yang,[160] Z. Yang,[17] W-M. Yao,[18] Y. C. Yap,[44] Y. Yasu,[79] E. Yatsenko,[58c,58d] J. Ye,[41] S. Ye,[29] I. Yeletskikh,[77] E. Yigitbasi,[25] E. Yildirim,[97] K. Yorita,[176] K. Yoshihara,[133] C. J. S. Young,[35] C. Young,[150] J. Yu,[8] J. Yu,[76] X. Yue,[59a] S. P. Y. Yuen,[24] I. Yusuff,[31,ww] B. Zabinski,[82] G. Zacharis,[10] E. Zaffaroni,[52] R. Zaidan,[14] A. M. Zaitsev,[140,ll] N. Zakharchuk,[44] J. Zalieckas,[17] S. Zambito,[57] D. Zanzi,[35] D. R. Zaripovas,[55] S. V. Zeißner,[45] C. Zeitnitz,[179] G. Zemaityte,[131] J. C. Zeng,[170] Q. Zeng,[150] O. Zenin,[140] D. Zerwas,[128] M. Zgubič,[131] D. F. Zhang,[58b] D. Zhang,[103] F. Zhang,[178] G. Zhang,[58a,vv] H. Zhang,[15c] J. Zhang,[6] L. Zhang,[50] L. Zhang,[58a] M. Zhang,[170] P. Zhang,[15c] R. Zhang,[58a,q] R. Zhang,[24] X. Zhang,[58b] Y. Zhang,[15d] Z. Zhang,[128] P. Zhao,[47] X. Zhao,[41] Y. Zhao,[58b,128,y] Z. Zhao,[58a] A. Zhemchugov,[77] B. Zhou,[103] C. Zhou,[178] L. Zhou,[41] M. S. Zhou,[15d] M. Zhou,[152] N. Zhou,[58c] Y. Zhou,[7] C. G. Zhu,[58b] H. L. Zhu,[58a] H. Zhu,[15a] J. Zhu,[103] Y. Zhu,[58a] X. Zhuang,[15a] K. Zhukov,[108] V. Zhulanov,[120b,120a] A. Zibell,[174] D. Zieminska,[63] N. I. Zimine,[77] S. Zimmermann,[50] Z. Zinonos,[113] M. Zinser,[97] M. Ziolkowski,[148] G. Zobernig,[178] A. Zoccoli,[23b,23a] K. Zoch,[51] T. G. Zorbas,[146] R. Zou,[36] M. Zur Nedden,[19] and L. Zwalinski[35]

(ATLAS Collaboration)

[1]*Department of Physics, University of Adelaide, Adelaide, Australia*
[2]*Physics Department, SUNY Albany, Albany, New York, USA*
[3]*Department of Physics, University of Alberta, Edmonton, Alberta, Canada*
[4a]*Department of Physics, Ankara University, Ankara, Turkey*
[4b]*Istanbul Aydin University, Istanbul, Turkey*
[4c]*Division of Physics, TOBB University of Economics and Technology, Ankara, Turkey*
[5]*LAPP, Université Grenoble Alpes, Université Savoie Mont Blanc, CNRS/IN2P3, Annecy, France*
[6]*High Energy Physics Division, Argonne National Laboratory, Argonne, Illinois, USA*
[7]*Department of Physics, University of Arizona, Tucson, Arizona, USA*
[8]*Department of Physics, University of Texas at Arlington, Arlington, Texas, USA*
[9]*Physics Department, National and Kapodistrian University of Athens, Athens, Greece*
[10]*Physics Department, National Technical University of Athens, Zografou, Greece*
[11]*Department of Physics, University of Texas at Austin, Austin, Texas, USA*
[12a]*Bahcesehir University, Faculty of Engineering and Natural Sciences, Istanbul, Turkey*
[12b]*Istanbul Bilgi University, Faculty of Engineering and Natural Sciences, Istanbul, Turkey*
[12c]*Department of Physics, Bogazici University, Istanbul, Turkey*
[12d]*Department of Physics Engineering, Gaziantep University, Gaziantep, Turkey*
[13]*Institute of Physics, Azerbaijan Academy of Sciences, Baku, Azerbaijan*
[14]*Institut de Física d'Altes Energies (IFAE), Barcelona Institute of Science and Technology, Barcelona, Spain*
[15a]*Institute of High Energy Physics, Chinese Academy of Sciences, Beijing, China*
[15b]*Physics Department, Tsinghua University, Beijing, China*
[15c]*Department of Physics, Nanjing University, Nanjing, China*

[15d]*University of Chinese Academy of Science (UCAS), Beijing, China*
[16]*Institute of Physics, University of Belgrade, Belgrade, Serbia*
[17]*Department for Physics and Technology, University of Bergen, Bergen, Norway*
[18]*Physics Division, Lawrence Berkeley National Laboratory and University of California, Berkeley, California, USA*
[19]*Institut für Physik, Humboldt Universität zu Berlin, Berlin, Germany*
[20]*Albert Einstein Center for Fundamental Physics and Laboratory for High Energy Physics, University of Bern, Bern, Switzerland*
[21]*School of Physics and Astronomy, University of Birmingham, Birmingham, United Kingdom*
[22]*Centro de Investigaciónes, Universidad Antonio Nariño, Bogota, Colombia*
[23a]*Dipartimento di Fisica e Astronomia, Università di Bologna, Bologna, Italy*
[23b]*INFN Sezione di Bologna, Italy*
[24]*Physikalisches Institut, Universität Bonn, Bonn, Germany*
[25]*Department of Physics, Boston University, Boston, Massachusetts, USA*
[26]*Department of Physics, Brandeis University, Waltham, Massachusetts, USA*
[27a]*Transilvania University of Brasov, Brasov, Romania*
[27b]*Horia Hulubei National Institute of Physics and Nuclear Engineering, Bucharest, Romania*
[27c]*Department of Physics, Alexandru Ioan Cuza University of Iasi, Iasi, Romania*
[27d]*National Institute for Research and Development of Isotopic and Molecular Technologies, Physics Department, Cluj-Napoca, Romania*
[27e]*University Politehnica Bucharest, Bucharest, Romania*
[27f]*West University in Timisoara, Timisoara, Romania*
[28a]*Faculty of Mathematics, Physics and Informatics, Comenius University, Bratislava, Slovak Republic*
[28b]*Department of Subnuclear Physics, Institute of Experimental Physics of the Slovak Academy of Sciences, Kosice, Slovak Republic*
[29]*Physics Department, Brookhaven National Laboratory, Upton, New York, USA*
[30]*Departamento de Física, Universidad de Buenos Aires, Buenos Aires, Argentina*
[31]*Cavendish Laboratory, University of Cambridge, Cambridge, United Kingdom*
[32a]*Department of Physics, University of Cape Town, Cape Town, South Africa*
[32b]*Department of Mechanical Engineering Science, University of Johannesburg, Johannesburg, South Africa*
[32c]*School of Physics, University of the Witwatersrand, Johannesburg, South Africa*
[33]*Department of Physics, Carleton University, Ottawa, Ontario, Canada*
[34a]*Faculté des Sciences Ain Chock, Réseau Universitaire de Physique des Hautes Energies—Université Hassan II, Casablanca, Morocco*
[34b]*Centre National de l'Energie des Sciences Techniques Nucleaires (CNESTEN), Rabat, Morocco*
[34c]*Faculté des Sciences Semlalia, Université Cadi Ayyad, LPHEA-Marrakech, Morocco*
[34d]*Faculté des Sciences, Université Mohamed Premier and LPTPM, Oujda, Morocco*
[34e]*Faculté des sciences, Université Mohammed V, Rabat, Morocco*
[35]*CERN, Geneva, Switzerland*
[36]*Enrico Fermi Institute, University of Chicago, Chicago, Illinois, USA*
[37]*LPC, Université Clermont Auvergne, CNRS/IN2P3, Clermont-Ferrand, France*
[38]*Nevis Laboratory, Columbia University, Irvington, New York, USA*
[39]*Niels Bohr Institute, University of Copenhagen, Copenhagen, Denmark*
[40a]*Dipartimento di Fisica, Università della Calabria, Rende, Italy*
[40b]*INFN Gruppo Collegato di Cosenza, Laboratori Nazionali di Frascati, Italy*
[41]*Physics Department, Southern Methodist University, Dallas, Texas, USA*
[42]*Physics Department, University of Texas at Dallas, Richardson, Texas, USA*
[43a]*Department of Physics, Stockholm University, Sweden*
[43b]*Oskar Klein Centre, Stockholm, Sweden*
[44]*Deutsches Elektronen-Synchrotron DESY, Hamburg and Zeuthen, Germany*
[45]*Lehrstuhl für Experimentelle Physik IV, Technische Universität Dortmund, Dortmund, Germany*
[46]*Institut für Kern- und Teilchenphysik, Technische Universität Dresden, Dresden, Germany*
[47]*Department of Physics, Duke University, Durham, North Carolina, USA*
[48]*SUPA—School of Physics and Astronomy, University of Edinburgh, Edinburgh, United Kingdom*
[49]*INFN e Laboratori Nazionali di Frascati, Frascati, Italy*
[50]*Physikalisches Institut, Albert-Ludwigs-Universität Freiburg, Freiburg, Germany*
[51]*II. Physikalisches Institut, Georg-August-Universität Göttingen, Göttingen, Germany*
[52]*Département de Physique Nucléaire et Corpusculaire, Université de Genève, Genève, Switzerland*
[53a]*Dipartimento di Fisica, Università di Genova, Genova, Italy*

[53b]INFN Sezione di Genova, Italy
[54]II. Physikalisches Institut, Justus-Liebig-Universität Giessen, Giessen, Germany
[55]SUPA—School of Physics and Astronomy, University of Glasgow, Glasgow, United Kingdom
[56]LPSC, Université Grenoble Alpes, CNRS/IN2P3, Grenoble INP, Grenoble, France
[57]Laboratory for Particle Physics and Cosmology, Harvard University, Cambridge, Massachusetts, USA
[58a]Department of Modern Physics and State Key Laboratory of Particle Detection and Electronics, University of Science and Technology of China, Hefei, China
[58b]Institute of Frontier and Interdisciplinary Science and Key Laboratory of Particle Physics and Particle Irradiation (MOE), Shandong University, Qingdao, China
[58c]School of Physics and Astronomy, Shanghai Jiao Tong University, KLPPAC-MoE, SKLPPC, Shanghai, China
[58d]Tsung-Dao Lee Institute, Shanghai, China
[59a]Kirchhoff-Institut für Physik, Ruprecht-Karls-Universität Heidelberg, Heidelberg, Germany
[59b]Physikalisches Institut, Ruprecht-Karls-Universität Heidelberg, Heidelberg, Germany
[60]Faculty of Applied Information Science, Hiroshima Institute of Technology, Hiroshima, Japan
[61a]Department of Physics, Chinese University of Hong Kong, Shatin, N.T., Hong Kong, China
[61b]Department of Physics, University of Hong Kong, Hong Kong, China
[61c]Department of Physics and Institute for Advanced Study, Hong Kong University of Science and Technology, Clear Water Bay, Kowloon, Hong Kong, China
[62]Department of Physics, National Tsing Hua University, Hsinchu, Taiwan
[63]Department of Physics, Indiana University, Bloomington, Indiana, USA
[64a]INFN Gruppo Collegato di Udine, Sezione di Trieste, Udine, Italy
[64b]ICTP, Trieste, Italy
[64c]Dipartimento di Chimica, Fisica e Ambiente, Università di Udine, Udine, Italy
[65a]INFN Sezione di Lecce, Italy
[65b]Dipartimento di Matematica e Fisica, Università del Salento, Lecce, Italy
[66a]INFN Sezione di Milano, Italy
[66b]Dipartimento di Fisica, Università di Milano, Milano, Italy
[67a]INFN Sezione di Napoli, Italy
[67b]Dipartimento di Fisica, Università di Napoli, Napoli, Italy
[68a]INFN Sezione di Pavia, Italy
[68b]Dipartimento di Fisica, Università di Pavia, Pavia, Italy
[69a]INFN Sezione di Pisa, Italy
[69b]Dipartimento di Fisica E. Fermi, Università di Pisa, Pisa, Italy
[70a]INFN Sezione di Roma, Italy
[70b]Dipartimento di Fisica, Sapienza Università di Roma, Roma, Italy
[71a]INFN Sezione di Roma Tor Vergata, Italy
[71b]Dipartimento di Fisica, Università di Roma Tor Vergata, Roma, Italy
[72a]INFN Sezione di Roma Tre, Italy
[72b]Dipartimento di Matematica e Fisica, Università Roma Tre, Roma, Italy
[73a]INFN-TIFPA, Italy
[73b]Università degli Studi di Trento, Trento, Italy
[74]Institut für Astro- und Teilchenphysik, Leopold-Franzens-Universität, Innsbruck, Austria
[75]University of Iowa, Iowa City, Iowa, USA
[76]Department of Physics and Astronomy, Iowa State University, Ames, Iowa, USA
[77]Joint Institute for Nuclear Research, Dubna, Russia
[78a]Departamento de Engenharia Elétrica, Universidade Federal de Juiz de Fora (UFJF), Juiz de Fora, Brazil
[78b]Universidade Federal do Rio De Janeiro COPPE/EE/IF, Rio de Janeiro, Brazil
[78c]Universidade Federal de São João del Rei (UFSJ), São João del Rei, Brazil
[78d]Instituto de Física, Universidade de São Paulo, São Paulo, Brazil
[79]KEK, High Energy Accelerator Research Organization, Tsukuba, Japan
[80]Graduate School of Science, Kobe University, Kobe, Japan
[81a]AGH University of Science and Technology, Faculty of Physics and Applied Computer Science, Krakow, Poland
[81b]Marian Smoluchowski Institute of Physics, Jagiellonian University, Krakow, Poland
[82]Institute of Nuclear Physics Polish Academy of Sciences, Krakow, Poland
[83]Faculty of Science, Kyoto University, Kyoto, Japan
[84]Kyoto University of Education, Kyoto, Japan

[85]*Research Center for Advanced Particle Physics and Department of Physics, Kyushu University, Fukuoka, Japan*
[86]*Instituto de Física La Plata, Universidad Nacional de La Plata and CONICET, La Plata, Argentina*
[87]*Physics Department, Lancaster University, Lancaster, United Kingdom*
[88]*Oliver Lodge Laboratory, University of Liverpool, Liverpool, United Kingdom*
[89]*Department of Experimental Particle Physics, Jožef Stefan Institute and Department of Physics, University of Ljubljana, Ljubljana, Slovenia*
[90]*School of Physics and Astronomy, Queen Mary University of London, London, United Kingdom*
[91]*Department of Physics, Royal Holloway University of London, Egham, United Kingdom*
[92]*Department of Physics and Astronomy, University College London, London, United Kingdom*
[93]*Louisiana Tech University, Ruston, Louisiana, USA*
[94]*Fysiska institutionen, Lunds universitet, Lund, Sweden*
[95]*Centre de Calcul de l'Institut National de Physique Nucléaire et de Physique des Particules (IN2P3), Villeurbanne, France*
[96]*Departamento de Física Teorica C-15 and CIAFF, Universidad Autónoma de Madrid, Madrid, Spain*
[97]*Institut für Physik, Universität Mainz, Mainz, Germany*
[98]*School of Physics and Astronomy, University of Manchester, Manchester, United Kingdom*
[99]*CPPM, Aix-Marseille Université, CNRS/IN2P3, Marseille, France*
[100]*Department of Physics, University of Massachusetts, Amherst, Massachusetts, USA*
[101]*Department of Physics, McGill University, Montreal, Québec, Canada*
[102]*School of Physics, University of Melbourne, Victoria, Australia*
[103]*Department of Physics, University of Michigan, Ann Arbor, Michigan, USA*
[104]*Department of Physics and Astronomy, Michigan State University, East Lansing, Michigan, USA*
[105]*B.I. Stepanov Institute of Physics, National Academy of Sciences of Belarus, Minsk, Belarus*
[106]*Research Institute for Nuclear Problems of Byelorussian State University, Minsk, Belarus*
[107]*Group of Particle Physics, University of Montreal, Montreal, Québec, Canada*
[108]*P.N. Lebedev Physical Institute of the Russian Academy of Sciences, Moscow, Russia*
[109]*Institute for Theoretical and Experimental Physics (ITEP), Moscow, Russia*
[110]*National Research Nuclear University MEPhI, Moscow, Russia*
[111]*D.V. Skobeltsyn Institute of Nuclear Physics, M.V. Lomonosov Moscow State University, Moscow, Russia*
[112]*Fakultät für Physik, Ludwig-Maximilians-Universität München, München, Germany*
[113]*Max-Planck-Institut für Physik (Werner-Heisenberg-Institut), München, Germany*
[114]*Nagasaki Institute of Applied Science, Nagasaki, Japan*
[115]*Graduate School of Science and Kobayashi-Maskawa Institute, Nagoya University, Nagoya, Japan*
[116]*Department of Physics and Astronomy, University of New Mexico, Albuquerque, New Mexico, USA*
[117]*Institute for Mathematics, Astrophysics and Particle Physics, Radboud University Nijmegen/Nikhef, Nijmegen, Netherlands*
[118]*Nikhef National Institute for Subatomic Physics and University of Amsterdam, Amsterdam, Netherlands*
[119]*Department of Physics, Northern Illinois University, DeKalb, Illinois, USA*
[120a]*Budker Institute of Nuclear Physics, SB RAS, Novosibirsk, Russia*
[120b]*Novosibirsk State University Novosibirsk, Russia*
[121]*Department of Physics, New York University, New York, New York, USA*
[122]*The Ohio State University, Columbus, Ohio, USA*
[123]*Faculty of Science, Okayama University, Okayama, Japan*
[124]*Homer L. Dodge Department of Physics and Astronomy, University of Oklahoma, Norman, Oklahoma, USA*
[125]*Department of Physics, Oklahoma State University, Stillwater, Oklahoma, USA*
[126]*Palacký University, RCPTM, Joint Laboratory of Optics, Olomouc, Czech Republic*
[127]*Center for High Energy Physics, University of Oregon, Eugene, Oregon, USA*
[128]*LAL, Université Paris-Sud, CNRS/IN2P3, Université Paris-Saclay, Orsay, France*
[129]*Graduate School of Science, Osaka University, Osaka, Japan*
[130]*Department of Physics, University of Oslo, Oslo, Norway*
[131]*Department of Physics, Oxford University, Oxford, United Kingdom*
[132]*LPNHE, Sorbonne Université, Paris Diderot Sorbonne Paris Cité, CNRS/IN2P3, Paris, France*
[133]*Department of Physics, University of Pennsylvania, Philadelphia, Pennsylvania, USA*
[134]*Konstantinov Nuclear Physics Institute of National Research Centre "Kurchatov Institute", PNPI, St. Petersburg, Russia*
[135]*Department of Physics and Astronomy, University of Pittsburgh, Pittsburgh, Pennsylvania, USA*
[136a]*Laboratório de Instrumentação e Física Experimental de Partículas—LIP, Portugal*

[136b]Departamento de Física, Faculdade de Ciências, Universidade de Lisboa, Lisboa, Portugal
[136c]Departamento de Física, Universidade de Coimbra, Coimbra, Portugal
[136d]Centro de Física Nuclear da Universidade de Lisboa, Lisboa, Portugal
[136e]Departamento de Física, Universidade do Minho, Braga, Portugal
[136f]Departamento de Física Teorica y del Cosmos, Universidad de Granada, Granada (Spain), Spain
[136g]Dep Física and CEFITEC of Faculdade de Ciências e Tecnologia, Universidade Nova de Lisboa, Caparica, Portugal
[137]Institute of Physics, Academy of Sciences of the Czech Republic, Prague, Czech Republic
[138]Czech Technical University in Prague, Prague, Czech Republic
[139]Charles University, Faculty of Mathematics and Physics, Prague, Czech Republic
[140]State Research Center Institute for High Energy Physics, NRC KI, Protvino, Russia
[141]Particle Physics Department, Rutherford Appleton Laboratory, Didcot, United Kingdom
[142]IRFU, CEA, Université Paris-Saclay, Gif-sur-Yvette, France
[143]Santa Cruz Institute for Particle Physics, University of California Santa Cruz, Santa Cruz, California, USA
[144a]Departamento de Física, Pontificia Universidad Católica de Chile, Santiago, Chile
[144b]Departamento de Física, Universidad Técnica Federico Santa María, Valparaíso, Chile
[145]Department of Physics, University of Washington, Seattle, Washington , USA
[146]Department of Physics and Astronomy, University of Sheffield, Sheffield, United Kingdom
[147]Department of Physics, Shinshu University, Nagano, Japan
[148]Department Physik, Universität Siegen, Siegen, Germany
[149]Department of Physics, Simon Fraser University, Burnaby, British Columbia, Canada
[150]SLAC National Accelerator Laboratory, Stanford, California, USA
[151]Physics Department, Royal Institute of Technology, Stockholm, Sweden
[152]Departments of Physics and Astronomy, Stony Brook University, Stony Brook, New York, USA
[153]Department of Physics and Astronomy, University of Sussex, Brighton, United Kingdom
[154]School of Physics, University of Sydney, Sydney, Australia
[155]Institute of Physics, Academia Sinica, Taipei, Taiwan
[156a]E. Andronikashvili Institute of Physics, Iv. Javakhishvili Tbilisi State University, Tbilisi, Georgia
[156b]High Energy Physics Institute, Tbilisi State University, Tbilisi, Georgia
[157]Department of Physics, Technion, Israel Institute of Technology, Haifa, Israel
[158]Raymond and Beverly Sackler School of Physics and Astronomy, Tel Aviv University, Tel Aviv, Israel
[159]Department of Physics, Aristotle University of Thessaloniki, Thessaloniki, Greece
[160]International Center for Elementary Particle Physics and Department of Physics, University of Tokyo, Tokyo, Japan
[161]Graduate School of Science and Technology, Tokyo Metropolitan University, Tokyo, Japan
[162]Department of Physics, Tokyo Institute of Technology, Tokyo, Japan
[163]Tomsk State University, Tomsk, Russia
[164]Department of Physics, University of Toronto, Toronto, Ontario, Canada
[165a]TRIUMF, Vancouver, British Columbia, Canada
[165b]Department of Physics and Astronomy, York University, Toronto, Ontario, Canada
[166]Division of Physics and Tomonaga Center for the History of the Universe, Faculty of Pure and Applied Sciences, University of Tsukuba, Tsukuba, Japan
[167]Department of Physics and Astronomy, Tufts University, Medford, Massachusetts, USA
[168]Department of Physics and Astronomy, University of California Irvine, Irvine, Massachusetts, USA
[169]Department of Physics and Astronomy, University of Uppsala, Uppsala, Sweden
[170]Department of Physics, University of Illinois, Urbana, Illinois, USA
[171]Instituto de Física Corpuscular (IFIC), Centro Mixto Universidad de Valencia—CSIC, Valencia, Spain
[172]Department of Physics, University of British Columbia, Vancouver, British Columbia, Canada
[173]Department of Physics and Astronomy, University of Victoria, Victoria, British Columbia, Canada
[174]Fakultät für Physik und Astronomie, Julius-Maximilians-Universität Würzburg, Würzburg, Germany
[175]Department of Physics, University of Warwick, Coventry, United Kingdom
[176]Waseda University, Tokyo, Japan
[177]Department of Particle Physics, Weizmann Institute of Science, Rehovot, Israel
[178]Department of Physics, University of Wisconsin, Madison, Wisconsin, USA
[179]Fakultät für Mathematik und Naturwissenschaften, Fachgruppe Physik, Bergische Universität Wuppertal, Wuppertal, Germany
[180]Department of Physics, Yale University, New Haven, Connecticut, USA
[181]Yerevan Physics Institute, Yerevan, Armenia

[a]Deceased.
[b]Also at Department of Physics, King's College London, London, United Kingdom.
[c]Also at Istanbul University, Dept. of Physics, Istanbul, Turkey.
[d]Also at Institute of Physics, Azerbaijan Academy of Sciences, Baku, Azerbaijan.
[e]Also at TRIUMF, Vancouver, British Columbia, Canada.
[f]Also at Department of Physics and Astronomy, University of Louisville, Louisville, Kentucky, USA.
[g]Also at Department of Physics, California State University, Fresno, California, USA.
[h]Also at Department of Physics, University of Fribourg, Fribourg, Switzerland.
[i]Also at II. Physikalisches Institut, Georg-August-Universität Göttingen, Göttingen, Germany.
[j]Also at Departament de Fisica de la Universitat Autonoma de Barcelona, Barcelona, Spain.
[k]Also at Tomsk State University, Tomsk, and Moscow Institute of Physics and Technology State University, Dolgoprudny, Russia.
[l]Also at The Collaborative Innovation Center of Quantum Matter (CICQM), Beijing, China.
[m]Also at Universita di Napoli Parthenope, Napoli, Italy.
[n]Also at Institute of Particle Physics (IPP), Canada.
[o]Also at Dipartimento di Fisica E. Fermi, Università di Pisa, Pisa, Italy.
[p]Also at Horia Hulubei National Institute of Physics and Nuclear Engineering, Bucharest, Romania.
[q]Also at CPPM, Aix-Marseille Université, CNRS/IN2P3, Marseille, France.
[r]Also at Department of Physics, St. Petersburg State Polytechnical University, St. Petersburg, Russia.
[s]Also at Borough of Manhattan Community College, City University of New York, New York, USA.
[t]Also at Department of Financial and Management Engineering, University of the Aegean, Chios, Greece.
[u]Also at Centre for High Performance Computing, CSIR Campus, Rosebank, Cape Town, South Africa.
[v]Also at Louisiana Tech University, Ruston, Louisiana, USA.
[w]Also at Institucio Catalana de Recerca i Estudis Avancats, ICREA, Barcelona, Spain.
[x]Also at Department of Physics, University of Michigan, Ann Arbor, Michigan, USA.
[y]Also at LAL, Université Paris-Sud, CNRS/IN2P3, Université Paris-Saclay, Orsay, France.
[z]Also at Graduate School of Science, Osaka University, Osaka, Japan.
[aa]Also at Physikalisches Institut, Albert-Ludwigs-Universität Freiburg, Freiburg, Germany.
[bb]Also at Institute for Mathematics, Astrophysics and Particle Physics, Radboud University Nijmegen/Nikhef, Nijmegen, Netherlands.
[cc]Also at Near East University, Nicosia, North Cyprus, Mersin, Turkey.
[dd]Also at Institute of Theoretical Physics, Ilia State University, Tbilisi, Georgia.
[ee]Also at CERN, Geneva, Switzerland.
[ff]Also at Department of Physics, Stanford University, Stanford, California, USA.
[gg]Also at Manhattan College, New York, New York, USA.
[hh]Also at Hellenic Open University, Patras, Greece.
[ii]Also at The City College of New York, New York, New York, USA.
[jj]Also at Departamento de Física Teorica y del Cosmos, Universidad de Granada, Granada (Spain), Spain.
[kk]Also at Department of Physics, California State University, Sacramento, California, USA.
[ll]Also at Moscow Institute of Physics and Technology State University, Dolgoprudny, Russia.
[mm]Also at Département de Physique Nucléaire et Corpusculaire, Université de Genève, Genève, Switzerland.
[nn]Also at Department of Physics and Astronomy, University of Sheffield, Sheffield, United Kingdom.
[oo]Also at School of Physics, Sun Yat-sen University, Guangzhou, China.
[pp]Also at Department of Applied Physics and Astronomy, University of Sharjah, Sharjah, United Arab Emirates.
[qq]Also at Institut für Experimentalphysik, Universität Hamburg, Hamburg, Germany.
[rr]Also at National Research Nuclear University MEPhI, Moscow, Russia.
[ss]Also at Institute for Particle and Nuclear Physics, Wigner Research Centre for Physics, Budapest, Hungary.
[tt]Also at Giresun University, Faculty of Engineering, Giresun, Turkey.
[uu]Also at Department of Physics, Nanjing University, Nanjing, China.
[vv]Also at Institute of Physics, Academia Sinica, Taipei, Taiwan.
[ww]Also at Department of Physics, University of Malaya, Kuala Lumpur, Malaysia.